COMPARISON OF EXTRATROPICAL CYCLONE CHARACTERISTICS FROM ATMOSPHERIC GLOBAL CLIMATE MODEL SIMULATIONS AT DIFFERENT RESOLUTIONS

Master Thesis
Climate Physics MSc
Faculty of Mathematics and Natural Sciences
Christian-Albrechts-Universität zu Kiel

Submitted by:
Robin Norbert Pilch Kedzierski
(1000327)

First supervisor: Douglas Maraun
Second supervisor: Wonsun Park

Kiel, October 2013

ABSTRACT

Extratropical cyclones play a key role in weather and climate at mid and high latitudes. They are simulated with Atmospheric Global Climate Models (AGCMs) for weather forecasting and future climate projections.

In order to determine how realistic the simulated extratropical cyclones are at different horizontal resolutions of an AGCM, this study compares the extratropical cyclone characteristics between the T31-42-63-106-159 resolutions of the ECHAM5 model (with prescribed SST and ice coverage) and the ERA-Interim reanalysis.

The results show that cyclone characteristics are indeed very dependent on resolution in the ECHAM5 runs. Fewer cyclones are detected at lower resolutions, and the cyclone characteristics get more realistic at higher resolutions compared to the ERA-Interim reanalysis, but not in a constant way.

The Atlantic Ocean is much more sensitive to resolution change than the Pacific, and the prescribed sea surface temperatures and ice coverage in the Atlantic do not force a similar NAO phase in the atmosphere in the ECHAM5 model runs compared to the predominant NAO phase captured in ERA-Interim (that happened in reality), which highly affects the cyclone spatial distribution and strength.

Resolutions T106 and T159 have a realistic representation of extratropical cyclone properties in most cases, but they do not match that well with ERA-Interim when taking the most extreme cases.

ZUSAMMENFASSUNG

Außertropische Zyklone spielen eine entscheidene Rolle in Bezug auf Wetter und Klima in den mittleren und hohen Breiten. Die Simulation dieser Sturmsysteme anhand atmosphärischer globaler Klimamodelle (AGCMs) dient der Wettervorhersage und zukünftigen Klimaprojektionen.

Um die Abhängigkeit der Vorhersagegüte von unterschiedlichen horizontalen Modellauflösungen zu quantifizieren, vergleicht die vorliegende Arbeit die Eigenschaften simulierter außertropischer Zyklone des ECHAM5 Models, welche auf festen Randbedingungen der SST und des Meereises sowie unterschiedlichen horizontalen Auflösungen (T31-42-63-106-159) basieren, mit Ergebnissen der ERA-Interim Reanalyse.

Die Ergebnisse zeigen, dass die Auflösung der ECHAM5 Läufe einen entscheidenden Einfluss auf die wirklichkeitsgetreue Darstellung der Zyklone hat. Während bei geringerer Auflösung weniger Zyklone nachgewiesen werden können, sind die Zyklooncharakteristiken bei höherer Auflösung realitätsnäher im Vergleich zu Ergebnisse der ERA-Interim Reanalyse, wobei kein linearer Zusammenhang besteht.

Die Modelergebnisse zeigen für den atlantischen Sektor eine weitaus stärkere Abhängigkeit von der Auflösung als die des Pazifikraums. Im Vergleich zu der vorherrschenden NAO Phase innerhalb der ERA-Interim Daten (welche der Realität entsprechen), treiben die festen SST- und Meereisrandbedingungen über dem Atlantik keine ähnliche NAO Phase in der atmosphärischen Komponenten der ECHAM5 Modellläufe an. Letzteres hat einen entscheidenen Einfluss auf die räumliche Verteilung sowie die Stärke der Zylone.

Die T106- und T159 Auslösungen produzieren größtenteils eine realistische Darstellung der Eigenschaften außertropischer Zyklone, wobei die Übereinstimmung mit der ERA-Interim Reanalyse im Falle von extremen Zyklonen abnimmt.

INDEX

INDEX (continues)

1: INTRODUCTION

1.1: Motivation

Extratropical cyclones are a key feature in the atmospheric circulation in the mid and high latitudes. They are synoptic-scale systems that account for an important part of the meridional transport of heat, moisture and momentum in the atmosphere, and they bring unstable weather to the places they affect. Extratropical cyclones are also associated with significant percentages of precipitation extremes *(Pfahl and Wernli, 2012)* and wind extremes *(Martinez-Alvarado et al., 2012),* which makes them one of the main atmospheric hazards over mid and high latitudes.

The simulation of extratropical cyclones is done using Atmospheric Global Climate Models (AGCMs), and this can be done for any timescale: from short-time simulations (in general from a couple of days to a week) used for weather forecasts, to centennial integrations for future climate projections.

The most important factors that control the realism of an AGCM are the representation of the physical laws governing the atmospheric processes, the interaction of the atmospheric component with the others (such as ocean, land and ice), the horizontal and vertical resolution of the model, and the inclusion of biological/geological/chemical processes.

Due to limited computational resources, integrations of an AGCM on a very long timescale are usually done at the expense of lower spatial resolution. The spatial scale of some of the processes that affect cyclone development might be not well-captured, leading to an underestimation of synoptic-scale activity and an unrealistic representation of extratropical cyclones.

The AGCMs used for climate change projections with increased greenhouse gas concentration scenarios have a relatively low spatial resolution compared to operational weather forecast models. The simulated response of extratropical cyclones to these scenarios depends on how realistically they are represented in the model.

This study will examine the characteristics of extratropical cyclones simulated with the ECHAM5 model *(Roeckner et al., 2003)* at different resolutions (T31-42-63-106-159). With the intention of addressing how realistic the simulated cyclones from the ECHAM5 runs are, their characteristics will be compared with the data from the ERA-Interim reanalysis *(Dee et al., 2011),* which is (up to date) the most accurate record of the cyclones that happened in the last

decades. The focus will be made on oceanic extratropical cyclones (Atlantic and Pacific) during winter time.

The two main goals of the study are to describe the sensitivity of the extratropical cyclone characteristics to changing horizontal resolution, and to address whether the simulated cyclones are realistic at some point.

This study will also compare its results with similar earlier investigations, in order to confirm their findings or report differences. The background about this topic follows below.

1.2: Background

-About the sensitivity to horizontal resolution:

Blender and Schubert (2000) used the relatively high resolution T106 of the ECHAM4 model *(Roeckner et al., 1996)*, interpolating its output onto lower resolutions (T21-42-63-84) to study the pure effect of truncation on the same pressure fields. They found that, with lower resolution, the number of detected cyclones decreased. The reason for this is that the small-scale features of the sea-level pressure fields (SLP) are smoothed out at lower resolution, meaning that some too small or too shallow cyclones are not captured.

Jung et al. (2006) found a similar relationship comparing seasonal integrations from resolutions T95 to T255 of the ECMWF model *(Simmons et al., 1989).* ECHAM models are derived from the ECMWF model. T95 produced just 60% of the cyclones found at T255.

Roeckner et al. (2006) studied the sensitivity to horizontal resolution of the mean climate at the ECHAM5 model *(Roeckner et al., 2003)* comparing different variables to the ERA-15 reanalysis *(Gibson et al., 1997).* They found that the root mean squared errors decreased monotonically with increasing resolution (from T42 to T159).

From the conclusions of these studies, one would expect fewer cyclones at lower resolutions and a constant convergence towards a realistic representation of extratropical cyclones with increasing resolution.

-What resolution of the ECHAM5 model simulates realistic extratropical cyclones?

The study by *Ulbrich et al. (2008)* suggests that the T63 resolution of the ECHAM5 model provides realistic results of storm track activity, when compared to other models of the Intergovernmental Panel on Climate Change *(IPCC, 2007).*

The results by *Pinto et al. (2009)* also suggest that the T63 resolution of the ECHAM5 model has realistic extratropical cyclones, comparing cyclone properties and their variability

with the North Atlantic Oscillation (NAO) to the NCEP-NCAR reanalysis data *(Kalnay et al., 1996).*

Although T63 is found to be realistic, it has to be pointed out that cyclone properties are still dependent on horizontal resolution at much higher resolutions:

Champion et al. (2011) find dependency between T213 and T319 resolutions of the ECHAM5 model, and *Jung et al. (2006)* address that, locally, resolution is a significant factor at even short and medium-range weather forecast models such as the T255 version of the ECMWF model.

2: FUNDAMENTALS

This section provides the concepts needed to understand what influences extratropical cyclone characteristics. It gives a detailed definition of what an extratropical cyclone is, the atmospheric conditions that determine their development, and their variability in the Atlantic and Pacific oceans.

2.1: Definition of extratropical cyclones

The definition of extratropical cyclones implies much more difficulties than that for tropical cyclones. The reasons are that extratropical cyclones are very common, that they form in different synoptic situations, and vary greatly in shape, structure and size, thus being much more asymmetric than a tropical cyclone. It is not unusual for an extratropical cyclone to have multiple centres of minimum pressure that can split and merge with others, this being a big handicap for their counting.

The naming itself classifies the common property of extratropical cyclones in a very wide sense: cyclone after the cyclonic (counter-clockwise in the Northern Hemisphere) circulation of the air around the centre, and extratropical referring to the latitudes it affects (simply not tropical) and also the main source of energy that drives the system (again, not the one that drives tropical cyclones, that is latent heat release from condensation in convective areas).

The main feature that differentiates extratropical from tropical cyclones is the core (centre) temperature compared to the outer surrounding areas. Since tropical cyclones are fed with latent heat release from deep convection, they develop a “warm core” being the deepest convection located near the centre, whereas extratropical cyclones show in contrast a “cold core” because the low pressure and minimum temperature centres tend to be closer when the energy from the baroclinic instability (misalignment of pressure and temperature fields) is released.

Some very strong extratropical cyclones develop a warm core in their mature state due to deep convective activity from a very baroclinic (unstable) situation, with the latest example being storm Jolle (January 2013).

To add even more intricacy, many tropical cyclones undergo an extratropical transition in their last stages (46% of tropical cyclones in the Atlantic*, Evans and Hart, 2003*) when they

reach higher latitudes and colder waters that don't fuel deep convection. Also, some extratropical lows experience tropical transition when they are pushed into tropical latitudes, and become tropical cyclones eventually. The first case of a cyclone going through extratropical transition and back into a tropical cyclone has been recorded recently (Hurricane Nadine in 2012). Also, an intermediate state has been termed for cyclones that have both tropical and extratropical characteristics: "subtropical cyclone", when a baroclinic situation allows the system to have deep convection and a tropical-like look over ocean waters far from reaching 26ºC (temperature required by tropical cyclones to sustain well-organized deep convection).

A simple and broad definition of extratropical cyclone would be any low pressure system in a background "baroclinic" zone (where the gradients of pressure and temperature are not parallel).

From a climatic perspective, extratropical cyclones convert the potential energy of the meridional temperature gradient into kinetic energy, reducing the pole-to-equator gradient and transporting energy poleward *(Holton, 1972).*

2.2: Conditions determining extratropical cyclone development

There are four parameters that describe the large-scale atmospheric conditions influencing extratropical cyclone development *(Pinto et al. 2009):*

-Baroclinicity: misalignment of temperature and pressure fields, as a measure of instability (fields less parallel: more unstable environment: conductive for cyclone development). The most "baroclinic" areas are placed in the North-Western part of the Atlantic and Pacific oceans, near strong sea surface temperature gradients (the Gulf Stream and the Kuroshio Current, respectively), and with cold air being advected from the continents by the westerlies. In climate simulations at low resolution, baroclinicity can be underestimated because of the smoothing of temperature and pressure gradients.

-The Jet Stream: it is the flow at the upper levels of the troposphere. A stronger jet leads to faster cyclone growth. Also, it has a strong influence on the steering of the cyclones, determining their paths.

-Upper air divergence: it induces upward motion in the underlying air column, decreasing the surface pressure and strengthening the extratropical cyclone. Areas of intense upper air divergence are found in the exit region north of the Jet Stream.

-Equivalent potential temperature: it indicates the effect of latent and sensible heat release. This effect, as explained earlier in section 2.1, becomes an extra (and important) source of energy for the development of the strongest extratropical cyclones.

2.3: Variability in the Atlantic

The extratropical cyclone's spatial variability in the North Atlantic Ocean is strongly related to the NAO *(Pinto et al. 2009)*.

Figure 2.1 shows the relative cyclone track densities occurring in winter from the NCEP-NCAR reanalysis. The upper map shows the cyclones that happened during a strongly positive (NAO++) daily index (i.e. stronger pressure difference between Iceland and the Azores and enhanced large-scale westerly flow). The lower map shows those cyclones happening during NAO- - index.

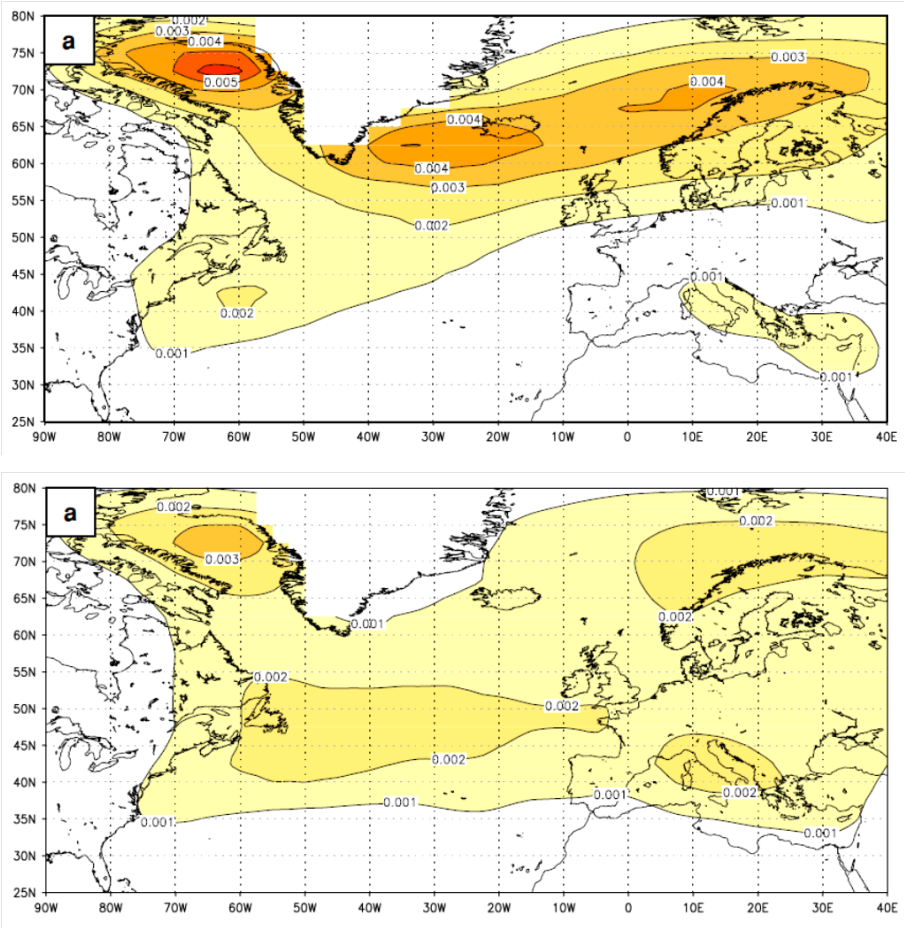

Figure 2.1: winter relative cyclone track density maps for:

NAO++ (upper map)

NAO- - (lower map)

Non-extreme cyclones.

(Pinto et al. 2009)

From figure 2.1 it can be deduced that during a NAO++ phase extratropical cyclones tend to be placed in the northernmost part of the North Atlantic and Europe, whereas during a NAO- - phase the occurrence of extratropical cyclones is much more homogeneous over those areas.

Figure 2.2 shows the same as fig. 2.1 (winter NAO++ / NAO- - relative cyclone track densities) but for extreme cyclones (in terms of relative vorticity).

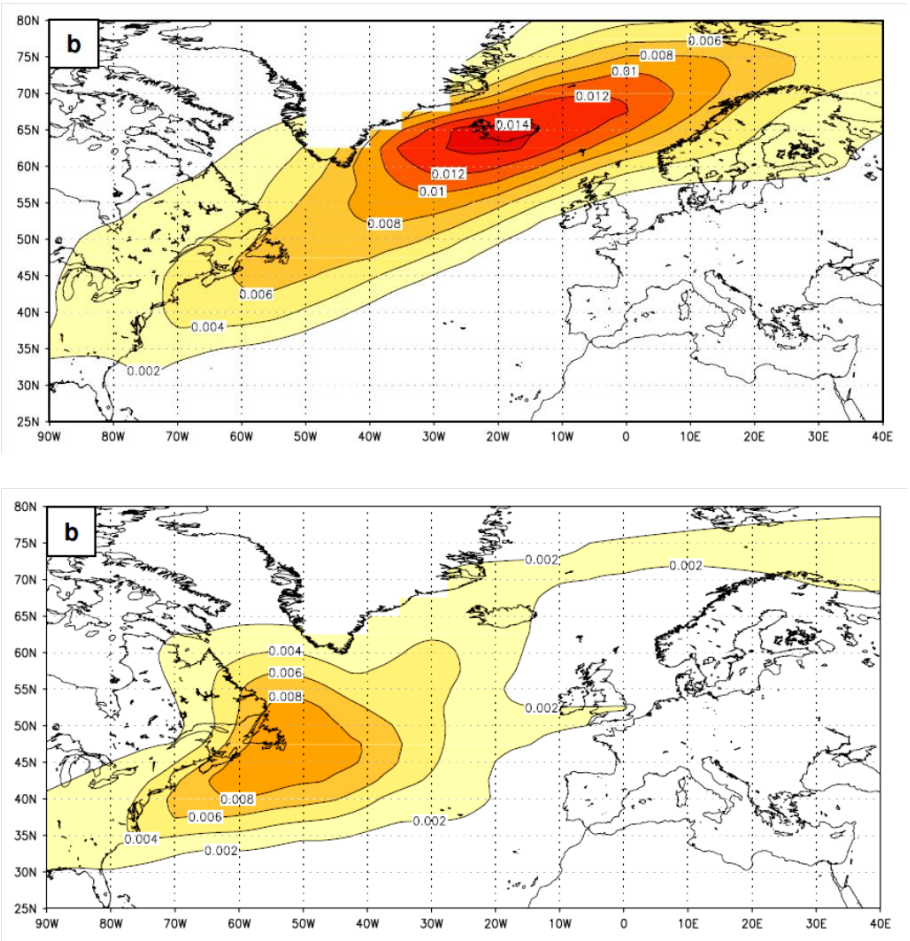

Figure 2.2: winter relative cyclone track density maps for:

NAO++ (upper map)

NAO- - (lower map)

Only extreme cyclones.

(Pinto et al. 2009)

Fig. 2.2 shows that extreme extratropical cyclones occur mostly over the northernmost portion of the Atlantic, and that their spatial distribution is also determined by the NAO phase. The area near Newfoundland has always a high density. During the NAO- - phase, extreme extratropical cyclones happen over the NW Atlantic, and during NAO++ phase this area of high density elongates towards Iceland and the Barents Sea. Also, extreme cyclones happen more often during NAO++ phase.

The cause for this behaviour of extreme cyclones is that during NAO++ phase all the large-scale atmospheric parameters disclosed in section 2.2 (baroclinicicy, jet strength, upper air divergence and equivalent potential temperature) reach extreme values over a wider area, and are better aligned together, giving a stronger forcing for cyclone growth over a longer portion of the cyclone's track, which allows the cyclone to develop faster over a longer period of time.

In the study by *Pinto et al. (2009),* the same track density relationship with the NAO is found in the simulated cyclones from the T63 resolution of the ECHAM5 model.

2.4: Variability in the Pacific

The extratropical cyclone's spatial variability in the North Pacific Ocean is strongly related to the Aleutian Low strength *(Zhu et al. 2007)*.

Figure 2.3 shows the extratropical cyclone tracks of three years with a strong Aleutian Low (left) and three years with a weak Aleutial Low (right).

It can be observed that during winters with strong Aleutian Low, extratropical cyclone tracks tend to be grouped together in a SW to NE direction (from near Japan to the Gulf of Alaska), while in winters with weak Aleutian Low, the cyclone tracks are more dispersed throughout the North Pacific, without preference for any particular area.

No difference in cyclone intensity between the two sets of winters (with strong and weak Aleutian Low) was found. In the case of extreme cyclones, their behaviour is related to other factors.

Yoshiike and Kawamura (2009) show the influence of the winter monsoon: with an enhanced winter monsoon, the low-level baroclinicity increases and concentrates closer to the Kuroshio Current near Japan, leading to more extreme cyclones in that area. Weaker winter monsoon leads to less unstable conditions in a wider area.

Yoshida and Asuma (2004) relate the placement of explosively developing extratropical cyclones to the intensity and extension of the cold air mass that develops over the East Asian continent during winter.

Nakamura and Sampe (2002) describe how a stronger Subtropical Jet over the Pacific tends to trap upper-level synoptic scale eddies into its core, not letting them propagate into the baroclinic area 10º to the N of the jet (near the Kuroshio Current). Then, vertical coupling

with low-level disturbances in the baroclinic area is not possible, suppressing extratropical cyclone growth even if the baroclinicity near the Kuroshio Current is higher.

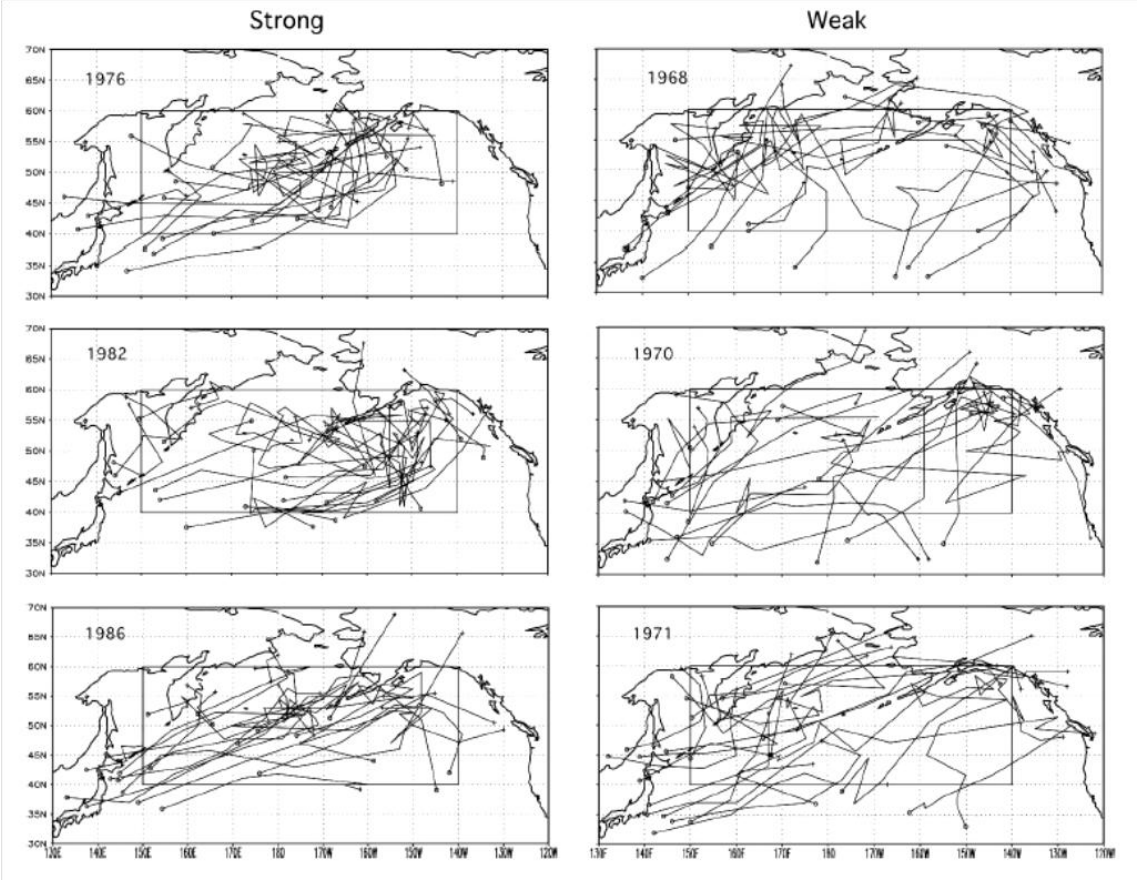

Figure 2.3: winter cyclone tracks for years with strong Aleutian Low (left) and weak Aleutian Low (right) *(Zhu et al., 2007)*

3: DATA

The data used for this study will be cyclone tracks obtained from simulations of the Atmospheric Global Climate model ECHAM 5 (*Roeckner et al., 2003*, description in section 3.1) at T31-42-63-106-159 resolutions, which will be compared between them and the cyclones from the ERA-Interim Reanalysis (*Dee et al., 2011*; description in section 3.2), that can be assumed as the representation of reality in the data. The time period investigated is 1982-2009.

In the data packages used in this study, the cyclone tracks are already prepared by the data source. The cyclone detection and tracking to obtain the cyclone tracks was carried out on the sea level pressure (SLP) fields at 6h time frequency from each of the 6 data sets (ECHAM5 runs T31-42-63-106-159 and the ERA-Interim reanalysis).

The SLP fields were interpolated onto a 0'5ºx0'5º grid in polar stereographic projection, making a 181x181 map (as in *Grigoriev et al. (2000), Zolina and Gulev (2002)* or *Rudeva and Gulev (2007 and 2011)*).

The cyclone detection and tracking was done with the software developed by *Grigoriev et al. (2000),* defining the cyclone centres as pressure minima across 13 neighbouring points, and tracking them with the "next-neighbour search". Cyclones shorter than 24h are discarded.

The format of the data packages is detailed in Appendix I.1, and a description of the problems associated with it can be found in Appendix I.2 (see also Appendix I.4 for the solution found for these problems).

In order to compute the original data with the software used in this study (mathematical software "R"), they are pre-processed to change their file extension (see Appendix I.3). The algorithm converts all six data packages (ECHAM5 resolutions T31/42/63/106/159 and the ERA-Interim Reanalysis) into six arrays of dimensions:
(28 x 4000 x 180 x 6), corresponding to [year, cyclone, step, information].
The information in the last dimension consists of 6 variables being: 1(longitude ºE), 2(latitude ºN), 3(time step), 4(pressure hPa), 5(intensification rate hPa/6h) and 6(distance km).

This array set will be referred as "DATA" from now on, in order to not repeat "array with cyclone track information of model output...", and to avoid redundancies, since other arrays are created later on for other purposes.

3.1: The ECHAM5 model

ECHAM5 *(Roeckner et al., 2003)* is the fifth generation atmospheric general circulation model developed at the Max Planck Institute of Meteorology (MPIM), and is currently the second most recent version (being ECHAM6 the newest). The ECHAM series of models have been evolved by the MPIM from the spectral weather prediction model used at the European Centre for Medium range Weather Forecasts (ECMWF, *Simmons et al., 1989*).

The ECHAM5 model uses a leapfrog semi-implicit time-differencing scheme for its computation. In its spectral dynamical core, a truncated series of spherical harmonics represents vorticity, divergence, temperature, and the logarithm of surface pressure in the horizontal coordinates. For the vertical coordinate, a hybrid sigma-pressure system is used.

A weak time filter is used to avoid the development of spurious computational modes.

Several changes were made in the physics and numerics of the model compared to its previous version ECHAM4. The newer components are: a semi-Lagrangian scheme for passive tracer transport (for example water in vapour, liquid or solid state), a longwave radiation scheme, increased number of spectral intervals for longwave and shortwave radiation, and improved cloud parameterization (microphysical scheme, prognostic statistics, equations for separated cloud ice and liquid water).

The representation of land-surface processes has also been improved, such as the implicit surface-atmosphere coupling, and the orographic drag forces.

The components that didn't undergo changes from the earlier version of the model are the horizontal and vertical diffusion, cumulus convection and the spectral dynamics.

The model has two configurations:

-Standard configuration: with 19 or 31 vertical levels in the atmosphere, and the top at 10hPa altitude (around 30Km). This will be the one used in this study.

-Middle atmosphere configuration: with 39 or 90 vertical levels in the atmosphere, and the top at 0.01hPa altitude (around 80Km).

Its spatial setting is done with triangular truncation, at wavenumbers 21, 31, 42, 63, 85, 106 and 159. The corresponding resolution of the grid boxes, as well as the computational time leap for the standard configuration is shown in fig. 3.1

Resolution	Grid (deg)	Δt (min)
T21 L19	5.62	40
T31 L19	3.75	40
T42 L19	2.81	30
T63 L19	1.87	20
T85 L19	1.41	15
T106 L19	1.12	12
T42 L31	2.81	20
T63 L31	1.87	12
T85 L31	1.41	8
T106 L31	1.12	6
T159 L31	0.75	4

Figure 3.1: Model resolutions at standard configuration (from left to right):
-T for horizontal wavenumber
-L for vertical levels
-Grid box resolution in º
-Temporal resolution in minutes

Roeckner et al. (2004)

Being an atmospheric general circulation model, the only free component of ECHAM5 is the atmosphere. Every model experiment is forced by the following components:

-In the standard model configuration no chemistry is included: the ozone concentration is prescribed as function of month, latitude and height *(Fortuin and Kelder, 1998).*

-Sea surface temperatures are also prescribed with data from "NOAA Optimum Interpolation (OI) Sea Surface Temperature (SST) V2" *(Reynolds, 2007),* with 0'25º grid resolution and daily coverage.

-Sea ice coverage is prescribed with observations at high resolution of 12.7km from the National Oceanic and Atmospheric Administration (NOAA) *(Grumbine, 1996).*

The different resolutions used in this study will be: T31 and T42 with 19 vertical levels, and T63, T106 and T159 with 31 vertical levels, all corresponding to the standard configuration of the model with the exact same forcings, but differing only in horizontal and vertical resolution.

3.2: The ERA-Interim reanalysis

The ERA-Interim reanalysis *(Dee et al., 2011)* is the latest global atmospheric reanalysis produced by the European Centre for Medium range Weather Forecasts (ECMWF).

Covering the time period from 1979 to present, it was conceived to carry on with the work completed by predecessor ERA-40 reanalysis, and also to prepare for a more ambitious reanalysis project at ECMWF in the future that will span all 20th century. Compared to ERA-40, ERA-Interim has improved the representation of the hydrological cycle and stratospheric circulation, and the quality of data assimilation, control and bias correction.

The ERA-Interim reanalysis is continuously updated with a sequential data assimilation using 12h analysis cycles, in which the observations (of the different variables fields like temperature, wind, humidity, surface pressure...) that are absorbed into the reanalysis are compared with short-range forecast model estimates (of those same variables) to compute the difference (bias) in space and time as a 4D operator (note that observations and forecasts are done with much higher time frequency than the analysis cycle). This operator is then used to minimize or correct future bias in the forecast.

The final achievement of the reanalysis is to extrapolate the observations into a gridded database in a consistent way. This gridded format then can be used for scientific investigation or further modelling.

All of the above is done with a spectral T255 horizontal resolution, approximately 79km (compared to T159 in ERA-40), 60 vertical layers with top of the atmosphere at 0.1hPa (around 65km altitude) and a time step of 30min.

4: METHODS

In this section various methods to automatically detect and track cyclones are explained. The different software settings influence how the cyclone properties are perceived.

4.1: Cyclone detection

For tracking intentions, extratropical cyclones are defined by their centre location at different times. This step done before the tracking is called cyclone detection, and there are two main techniques to carry it out:

-Looking for minima in pressure or geopotential height fields (for example: *Wernli and Schwierz, 2006*).

-Looking at vorticity fields (laplacian of the pressure field) for vorticity maxima (for example: *Simmonds et al. 2008*).

In both techniques the minima/maxima are defined compared to their neighbouring grid points. A different number of points are taken depending on the truncation (distribution of the grid boxes / parcels in the simulated Earth) and resolutions of the models used. All this can be done with surface, 1000hPa or 850hPa altitude fields.

Raible et al. (2008) and *Neu et al. (2013)* show that the choosing of different cyclone detection and tracking techniques might alter some aspects of the cyclone that is tracked. For example: the vorticity maximum centre appears earlier than the pressure minimum centre in many cases, and thus the cyclone detected by vorticity maxima will have a longer lifetime. Cyclone detection with vorticity maxima also performs better for smaller spatial scales, compared to detection with pressure minima *(Hoskins and Hodges, 2002).*

Also, recent studies are starting to add the condition of a closed pressure contour around the pressure minima to detect a cyclone (as in *Wernli and Schwierz, 2006*), and remarkable is the study by *Hanley and Caballero (2012)* that use contour mapping to deal with multicentre cyclones and merging-splitting events in an objective way, by taking many centres surrounded by the same contour line as one single cyclone. This helps making the cyclone statistics and track densities (number of cyclones that pass over one designated area) much more realistic, since it avoids double-counting of a cyclone that has several centres.

4.2: Cyclone tracking

After the cyclone detection algorithm has defined the position of cyclone centres at different times, the connection of the centres into a track is done by the tracking scheme / algorithm. One track consists of the positions of a cyclone during its lifetime linked together.

A detailed description and comparison of tracking techniques can be found in the publications by *Raible et al. (2008)* and *Neu et al. (2013).*

Polar projections are used preferably at this stage, because they conserve better the area at mid and high latitudes when mapping the pressure / geopotential height / vorticity fields.

Since the tracking scheme works with a timeline of maps with cyclone centres, it will go step by step in time from the beginning. For the first step, the algorithm searches around the cyclone centres within a predefined distance D (usually 1000km). Then it picks the closest centre in the next step (next-neighbour search) if it lays inside that radius of search in the previous step. When the track has more than one point, the trajectory of the cyclone can be calculated.

Some tracking schemes don't take the trajectory of the cyclone into account and keep searching in the same way in the subsequent steps, but this may bring trouble when tracking fast-moving cyclones, or when two cyclones are close to each other and their paths converge, giving the possibility to continue tracking the wrong cyclone afterwards.

Therefore, other schemes do not search around the last position of the cyclone track, but make a "first-guess" projection onto the next time step and search around that position (here distance D can be reduced since this technique is more accurate).

The "first-guess" projection can be done computing the distance and direction travelled by the cyclone between the last two steps and adding it to the last position, as if the cyclone didn't suffer acceleration of any type. In the studies by *Wernli and Schwierz (2006)* and *Hanley and Caballero (2012)* the full distance is not used, but just 75% of it, stating that it accounts for cyclone deceleration during its lifetime.

Once no cyclone centre meets these criteria, the cyclone's lifetime is presumed to have ended, and the track to be finished.

Before saving the cyclone track in a database, further limitations can be applied depending on the goals of the study. These can be: terrain filtering (not taking into account cyclone centres over land of certain altitude, like over 1500m), eliminating short cyclones (of lifetime <24h, for example) or those that do not travel a minimum distance.

5: RESULTS

A quick overlook at this point: apart from sections 5.1.1 and 5.1.2 where the seasonal cycles are obtained (meaning all seasons are taken into account), all climatologies are done for winters 1982/83 to 2008/09 (a total of 27 winters, taking December-January-February). The exception is resolution T63 of model output ECHAM5 where the winter 2003/04 is discarded, so its climatology consists of 26 winters (see Appendix I.2).

For every DATA array (the 6 datasets from T31/42/63/106/159 ECHAM5 model and the one from ERA-Interim), the properties of cyclones happening over the Atlantic and Pacific oceans are obtained from section 5.1.1 to 5.1.6 for their comparison. Sections 5.1.7 and 5.1.8 are to obtain Northern Hemisphere cyclone track / deepening / generation density maps, respectively.

The areas designated as Atlantic and Pacific oceans are shown in figure 5.1. Pacific is the area within 30-70ºN and 120-240ºE and the Atlantic consists of two boxes: 30-80ºN, 280-340ºE plus 45-80ºN, 20ºW-20ºE.

This is to avoid the thermal lows that appear over the Iberian Peninsula in summer, since only oceanic cyclones are wanted. If one looks at Appendix II, figure II.1, the lifetime and track length limitation criteria don't avoid cyclone generation maxima over land in summer.

The cyclone tracks that are taken into account will be those that are over one ocean for more than 24h (5 time steps or more), and that travel more than 1000km within the area designated for that ocean.

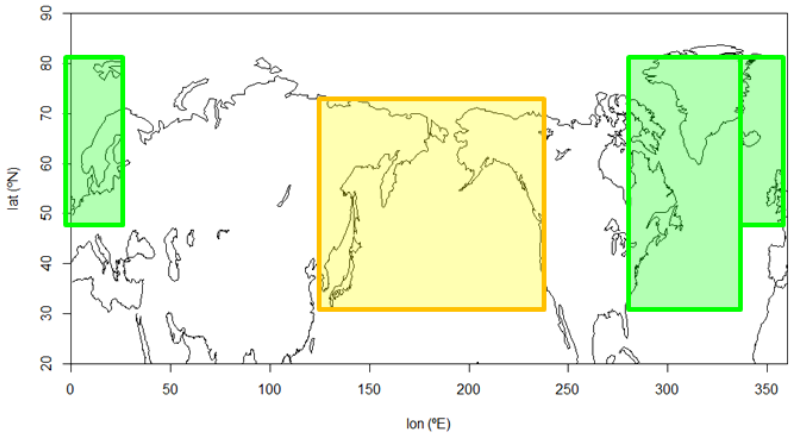

Figure 5.1: Areas to define the oceans:
-Atlantic: green boxes
-Pacific: orange box

5.1: Climatologies (1982-2009 time period)

5.1.1: Seasonal cycle of minimum pressure

Procedure:

Here the minimum pressure existing over the Atlantic and Pacific oceans throughout the year is to be compared. 29th of February in leap years is discarded, so the climatology goes from day 1 to 365. For each of the 6 DATA arrays available, the algorithm first creates a timeline of 28 years with 1460 time-steps each (365 days) for every ocean, and starts reading the information of all cyclones.

When does a cyclone meet the criteria to be considered in one ocean? (24h and 1000km over that ocean). From here on, the variables used by the algorithm refer to the setting of the DATA array in section 3.

This cyclone selection is done by the algorithm by looking at variables 1 and 2 (lon, lat) from the last dimension of the DATA array at each step of the cyclone and confirming if they lay in the designated areas for every ocean (fig. 5.1). Then computes the sum of variable 6 (distance) of those steps that are over the ocean to confirm if it is more than 1000km.

If the cyclone fulfils all of the above, its centre pressure (variable 4 in the array) is saved in that ocean's timeline in the corresponding year (first dimension in the array) and the corresponding time-steps that it was over the ocean (variable 3: time coordinate).

In the end, each step of the timeline has a list of centre pressures occurring at that step, over that ocean. This timeline will be used to compute the minimum pressures as well as the simultaneous number of cyclones over the oceans.

For the minimum pressure seasonal cycle, at each step of the timeline, the algorithm saves the lowest one, and then makes the mean of the 28 years for that time-step, being this the climatology of the minimum pressure throughout the year.

To finish, the algorithm makes a 7-day smoothing to remove noise, by making a mean of each time-step and the corresponding to -3.5 to +3.5 days (14 time-steps before and after: a mean of a total of 29 points), and represents all 6 DATA seasonal cycle in the same graphic for days 4 to 361 of the year, for every ocean.

Results

The seasonal cycle of minimum pressure at the Atlantic and the Pacific is shown in figure 5.2:

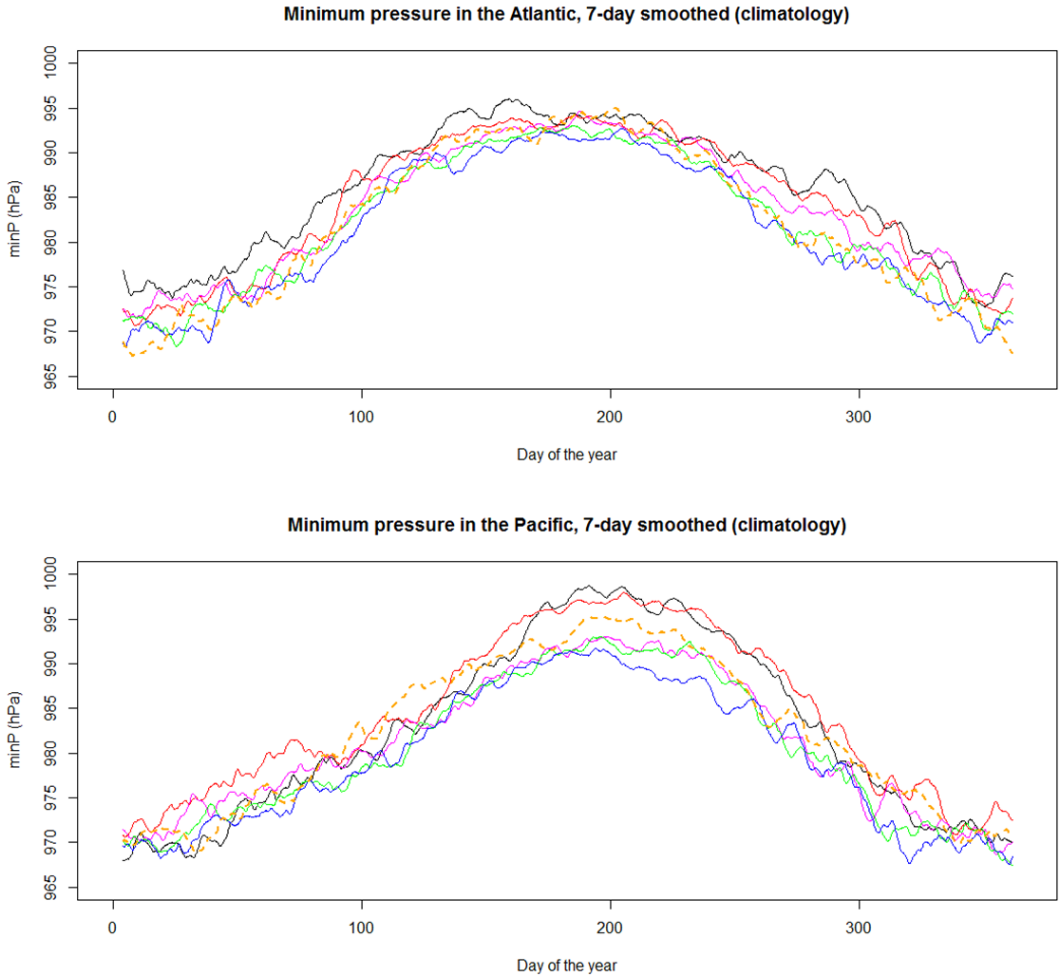

Figure 5.2: Climatology of the seasonal cycle of minimum pressure at the Atlantic (top) and Pacific (bottom).
Line colors correspond to:

- T31
- T42
- T63
- T106
- T159
- ERA- Interim

One can see that the two lower resolutions (T31 and T42, black and red lines respectively) tend to show higher min P than ERA-Interim (reality, orange dotted line), and that the highest resolution (T159, blue line) tends to do the opposite: it shows lower min P than reality.

Apart from this fact, all models agree in the timing of the seasonal cycle climatology: the time of the year when the lowest (~970hPa) and the highest (~995hPa) min P is reached at each ocean are almost the same for all the DATA sets.

The time when the min P is highest at the Atlantic appears to be earlier in the year compared to the Pacific. This can be explained with the East-Siberian High and Canadian High development and dissipation.

Both anticyclones form and are strongest in winter, and advect cold and dry continental air over the oceans, where it meets the relatively warm and wet air near the Gulf current in the Atlantic and the Kuroshio current in the Pacific. This situation increases baroclinicity and enhances cyclone growth and deepening: lowering the minimum pressure during winter time.

The East-Siberian High is much stronger than the Canadian High, and also lasts longer before dissipating, then advecting more cold air and increasing baroclinicity over the North West Pacific. In the cyclone generation maps from Appendix II it can be seen that, for cyclones with min P < 990hPa (figure II.2), the area near Japan remains active from the end of winter until May, whereas near the US east coast cyclone generation activity has totally decayed by then. Also, in the Atlantic there has been relatively lower activity in March and April at both T31 and T159 resolutions and ERA-Interim reanalysis than in the Pacific.

This supports the idea that the longer and stronger living of the East-Siberian High enhances cyclone activity in the North-West Pacific during spring, compared to the NW Atlantic, thus making the minimum pressure over the Pacific reach its highest value more-less two months after the same happens in the Atlantic.

5.1.2: Seasonal cycle of cyclone number

Procedure:

From the same timeline with stored cyclone centre pressures from the previous section, the algorithm computes the number of pressures recorded at each time-step (instead of saving the lowest as before) and makes the mean of the 28 years for that time-step: this is the climatology of the simultaneous number of cyclones over each ocean throughout the year. The same 7-day smoothing is applied as in 5.1.1 and a graphic for every ocean comparing the 6 DATA seasonal cycle is created.

Results:

The seasonal cycle of the number of simultaneous cyclones at the Atlantic and the Pacific is shown in figure 5.3. For the case of ECHAM5 resolutions, the higher the resolution is, the more cyclones it produces. Each resolution has higher cyclone numbers than the immediately lower resolution, and the highest (T159, blue) doubles the number of cyclones of the lowest (T31, black): 5-7 against less than 3 over both oceans.

The T31-42-63 resolutions show a more-less constant number of cyclones throughout the year. T106 (green line) is closest to ERA-Interim cyclone number (orange dotted line) apart from the Atlantic during summer.

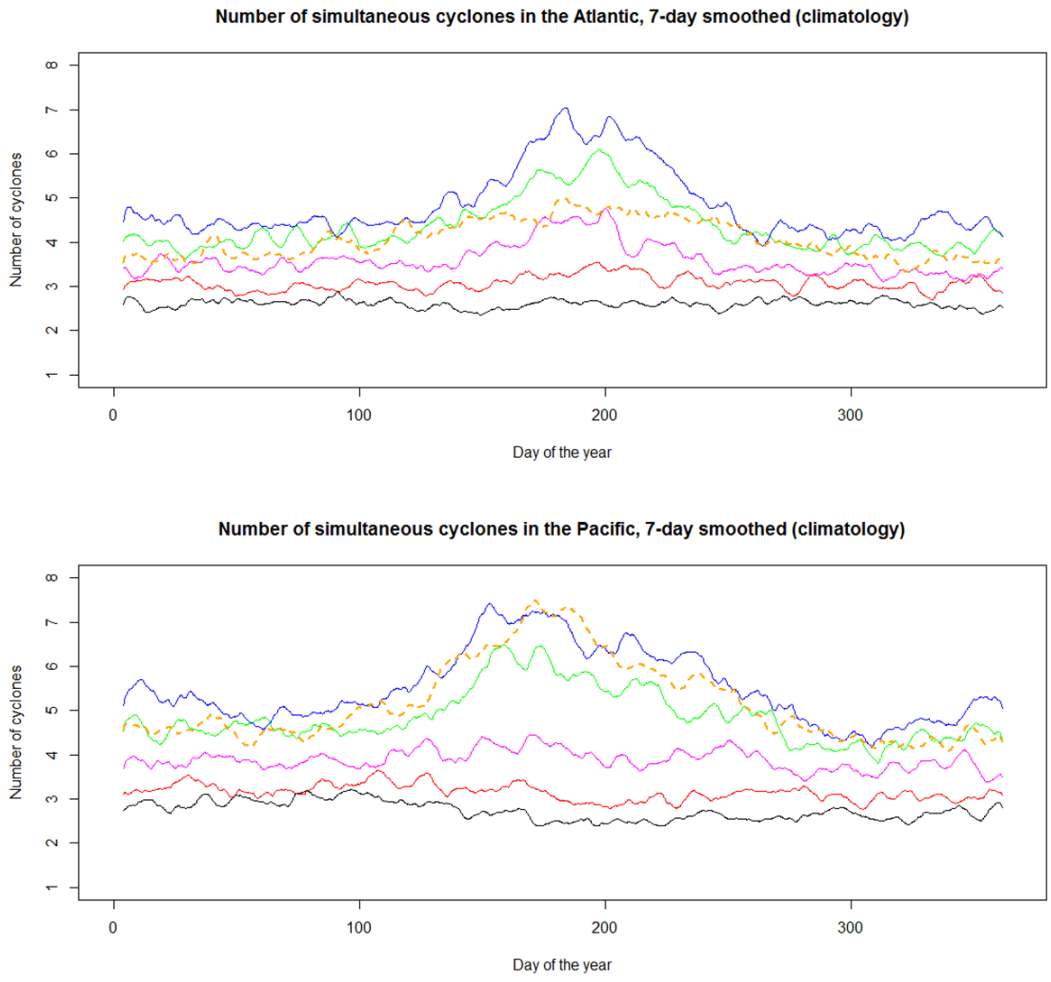

Figure 5.3: Climatology of the seasonal cycle of simultaneous number of cyclones at the Atlantic (top) and Pacific (bottom). Line colors correspond to:

- T31
- T42
- T63
- T106
- T159
- ERA- Interim

T159 (blue line) exaggerates the number of cyclones in both oceans. T159 (blue) and T106 (green) have a peak during summer in both oceans, a feature that the ERA-Interim only follows in the Pacific. The reason for this behaviour will be explained in section 5.2.3.

It has to be pointed out that for fig. 5.3 only oceanic cyclones with >24h and >1000km are taken into account, which excludes thermal lows.

The higher number of cyclones at higher resolutions could be because the increased resolution can capture more pressure minima that would be smoothed out at lower resolutions. Cyclones with multiple centres would be able to appear then, but why this would happen too much in the Atlantic during summer at T106 and T159 cannot be answered with this graphic.

The track reconstruction (detailed in Appendix I.4) has helped the cyclone number not to fall dramatically at the beginning and end of the year. In the cases that a number drop exists, it is not sharper than any other fluctuation throughout the year.

The algorithm recognizes more cyclones that fulfil the selection criteria (now that the missing part of their lifetime has been added) than without any track reconstruction, where the cyclone number fell suddenly down to less than half at the beginning and end of the year (not shown). This means that the information that could be recovered by the track reconstruction was the majority of which was cut during the production of the original data packages.

5.1.3: Cyclone minimum pressure distribution

Procedure:

For cyclones that are longer than 24h and 1000km over one ocean during winter time, the algorithm computes each cyclone's minimum pressure (the lowest pressure during its lifetime) and makes 6 lists (from every DATA array) of minimum pressures for every ocean (taking all winters).

Then takes each list as a distribution and computes a histogram of it with the relative frequencies of the minimum pressure intervals in logarithmic scale (relative frequencies are better than absolute frequencies since the number of cyclones detected on each ECHAM5 resolution and ERA-Interim reanalysis varies greatly; and logarithmic scale lets a reasonable

scale for the frequencies since the frequency of the pressures at the extremes are of several orders of magnitude lower than the rest).

For every ocean, a graphic comparing the 6 distributions is created. Lines are used instead of bars for better visibility.

Results:

The winter cyclone minimum pressure distributions at the Atlantic and the Pacific are shown in figure 5.4. The Atlantic holds more relative frequency of the lowest minimum pressures, supporting the observational fact that the deepest, record-breaking cyclones in therms of minimum pressure, occurred over the Atlantic.

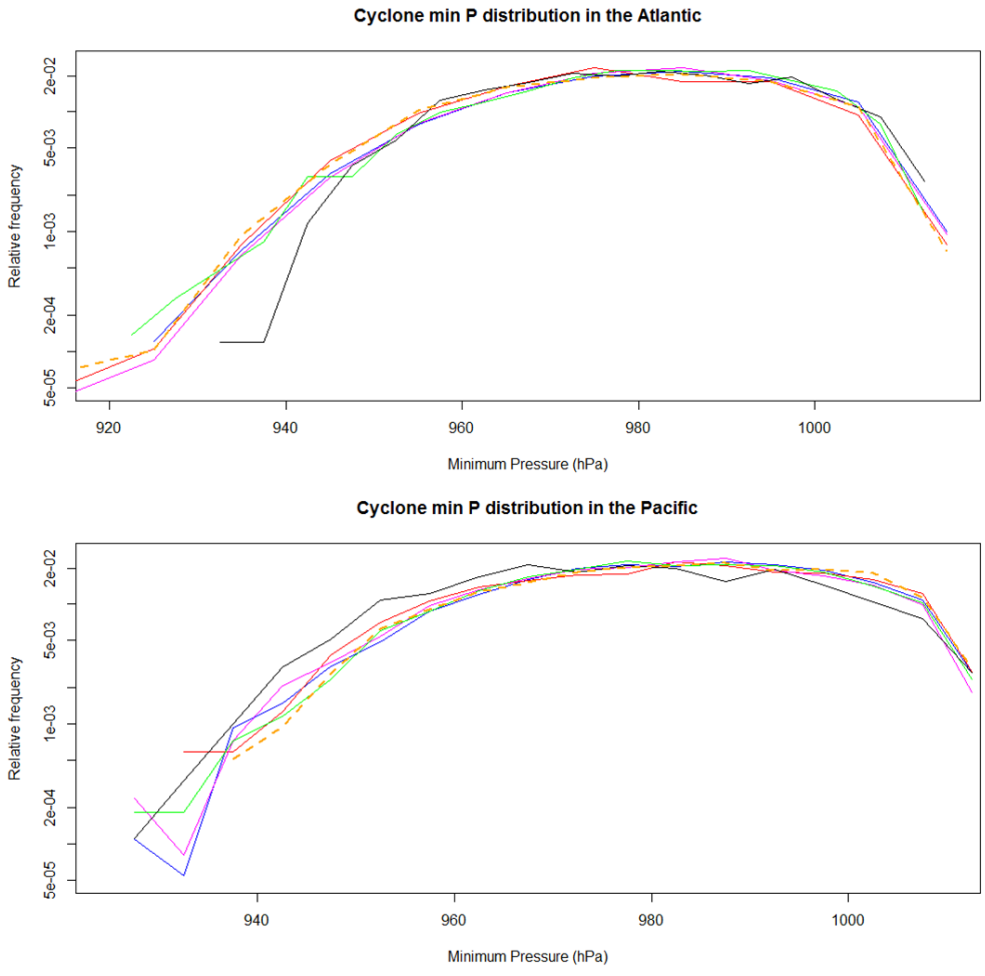

Figure 5.4: Climatological distribution of winter cyclone minimum pressures at the Atlantic (top) and Pacific (bottom). Line colors correspond to:

- T31
- T42
- T63
- T106
- T159
- ERA- Interim

In the Pacific, the ECHAM5 resolutions overestimate the occurrence of extreme low min P: the ERA-Interim (orange, dotted line) shows the lowest relative frequency at the lowest min P, and ends at roughly 940hPa, whereas the rest of lines continue into lower min P.

In the Atlantic the opposite happens: the occurrence of extreme min P at the lower side is underestimated by the ECHAM5 runs.

The middle parts of the distributions agree quite well, and the higher tail of the Atlantic distributions shows a higher relative frequency than in reality of the higher min P at the ECHAM5 resolutions. In the Pacific, the relative frequency of this higher min P is in contrast underestimated by the ECHAM5 model runs.

All this indicates that the ECHAM5 distributions are biased towards higher min P in the Atlantic, and towards lower min P in the Pacific.

In all cases, the T31 (black) distribution is the one that is furthest from the real (ERA-Interim) distribution, and there is a tendency for the rest of the lines to come closer to the real distribution as their corresponding resolution increases.

5.1.4: Cyclone lifetime distribution

Procedure:

The procedure is similar to that from 5.1.3. For the same cyclones detected, instead of computing the minimum pressure from each cyclone's pressure information, the algorithm counts the number of time-steps that the cyclone has lasted, and saves that number into a list (again, 6 lists, for every ocean)

(steps -1)/4 will be the lifetime in days of the cyclone (each step interval is 6h, first step has lifetime 0).

The same graphic procedure is done as in 5.1.3 but for the lifetime distributions (relative frequencies of the lifetime intervals, at log scale).

Results:

The winter cyclone lifetime distributions at the Atlantic and the Pacific are shown in fig. 5.5.

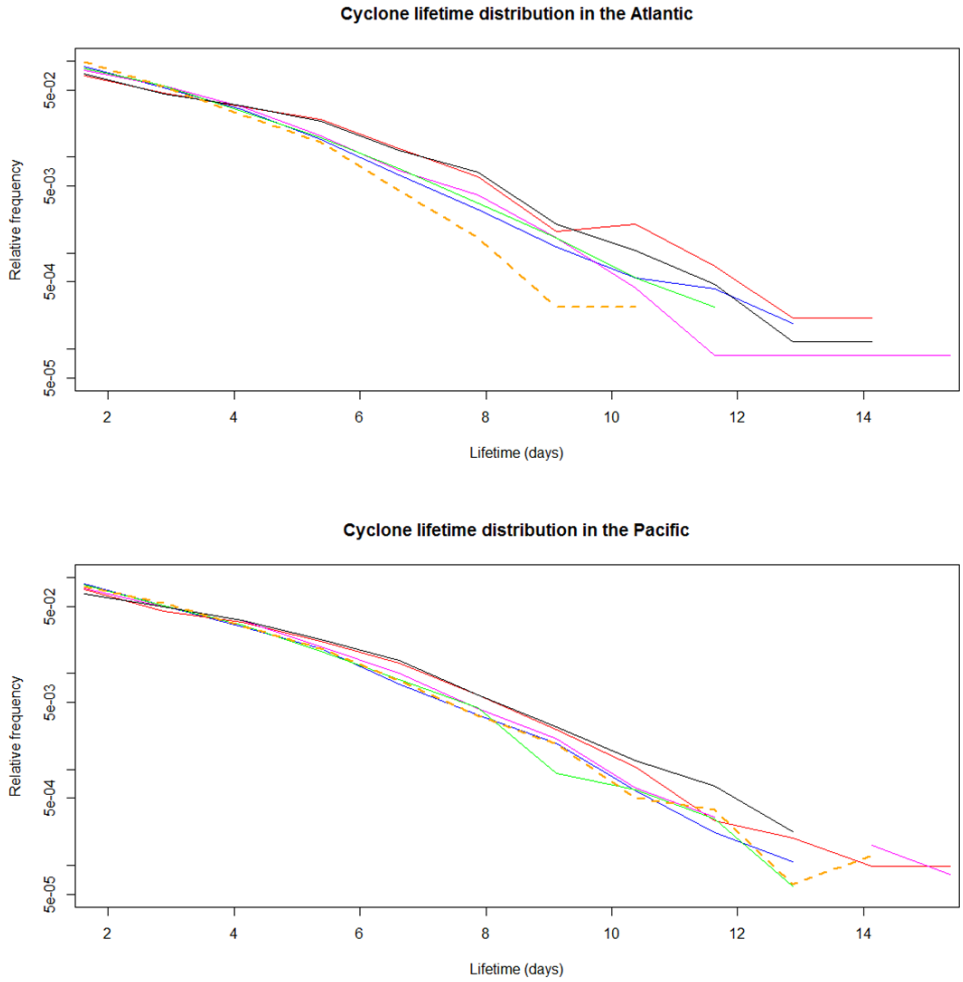

Figure 5.5: Climatological distribution of winter cyclone lifetime at the Atlantic (top) and Pacific (bottom).
Line colors correspond to:

- T31
- T42
- T63
- T106
- T159
- ERA- Interim

There is much more agreement between the lifetime distributions in the Pacific. T63-106-159 resolutions of the ECHAM5 model follow the real distribution (ERA-Interim) with very little difference. The two lowest resolutions T31-42 are more separated, overestimating the relative frequency of the longer-living cyclones.

In the Atlantic, all ECHAM5 resolutions overestimate the relative frequency of the longer-living cyclones. The distributions come closer to the real one with increasing resolution, but still all of them are quite separated from it.

This shows that the fact that the cyclones have a shorter lifetime over the Atlantic compared to the Pacific (orange, dotted line decaying at lower lifetime in fig. 5.5, meaning that cyclones develop faster in the Atlantic), is not well captured by any of the ECHAM5 runs.

A possible explanation for this is that the temperature gradient of the sea surface temperatures and the air masses in the Atlantic required for fast cyclone development happens at a smaller spatial scale and is partly smoothed out at lower resolutions. This would mean that the cyclones over the Atlantic will have a slower development in the model runs than in reality because of the lack of enough forcing for strengthening from the smoothed temperature gradients.

5.1.5: Track length distribution

Procedure:

For the same cyclones as in 5.1.3 and 5.1.4, this time the algorithm computes the sum of the distance travelled by each cyclone between its successive locations at each step, over each ocean (this is: the integrated length of all the lines linking the track points (variable 6 in the DATA array), for those points laying over the designated area of the oceans in fig. 5.1).

Then it saves that distance in a list (again, 6 lists, for every ocean).

The same graphic procedure is done as in 5.1.3 and 5.1.4 but for the track length distributions (relative frequencies of the track length intervals, at log scale).

Results:

The winter cyclone's track length distributions at the Atlantic and the Pacific are shown in fig. 5.6. As in section 5.1.4, there is better agreement between all distributions in the Pacific.

In the Atlantic, all ECHAM5 resolutions underestimate de relative frequency of the cyclones with longest tracks. This time, only the lowest resolutions T31-42 are very separated from the real distribution, being the rest (T63-106-159) quite close to the ERA-Interim distribution, except for T106 at the very longest track lengths.

Note that longer tracks are achieved in the Pacific, an expectable feature from the different size of the Atlantic and Pacific oceans.

For the shortest track lengths, in both oceans the (real) ERA-Interim distribution shows higher relative frequency of the shortest-travelling cyclones. Again, the ECHAM5 distributions differ more from the real distribution with decreasing resolutions.

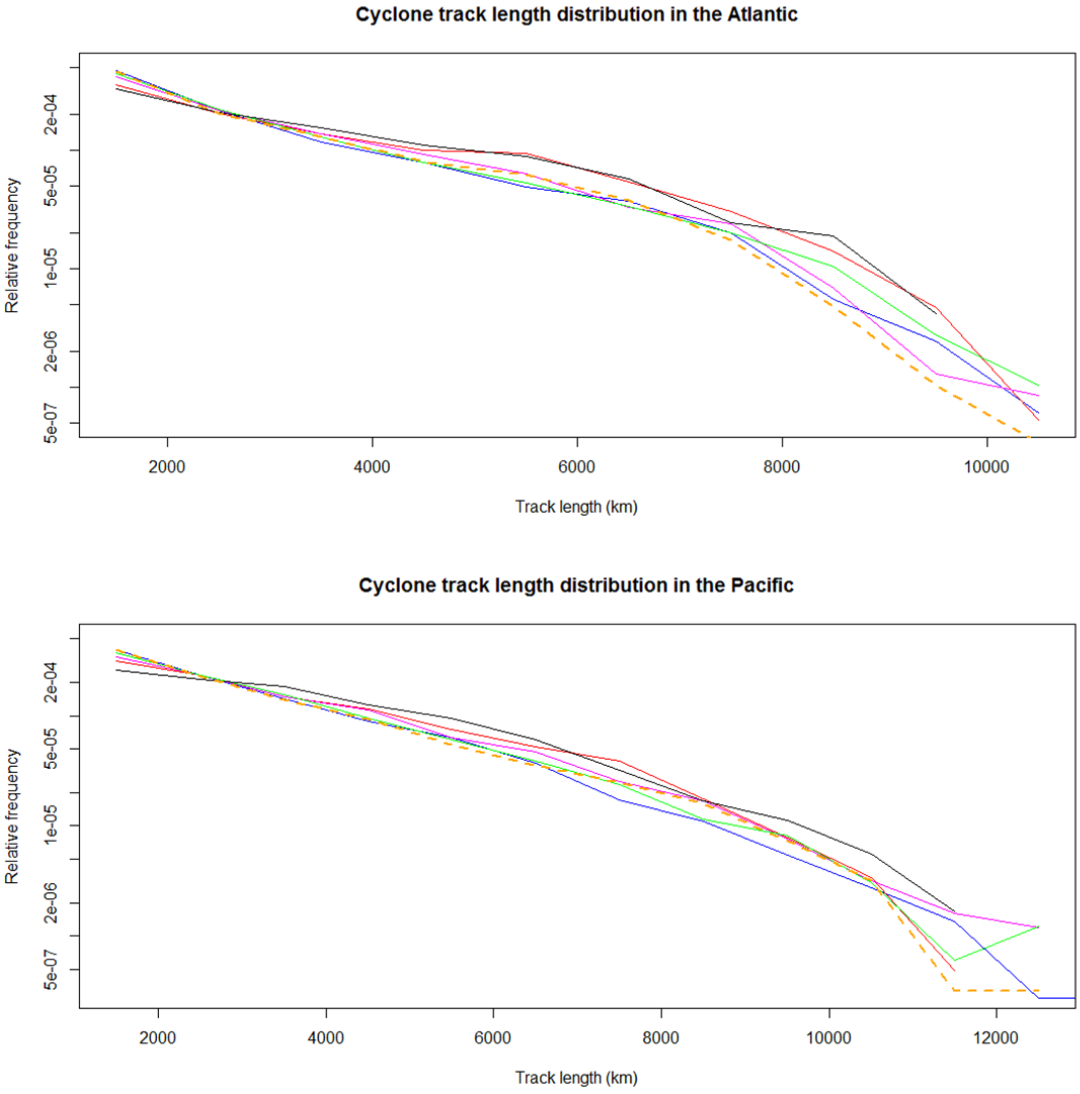

Figure 5.6: Climatological distribution of winter cyclone track length at the Atlantic (top) and Pacific (bottom).
Line colors correspond to:

- T31
- T42
- T63
- T106
- T159
- ERA- Interim

5.1.6: Intensification rate distribution

Procedure:

Again, the same cyclones as in 5.1.3, 5.1.4 and 5.1.5 are computed. The algorithm takes the intensification rate (variable 5 in the DATA array) of all the steps of the cyclone track that happen over ocean, and saves all into a list. This time, multiple values are stored for every

cyclone (all its pressure change history) instead of just one value (minimum pressure, lifetime or track length)

Again there are 6 lists/distributions, and the same graphic procedure is done as in 5.1.3-5.1.4-5.1.5 but for the intensification rates (relative frequencies of the intensification intervals, at log scale).

Results:

Figure 5.7 shows the distribution of the intensification rates during the winter cyclone's lifetimes in the Atlantic and the Pacific oceans.

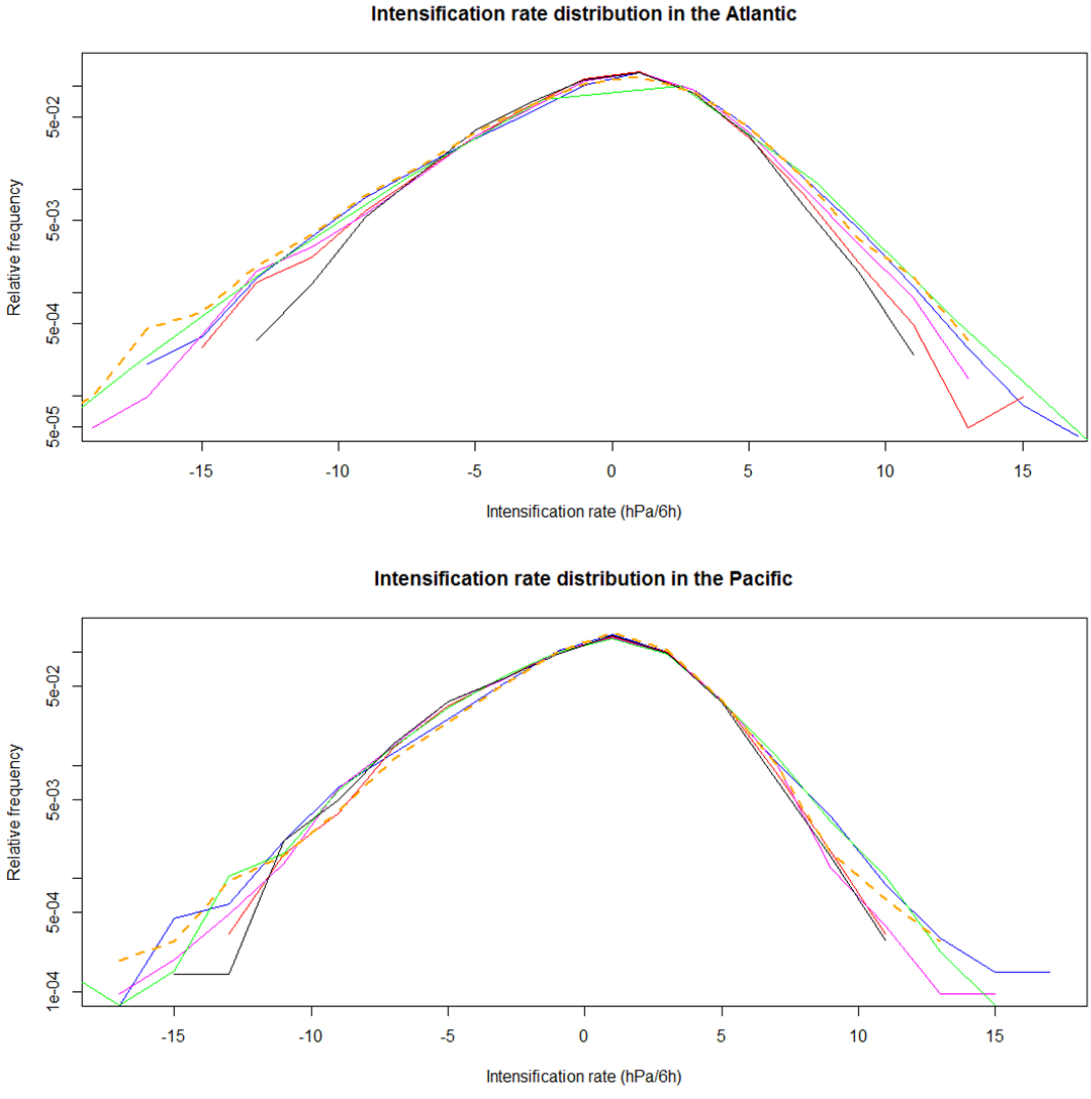

Figure 5.7: Climatological distribution of winter intensification rates (hPa/6h) at the Atlantic (top) and Pacific (bottom).
Line colors correspond to:

- T31
- T42
- T63
- T106
- T159
- ERA- Interim

The distributions in the Atlantic are wider, meaning that they reach more extreme values than in the Pacific, both at negative intensification rate (cyclone deepening / strengthening) and positive intensification rates.

This is in concordance with results in earlier sections: generally, the cyclones need to reach lower min P in the Atlantic than in the Pacific (section 5.1.3) in a shorter lifetime and track (sections 5.1.4 and 5.1.5, respectively).

In both oceans, the T106-159 (green and blue) distributions follow the real distribution (orange, dotted line) very closely. The rest of the ECHAM5 resolutions tend to underestimate the occurrence of extreme intensification rates, especially in the Atlantic.

This could be again the result of the temperature gradient smoothing at lower resolutions which doesn't give enough forcing for the fast development / decay of a cyclone, as explained in section 5.1.4.

5.1.7: Track density maps

Procedure:

-Cyclone selection criteria:

Here all winter cyclone tracks of more than 24h and 1000km are considered without any spatial restrictions by the algorithm, since the goal is to make Northern Hemisphere maps of winter track density.

For every DATA array, three different track density maps will be made: counting all cyclones, the 10% strongest cyclones of each of the six sets, and the 1% strongest cyclones. To define the 10% and 1% strongest cyclones of each DATA array, the winter cyclone minimum pressure distributions from section 5.1.3 are taken into account. Since wind or vorticity fields are not used in this study (only min P along the tracks), this is the best way available to define cyclone strength.

The algorithm computes the 0.1 and 0.01 quantiles of each of the 6 distributions: that will give two limits for every DATA set. The minimum pressure of 10% and 1% (respectively) of the cyclones will be lower than those limits.

The algorithm will obtain three maps from every DATA set. It will compute the lifetime and track length of every cyclone: if the cyclone track is longer than 24h and 1000km, it computes its minimum pressure. Then compares the min P with the limits: "no limit" for the

map with all cyclones, and the 0.1 and 0.01 quantiles of the DATA set (winter min P) distribution.

If the min P of the cyclone lays below one limit, the algorithm will add one count to the corresponding map at all the positions that the cyclone centre has passed over. How the counting is made and the mapping procedure is described next.

-Mapping settings:

The maps of cyclone track density are presented in normal cylindrical projection: as in figure 5.1, the Greenwich Meridian is placed left and the X axis will be the longitude in ºE. Only the Northern Hemisphere is shown from 20ºN polewards, since no extratropical cyclones occur nearer to the equator. Continent's contours are added to all maps.

The maps will have a grid spacing of 2ºx2º (resulting in 180x45 maps, and since they will be represented 20º polewards, 180x35 in the figures). This is a bit bigger than the spacing used for T63 model simulations (1.87º, see fig. 3.1 and section 3). That resolution was chosen because it is intermediate to the resolutions used in the model simulations and reanalysis from the DATA sets (T31/42/63/106/159 for ECHAM5 and T255 in ERA-Interim).

When it comes to the cyclone centre counts, normally it is done by summing up the number of cyclone centres that were over a certain grid. In the study by *Zolina and Gulev (2002)* it is addressed that, depending on the grid spacing, uncertainties appear depending on the interpolation done for the cyclone tracking: for the same tracks, different densities will appear when counting them over a bigger or a smaller grid, and fast-moving cyclones might "jump" several grids each step on their way.

To minimize these uncertainties, the position of the cyclone track is not counted alone, but an area of roughly 1000x1000 km around it, which can be assumed as the area affected by the cyclone centre's meteorological processes.

For computational simplicity, when the cyclone fulfils the criteria to be counted, the algorithm detects which grid box corresponds to the position of the cyclone centre, and adds one count to an area of 5x5 grid boxes centred at the cyclone centre. This being done at all steps, the 5x5 grids area counts usually overlap in the same track, but the algorithm adds just a +1 count for every single cyclone track.

For high latitudes, that 5x5 grids area becomes quite deformed, but making the zonal width of the area for +1 counts dependant on latitude would add a very big computational cost for making the maps. Nevertheless, this study concentrates on the Atlantic and Pacific oceans and mid-latitudes, where this effect is negligible. One could even argue that the difference in

Coriolis force would imply that a smaller gradient of pressure is needed for the same wind at lower latitudes (at geostrophic balance): so a cyclone of same min P and winds would be wider at lower latitudes, making this counting procedure perfectly correct with those simplistic assumptions.

The algorithm adds up the counts for each winter, saves the track densities for every winter (27 winters, except ECHAM5 T63 with 26 winters), and makes the mean at each grid box: obtaining the climatological winter track density maps (cyclones per winter) of the six DATA sets for all winter cyclones, and the 10% and 1% strongest cyclones.

Results

In this section, maps of the climatological winter (DJF) track density of all cyclones, the 10% strongest cyclones and the 1% strongest cyclones in terms of minimum pressure are shown (cyclones of >24h and >1000km). For each of the cyclone groups, maps from the ECHAM5 runs are compared with the ERA-Interim reanalysis (taken as the real track density).

- Figure 5.8 shows the track densities <u>taking all cyclones</u>:

One can see that in the ERA-Interim reanalysis (lower right map) there are three areas with track density maxima (magenta colour): two that cross the Pacific and Atlantic oceans in a North-East direction, and another between Mid-West US and Canada.

Only T106 and T159 resolutions from ECHAM5 runs represent the track density in a quite realistic way (at least over the oceans) in terms of shape and magnitude (22-25 cyclones/year) of the maxima. Yet, there are a few little differences in these two resolutions, compared to reality (ERA-Interim):

-The maximum over Mid-West US / Canada is underestimated (~18 instead of 22 cyclones/year).

-The area with high density over the Pacific is broader, especially towards the East, and has a more zonal look than in ERA-Interim (less slope).

-There is an area over South-Eastern Europe with high cyclone track density in T106-159 (~18 cyclones/year) that doesn't show up in ERA-Interim (where there is a small local maximum of ~13 cyclones/year). This makes a contrast between Southern and Northern Europe: in T106-159 there is more track density in the South and in ERA-Interim there is more in the North.

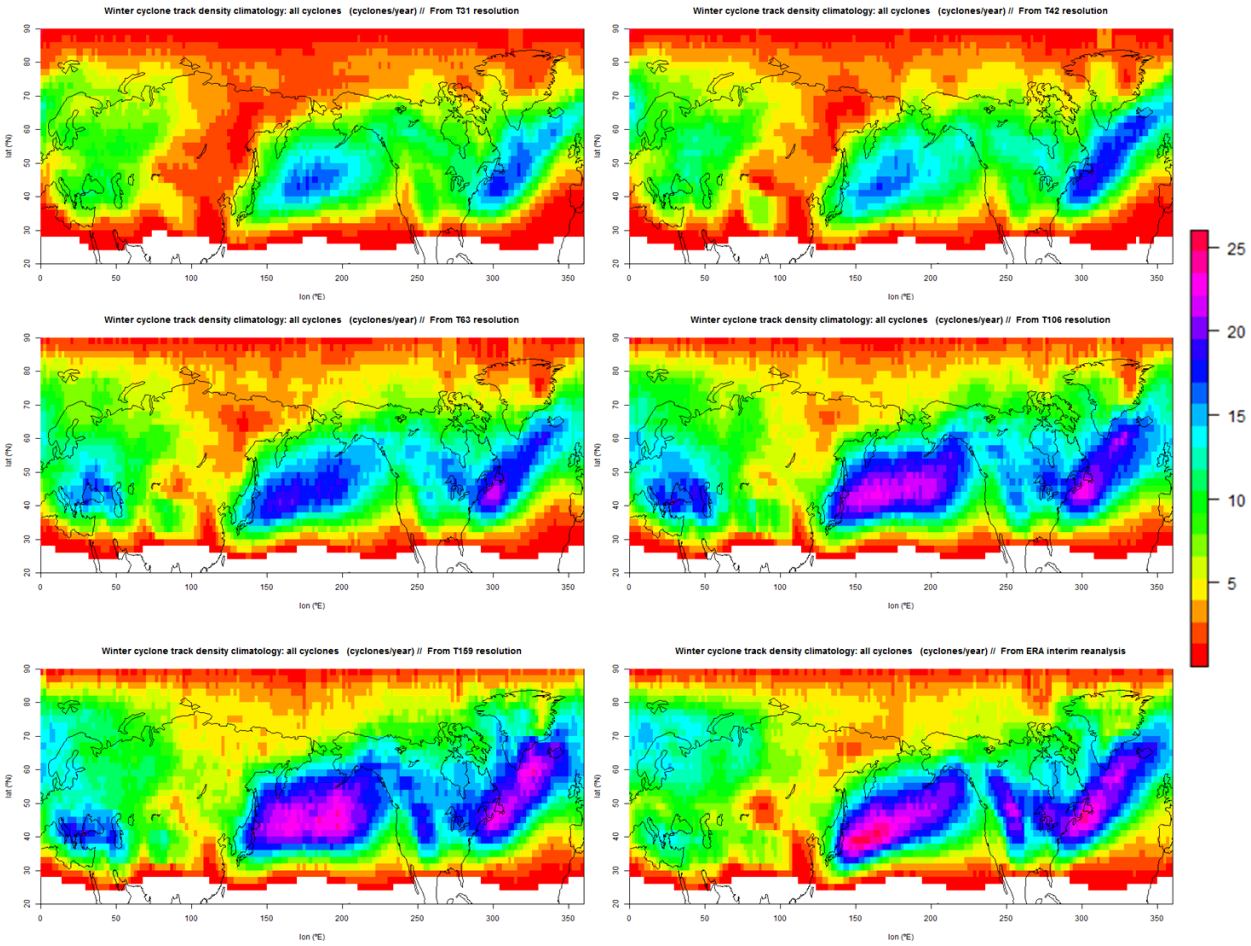

Figure 5.8: Climatological winter track density maps of all cyclones of >24h and >1000km. Shown are ECHAM5 runs at resolutions T31 (upper left), T42 (upper right), T63 (middle left), T106 (middle right), T159 (lower left), compared to ERA-Interim reanalysis (lower right). White spaces in the maps correspond to 0 or no track density of extratropical

The possible reasons for these differences will be studied further on in section 5.2.3, where maps with track density difference from ERA-Interim will be introduced, showing the spatial distribution of the track density differences in a clearer way. These differences don't have to be attributed to an incomplete representation of atmospheric processes by the ECHAM5 model.

The rest of the ECHAM5 resolutions (T31-42-63) show an overall lower track density, in a similar way as in section 5.1.2 (lower cyclone number at those resolutions in the seasonal cycle).

At T63 the maximum over SE Europe also does appear. There is a higher maximum of track density over the Atlantic at T42 and T63 (less track density over the Pacific, whereas at T106-159 and ERA-Interim the maxima at both oceans are of similar magnitude, ~24 cyclones/year).

At T31, the maxima are very low compared to reality (~16 against ~24 cyclones/year over both oceans), and the one in the Pacific is placed in the middle of the ocean (instead of crossing it from SW to NE).

- Figure 5.9 shows the track densities taking the 10% strongest cyclones:

The 10% strongest cyclones of each DATA set are taken; therefore the min P limit is a bit different in each DATA set. In this case, only two maxima are differentiated over the Atlantic and over the Pacific oceans, meaning that the strongest cyclones are mostly oceanic.

The maximum over the Atlantic (~9 cyclones/year) reaches N Europe, and is a bit higher than the one over the Pacific (~7 cyclones/year) in the ERA-Interim reanalysis. The continental areas mostly show lower track densities, with an increase crossing Canada and the US from NW to SE.

As in the case with all cyclones, T106 and T159 resolutions show a realistic representation of the track densities, very similar to the one from ERA-Interim reanalysis: they capture the magnitude of both maxima over the Atlantic and the Pacific and the increase in track density crossing Canada and the US from NW to SE.

Again the area with maximum density is broader in the Pacific and has less meridional slope (i.e. is more zonal) at T106-159.

In both T106 and T159 the Atlantic track density maximum doesn't reach N Europe as far to the East into Siberia as it does in the ERA-Interim reanalysis.

The rest of the ECHAM5 resolutions (T31-42-63) show much weaker maxima (5-6 cyclones/year). T31 puts more track density over the Pacific, and T63 puts the same track density over both oceans, contrary to the (real) track densities from ERA-Interim reanalysis where track density is higher in the Atlantic.

It can be said that, in this case (taking the 10% strongest cyclones), the model resolution makes a bigger difference on the results in the Atlantic. Track density increases with higher resolution in both oceans, but at the lowest resolution there is less over the Atlantic, and at the higher resolutions (and reality) there is more track density over the Atlantic than in the Pacific.

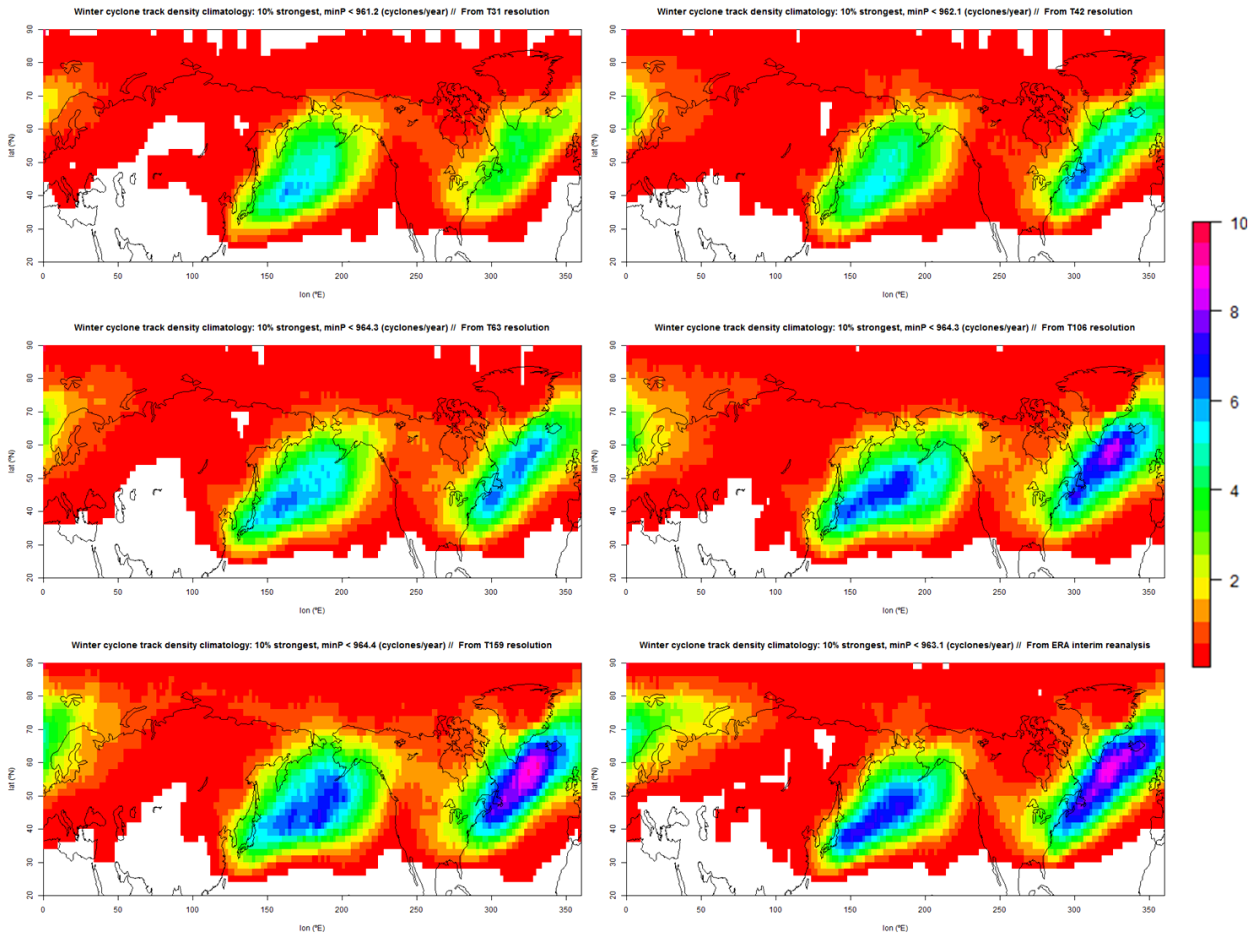

Figure 5.9: Climatological winter track density maps of the 10% strongest cyclones of each DATA set. Min P limits on top of each map. Shown are ECHAM5 runs at resolutions T31 (upper left), T42 (upper right), T63 (middle left), T106 (middle right), T159 (lower left), compared to ERA-Interim reanalysis (lower right). White spaces in the maps correspond to 0 or no track density of extratropical cyclones. The rest of colors correspond to the same color scale in all maps.

- Figure 5.10 shows the track densities taking the 1% strongest cyclones:

The 1% strongest cyclones of each DATA set are taken; therefore the min P limit is a bit different in each DATA set again.

This being the most extreme case in the section, it shows the biggest disagreement between the 6 DATA sets.

T159 has a too wide and too high density maximum over the Pacific (~0.7 cyclones/year at ERA-Interim reanalysis, against ~1 cyclones/year in the model run), and it lacks the peak near Iceland (~1.6 in reality, ~0.7 cyclones/year in the model run)

T106 shows the closest representation to reality: the maxima over the Pacific (~0.7 cyclones/year) and over the Atlantic (~1.5 cyclones/year in the model run, ~1.7 in reality) are quite close to ERA-Interim. Still, the maximum over the Pacific is too wide, and the one over the Atlantic doesn't reach and peak over Iceland. Also, there is a track density increase over Canada that is not appearing in ERA-Interim.

T63 and T42 are very similar to each other, with maximum of 0.7-0.8 cyclones/year over the Pacific and 1.0-1.1 cyclones/year over the Atlantic (too low).

The lowest resolution, T31, exaggerates the track density over the Pacific (~1.2 cyclones/year maximum) and has an extremely low density over the Atlantic (~0.3 cyclones/year maximum), meaning that it places almost all the extreme cyclones over the Pacific, totally opposite to ERA-Interim where most of them happen in the Atlantic.

To sum up, in this extreme case, the performance of all the ECHAM5 model runs gets worse than in the other cases (all cyclones and 10% strongest cyclones). Only T106 can be said to be quite close to the real distribution of track density of the 1% strongest cyclones, and it is not the highest resolution available in this study.

As in the case taking the 10% strongest cyclones, looking at this more extreme case taking just the 1% strongest cyclones shows again that the model resolution makes a bigger difference in the Atlantic, being this difference exaggerated this time:

Track density decreases a little bit with higher resolution over the Pacific. On the Atlantic, track density increases very much with higher resolutions: from almost no density at T31 (~0.3 cyclones/year), to about five times more at the higher resolutions.

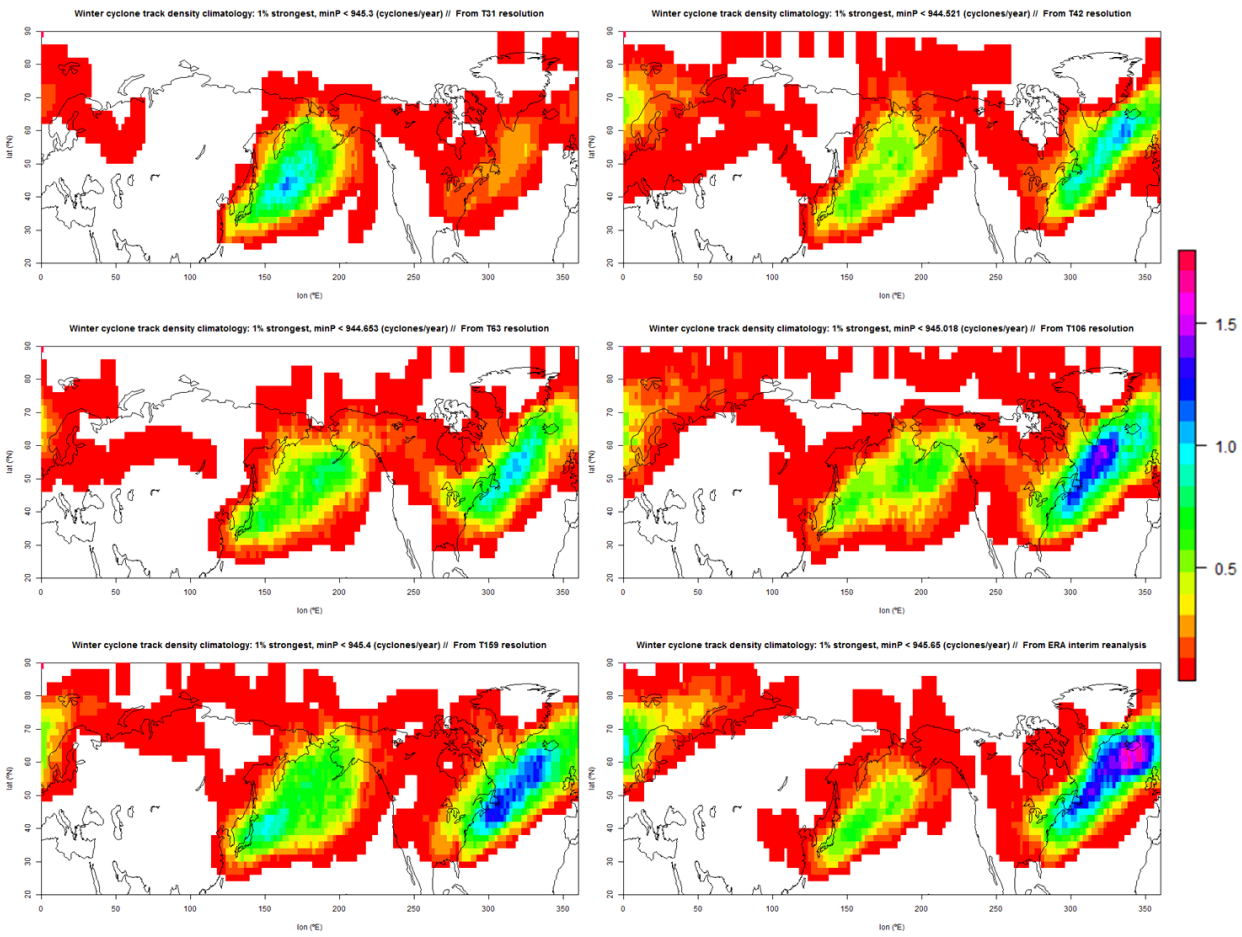

Figure 5.10: Climatological winter track density maps of the 1% strongest cyclones of each DATA set. Min P limits on top of each map. Shown are ECHAM5 runs at resolutions T31 (upper left), T42 (upper right), T63 (middle left), T106 (middle right), T159 (lower left), compared to ERA-Interim reanalysis (lower right). White spaces in the maps correspond to 0 or no track density of extratropical cyclones. The rest of colors correspond to the same color scale in all maps.

5.1.8: Strong deepening event maps

Procedure:

Strong or "explosive" / "bombing" cyclone deepening occurs when the central pressure of a cyclone falls very fast. This study looks for pressure drops of 20hPa/24h and 32hPa/24h.

Usually the limit used to define a "bombing" cyclone is around 1hPa/h, weighted with latitude (as in *Sanders and Gyakum, 1980*). Other studies suggest the better objectivity of using the drop of the *relative pressure* respect to the climatological mean pressure at the cyclone's

location at each step (*Sinclair, 1995; Lim and Simmonds, 2002*). The constant limits used here are for simplicity.

The algorithm takes the same cyclones as in 5.1.7 (winter tracks of more than 24h and 1000km), but instead of computing their min P, it looks at their intensification rates during their lifetime (variable 5 in the DATA arrays). From the fifth step to the last, the algorithm makes the sum of that step's and the 3 preceding intensification rates (there is no intensification rate in the first step since it is made subtracting step-1).

The intensification rates are in hPa/6h, so the sum of four gives the rate in hPa/24h. If the sum is lower than -20 (or -32) at any point of the cyclone's lifetime, the algorithm detects those time-steps where the pressure drop is stronger than -5hPa/6h. Then, for the locations of the cyclone at those times, it detects the corresponding grid box, and makes a +1 count on the corresponding map (limit -20 or -32) in the 5x5grids area centred at those locations. As in 5.1.7, if any overlapping exists in the same track, just a +1 count is added.

Also like in 5.1.7, the algorithm adds up the counts for each winter, saves the track densities for every winter (27 winters, except ECHAM5 T63 with 26 winters), and makes the mean at each grid box: obtaining the climatological winter deepening event maps (events per winter, both types -20hPa/24h and -32hPa/24h) for every DATA set.

Results:

In this section, maps of the climatological winter deepening event density are shown (for cyclones of >24h and >1000km). A strong deepening event is an extreme pressure drop during a cyclone's lifetime. Here two types are distinguished:

Drops of 20hPa/24h (more-less the pressure drop to define an "explosive" or "bombing" cyclone by different authors, see comment at section 5.1.8), and drops of 32hPa/24h (to have an even more extreme scenario to compare the ECHAM5 performance).

For each of the deepening types, maps from the ECHAM5 runs are compared with the ERA-Interim reanalysis (taken as the real deepening event density).

- Figure 5.11 shows the deepening event density of 20hPa/24h drop events:

It can be observed that extreme cyclone deepening is restricted to the oceans. At the ERA-Interim reanalysis (lower left) the Pacific has an event density maximum (~8.5 events/year) a bit higher than in the Atlantic (~7 events/year).

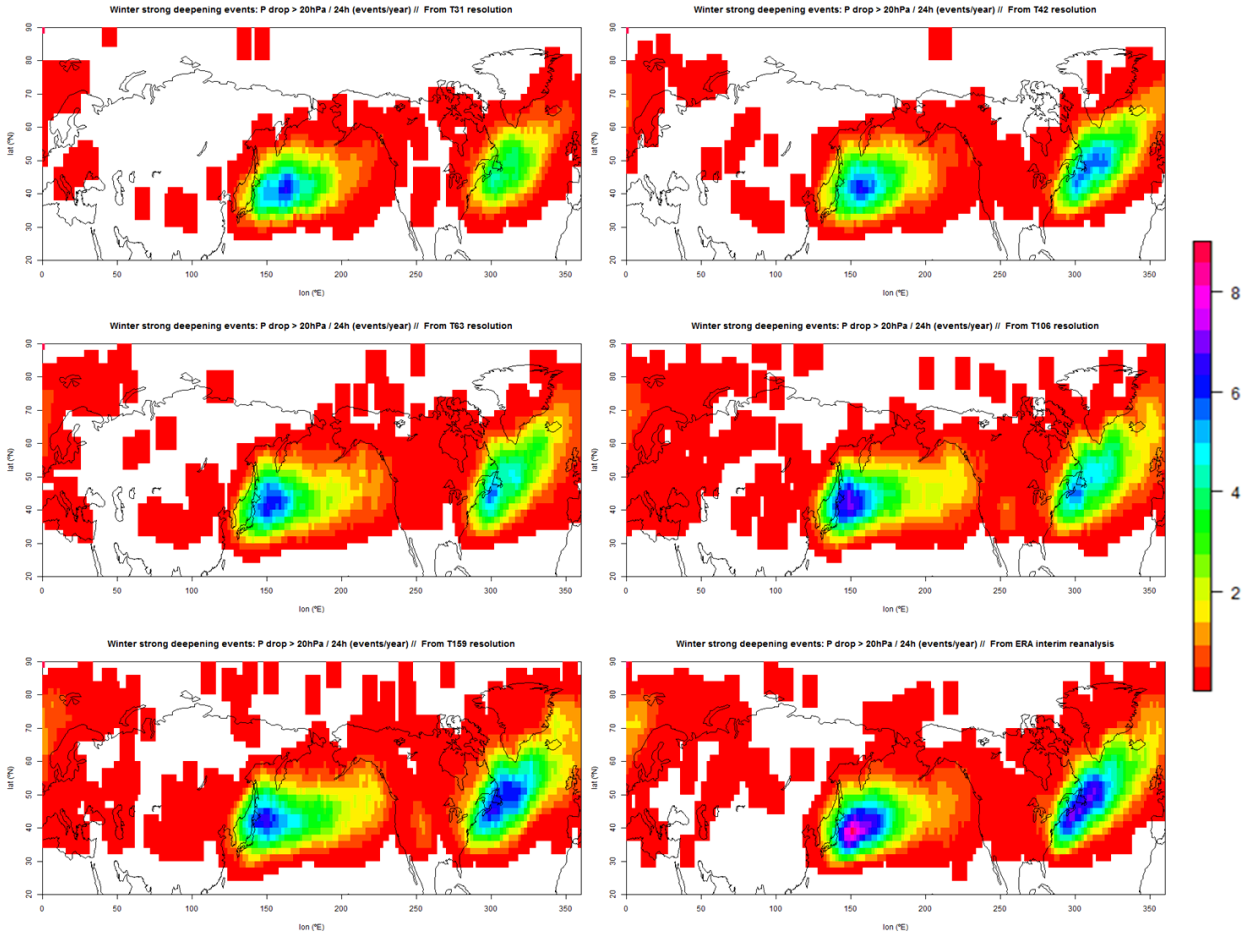

Figure 5.11: Climatological winter deepening event density maps of 20hPa/24h drop events. Shown are ECHAM5 runs at resolutions T31 (upper left), T42 (upper right), T63 (middle left), T106 (middle right), T159 (lower left), compared to ERA-Interim reanalysis (lower right). White spaces in the maps correspond to 0 or no deepening event density. The rest of colors correspond to the same color scale in all maps.

No ECHAM5 run reaches those maxima values, they all show lower event densities. All runs show a maximum in the Pacific of 5.5-6.5 events/year, and the biggest difference is seen in the Atlantic: from ~6 events/year, at T159 to just ~3.5 events/year at T31.

Also, T106 and T159 show an increased event density over Mid-West US that does not exist in ERA-Interim.

Although all resolutions underestimate the occurrence of this type of events, higher resolution improves the representation of this events, the highest one (T159) being the closest to reality. Still, higher resolutions would be needed in the study, to see if they achieve realistic deepening event densities.

In general, all this shows that, for this type of events, model resolution has an important influence over the Atlantic event density (again as in section 5.1.7 for the 10% and 1% strongest cyclone's track density), and makes almost no difference in the Pacific.

- Figure 5.12 shows the deepening event density of 32hPa/24h drop events:

This is the most extreme case of section 5.1. As for deepening events of 20hPa/24h, no ECHAM5 resolution shows a picture very similar to ERA-Interim reanalysis.

In this case, all resolutions underestimate the occurrence of this type of events in the Pacific. The maxima over the Pacific are around 1.5-1.7 events/year in all resolutions, except for T63 that shows a ~2.2 events/year maximum density. None of the ECHAM5 runs reach the ~2.7 events/year maximum from ERA-Interim (reality). As earlier, very little variation is seen in the Pacific with increasing resolution.

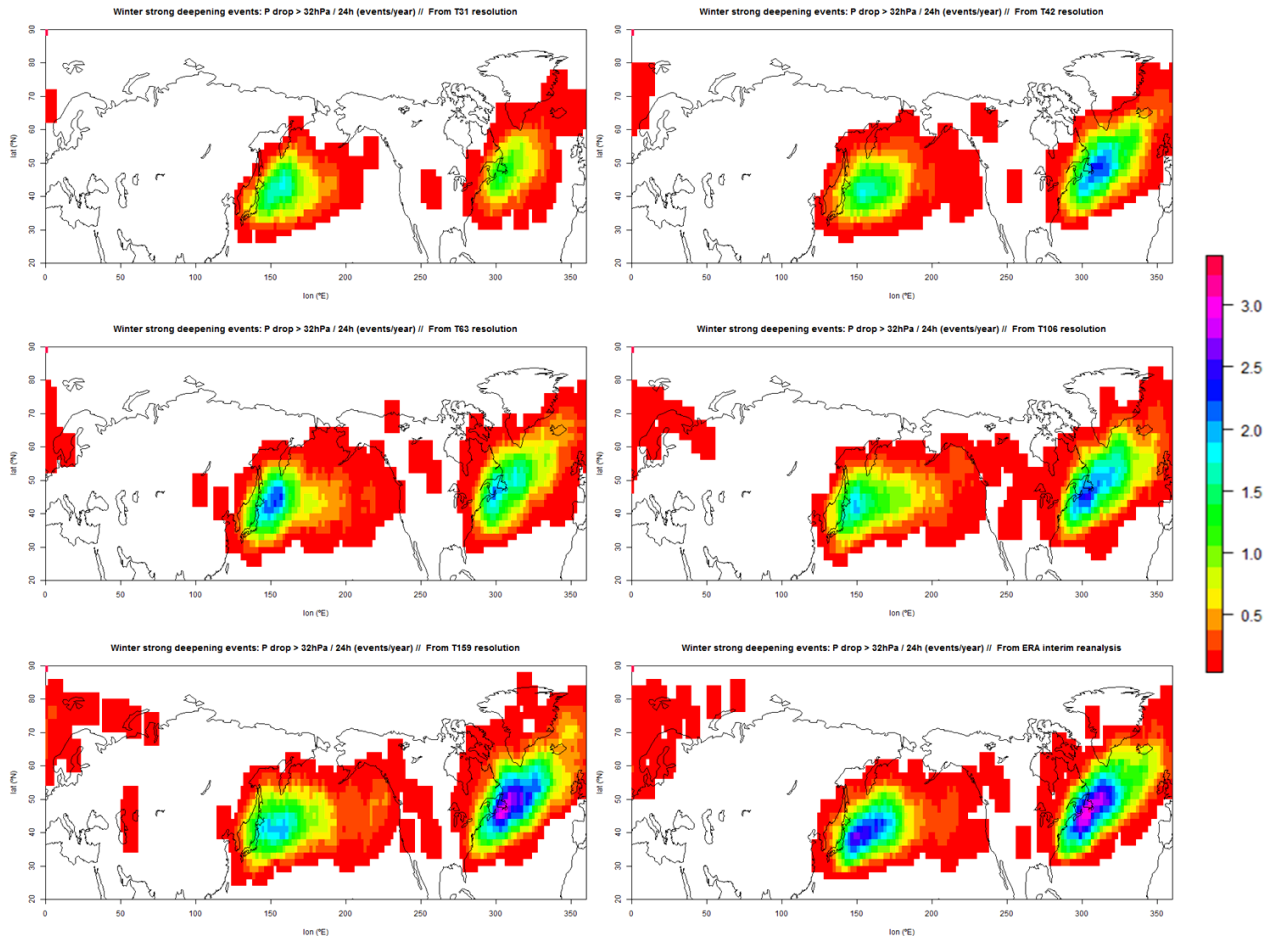

Figure 5.12: Climatological winter deepening event density maps of 32hPa/24h drop events. Shown are ECHAM5 runs at resolutions T31 (upper left), T42 (upper right), T63 (middle left), T106 (middle right), T159 (lower left), compared to ERA-Interim reanalysis (lower right). White spaces in the maps correspond to 0 or no deepening event density. The rest of colors correspond to the same color scale in all maps.

The lowest resolution (T31) shows more events in the Pacific than in the Atlantic, contrary to higher resolutions and ERA-Interim where more events are captured in the Atlantic.

In the Atlantic, deepening event density increases with higher resolutions, from ~1.4 events/year at T31 to ~3.0 events/year at T159. This ocean is again the most sensitive to resolution change, as for 20hPa/24h deepening events, and also track densities in the earlier section 5.1.7 (10% and 1% strongest cyclone's track density). In this case, T159 represents the event density in the Atlantic properly, but doesn't do so in the Pacific where it is underestimated.

As for deepening events of 20hPa/24h, the 32hPa/24h type would also need of higher resolutions to see if they capture the event density in a realistic way.

A quick outlook of section 5.1 (Climatologies):

All ECHAM5 resolutions capture the seasonal cycle of min P over both oceans properly (5.1.1). With increasing resolution, more cyclones are created in this runs (5.1.2); and in the Atlantic the number of cyclones during summer is exaggerated at high resolutions (T106-159).

The min P distributions are moved towards higher P than in reality (less intense cyclones) in the Atlantic, and the contrary is seen in the Pacific (bias towards lower min P) in section 5.1.3.

The Atlantic ocean is much more sensitive to resolution changes than the Pacific. This is palpable seeing the winter cyclone's lifetime (5.1.4) and track length distributions (5.1.5) where there is more discrepancy between the different ECHAM5 resolutions in the Atlantic, and a tendency to simulate cyclones with longer lifetime and track length than in reality: meaning that the tendency is to underestimate the cyclone's development pace.

A similar feature is seen in section 5.1.6 where there is more difference at extreme intensification rates between the different resolutions.

Up to here, resolutions T106 and T159 (and sometimes T63) show statistics very close to those from ERA-Interim (reality), but when it comes to mapping, T106-159 only do a good job at all cyclones and 10% strongest cyclone's track density (5.1.7).

The performance of all resolutions gets worse when a more extreme case is studied: for just the 1% strongest cyclone's track density (last case at 5.1.7) and both types of the extreme cyclone deepening event densities (5.1.8), the higher resolutions perform closer to

reality (ERA-Interim) but none of them captures de spatial distribution and magnitude of the densities properly.

In these cases, the Atlantic Ocean gets more sensitive to resolution changes the more extreme the case study is.

The lower resolutions underestimate the extreme cyclone activity over the Atlantic systematically, hinting that the processes that force rapid cyclone development and intensification happen at a smaller scale than in the Pacific. Thus, the smoothing caused by a lower spatial resolution would make the model run to miss those events.

The possible reasons for all of the above mentioned features will be studied in more detail in the next section (5.2) where the focus is made for specific relationships of different variables.

5.2: Relationships between variables

5.2.1: Minimum pressure vs lifetime

Procedure:

The distributions of minimum pressure (obtained in section 5.1.3) and lifetime (5.1.4) are used, both done for the same winter cyclones at the Atlantic and Pacific. One list with the min P and lifetime of each cyclone is created combining both distributions. To look at the relationship of the two variables, min P will go in the X-axis and lifetime in the Y-axis. Scatter plots would be very difficult to compare the 6 DATA sets, so they are turned into lines.

First, the list is organized by the min P in increasing order. Then the algorithm takes groups of 100 cyclones (from the sorted list with increasing min P) and computes their mean min P and lifetime, which will be the values that will appear in the graphic. This way it will show how the lifetime of a cyclone varies for a certain min P.

For the case of the ERA-Interim reanalysis dataset, confidence intervals at the 95% confidence are computed in the following way:

For every group of 100 cyclones, their different lifetimes are taken as a normal distribution, and the mean and standard deviation (sigma) are calculated.

$\frac{1\prime 96 \times sigma}{\sqrt{100}}$ is the interval around the calculated sample mean where the *true* mean will lay with 95% of confidence.

The means of the 100-cyclone groups, plus their (lifetime) 95% confidence intervals in the positive and negative direction will appear in the graphic for the ERA-Interim DATA set, and just the means for the rest of the DATA sets. This is to see how much they differ from the reanalysis (reality). One graph comparing the 6 DATA sets is done for each ocean.

Results:

Figure 5.13 shows the 100-cyclone-averaged relationship between the cyclone's minimum pressure and the lifetime it has.

It can be noted that there exists a linear relationship between the cyclone's min P and their mean lifetime: cyclones generally need a longer lifetime in order to intensify and reach lower min P.

In the Pacific all ECHAM5 distributions are very similar to that from ERA-Interim, laying within the interval of the corresponding error bars the vast majority of the times.

In the Atlantic, lower min P are reached and the lifetime of the cyclones is shorter in general compared to the Pacific. Besides, the different distributions of the ECHAM5 runs disagree from ERA-Interim much more than they do in the Pacific (where there is very little disagreement).

For the same min P, Atlantic cyclone lifetimes get longer with decreasing resolution. The T106 and T159 resolutions are very close to the real distribution, but still differ fairly from the ERA-Interim relationship, laying outside of its error bars at the lowest min P. At lower resolutions it can be seen that the linear relationship of the cyclone's min P and lifetime is clearly different from that observed in ERA-Interim.

A similar feature happens in the Pacific: for the same min P, Pacific cyclone lifetimes also get longer with decreasing resolution, but in this case the difference happens in a much smaller scale and, in general, no ECHAM5 run lays outside the ERA-Interim confidence interval.

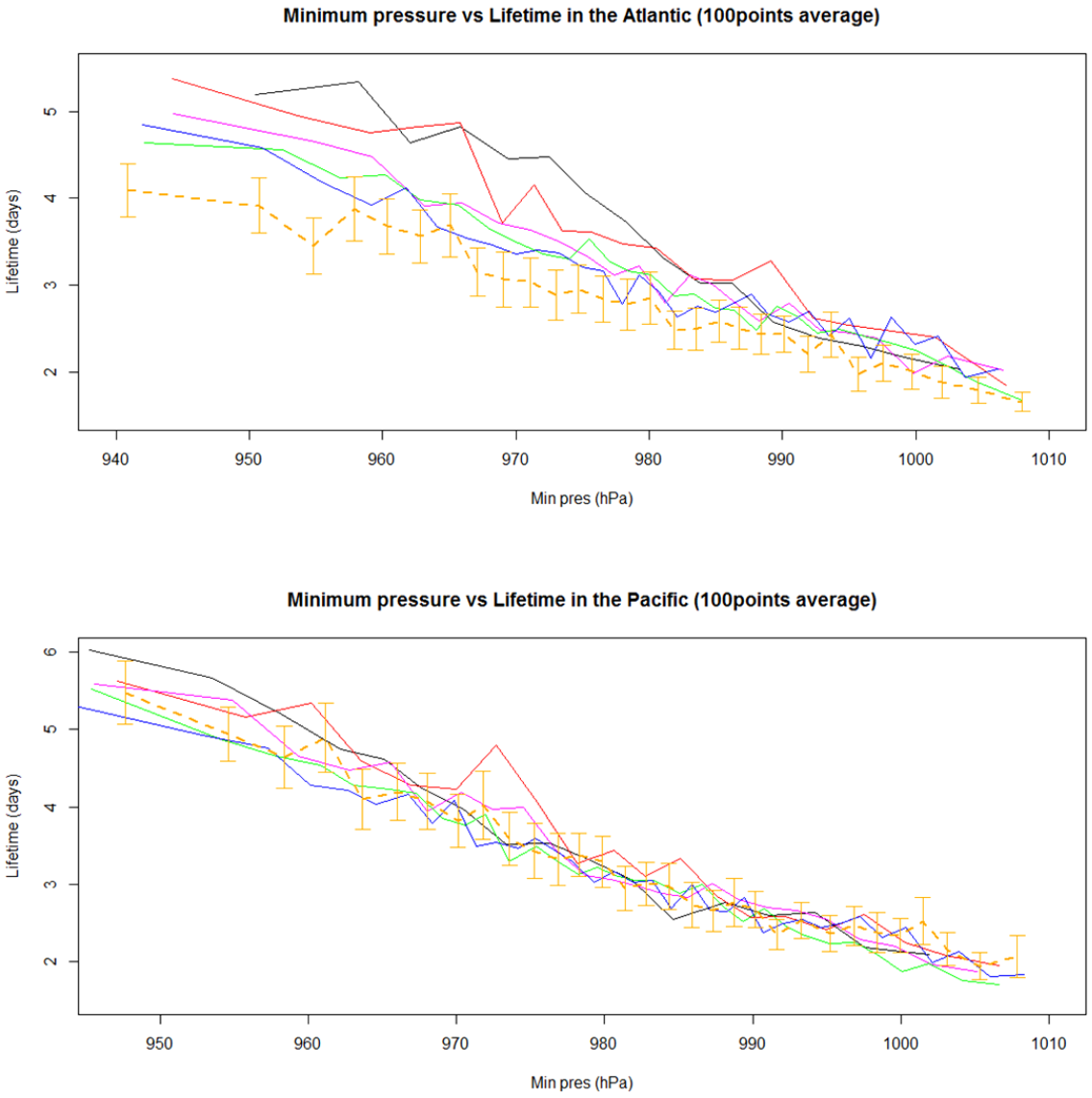

Figure 5.13: 100-cyclone-averaged relationship of the climatological distributions of winter cyclone's lifetime against their min P. Atlantic at the top and Pacific at the bottom.
Line colors correspond to:

As addressed in section 5.1, the Atlantic cyclone's characteristics are again very dependent on resolution, and the different ECHAM5 runs tend to underestimate the development / intensification pace of those cyclones with decreasing resolution.

5.2.2: Track length vs lifetime

Procedure:

The same procedure is applied as in 5.2.1, but instead of the min P distribution, the track length distribution is taken (obtained in section 5.1.5), a list with the track length and the lifetime of each cyclone is created and ordered with decreasing track length, and is divided into groups of 100 cyclones.

Then the mean track length and mean lifetime are computed for every group of 100 cyclones, and also the 95% confidence intervals for lifetime in the case of ERA-Interim reanalysis DATA set.

Track length goes in the X-axis and lifetime in the Y-axis, and again one graph comparing the 6 DATA sets is done for each ocean.

Results:

Figure 5.14 shows the 100-cyclone-averaged relationship between the cyclone's track length and the cyclone's corresponding lifetime.

Analogously to section 5.2.1, a linear relationship can be noted for the mean cyclone lifetime and track length. This time better agreement can be seen at both oceans compared to the min P – lifetime relationship (section 5.2.1).

A longer lifetime corresponds to the same track length with decreasing resolution (same as for min P in 5.2.1) but the differences are much smaller than in the earlier section.

Still in the Atlantic the differences are enough for the lower resolution's relationships to lay outside of the confidence interval of ERA-Interim (the higher resolutions lay inside at many of the track lengths).

These differences addressed in the Atlantic are again bigger than the ones seen between the relationships in the Pacific, so once more the Atlantic cyclones appear to be more dependent on resolution than the Pacific ones (as in 5.1 and 5.2.1).

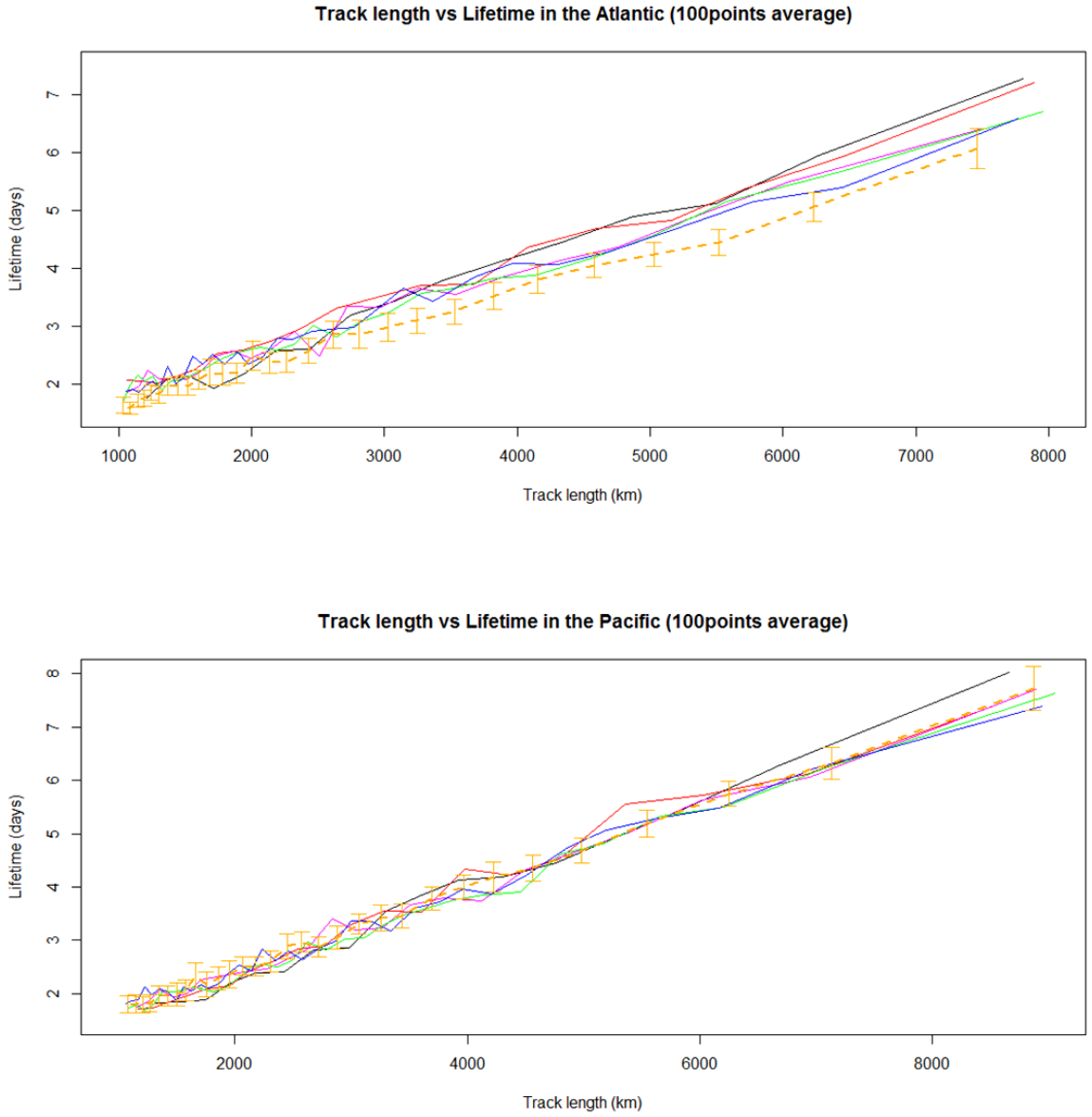

Figure 5.14: 100-cyclone-averaged relationship of the climatological distributions of winter cyclone's lifetime against their track length. Atlantic at the top and Pacific at the bottom.
Line colors correspond to:

- T31
- T42
- T63
- T106
- T159
- ERA- Interim

5.2.3: Track density differences with ERA-Interim

Procedure:

In this section, maps with the difference of track density of the ECHAM5 DATA sets with the ERA-Interim DATA set will be done for winter and summer climatologies, in a similar way as in section 5.1.7.

In section 5.1.7 winter track density maps are obtained, so the same procedure is done, but also for summer tracks (5x5 grids area around cyclone centre for +1 counts, only summer tracks longer than 24h and 1000km).

Then for every ECHAM5 DATA set (resolution) the track density from ERA-Interim is subtracted at each grid box of the map, the same being done for both winter and summer. As in sections 5.1.7 and 5.1.8, the maps are done with 2ºx2º grids, representing all longitudes and latitudes from 20ºN to 90ºN, resulting in 180x35 maps.

To finish, contours with ERA-Interim track density are added to every map (one contour every 5 cyclones/year density) to see whether the biggest differences happen in areas where track density is high or low in the reanalysis (reality). This way, 5 maps (each of the ECHAM5 resolutions) are obtained for both winter and summer.

Results:

The maps in this section contain more information than any other in the study. The maps show, for each of the five ECHAM5 runs, where there is more (magenta) or less (blue) track density than in the ERA-Interim reanalysis. This is done for summer (JJA) and winter (DJF).

At each map, contours with the ERA-Interim (summer or winter) cyclone track density are included to help seeing where the biggest differences occur (whether it happens near high or low cyclone activity areas).

- Figure 5.15 shows the summer track density differences from ERA-Interim:

In figure 5.15 it can be observed that the maps corresponding ECHAM5 resolutions T31 and T42 (upper row) show mostly blue colour, meaning that they have lower track density almost over the entire NH.

The areas with bigger difference are placed on the ERA-Interim higher track density areas: (from left to right on the map) the Mediterranean Sea, Middle East, Tibet-Himalayan area, near Japan, the Rocky Mountains, the American East Coast and Greenland.

The predominant blue colour is not a surprise since it has been addressed earlier that the lower resolutions produce much less cyclones than the higher ones and the ERA-Interim reanalysis.

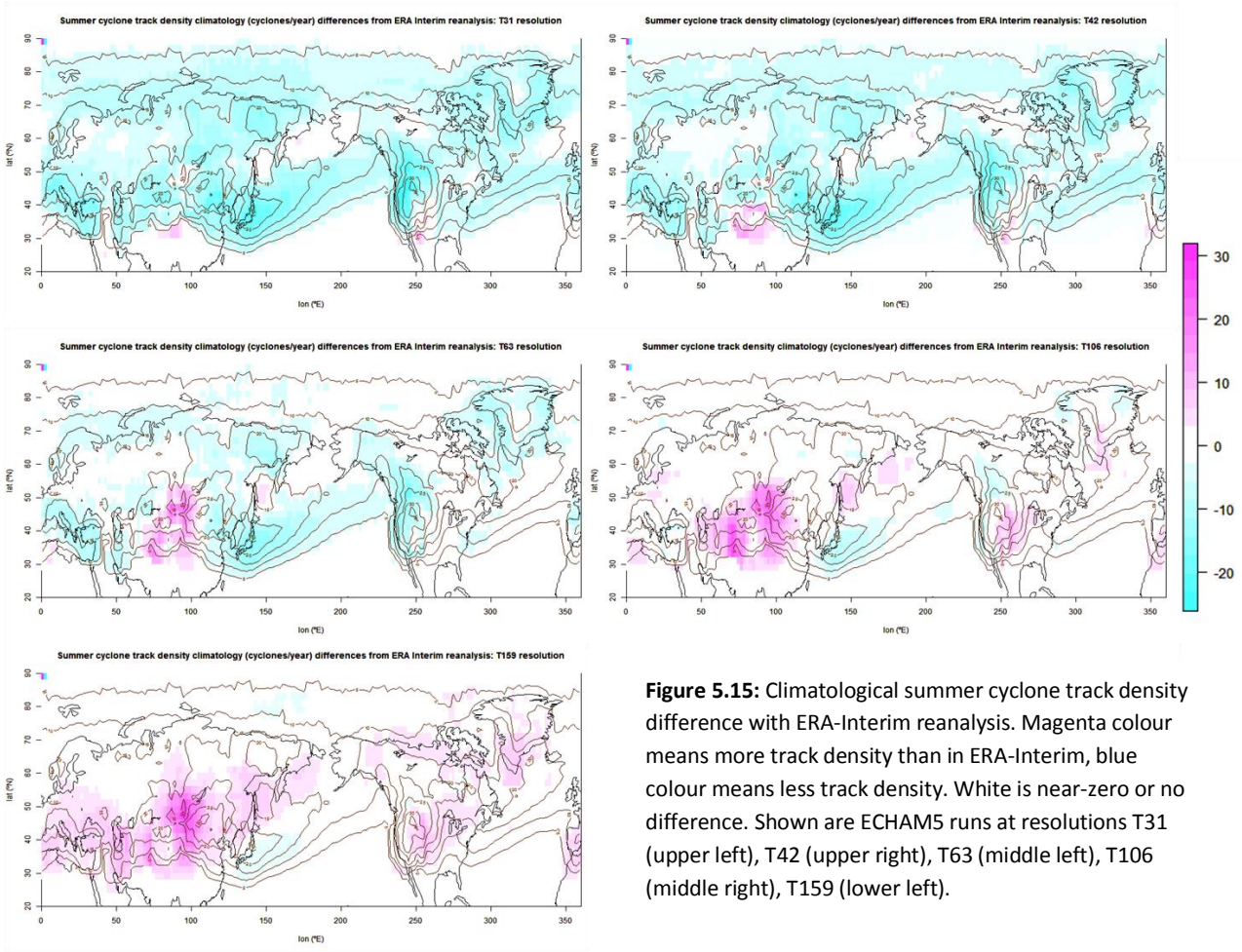

Figure 5.15: Climatological summer cyclone track density difference with ERA-Interim reanalysis. Magenta colour means more track density than in ERA-Interim, blue colour means less track density. White is near-zero or no difference. Shown are ECHAM5 runs at resolutions T31 (upper left), T42 (upper right), T63 (middle left), T106 (middle right), T159 (lower left).

Yet, there are two small areas S of the Himalayas and SE of the Rockies that show higher track density than ERA-Interim. Being T31-42 resolutions lower than the interpolation used for the mapping in this study, this could be explained with the increased cyclonic activity due to a lee-trough effect of the Himalayas and Rockies being extrapolated further away from these mountains because of the smoothed sea level pressure fields.

T63 resolution (middle left map) also shows a predominant lower track density over the Mediterranean Sea, N Europe, Siberia and eastern Asia, NE Pacific, the Rockies and Greenland. These lower values were also expectable since T63 had lower cyclone number in earlier sections.

The feature that differentiates T63 from T31-42 is a broad area of positive anomaly over central Asia, that makes the T63 map look like an intermediate distribution of track density between the lower and higher resolutions.

In the higher resolutions, T106 (middle right map) and T159 (lower left map), the positive anomaly over central Asia broadens and strengthens compared to T63. The positive anomalies turn to be predominant in these higher resolutions: they appear also over the Mid-West US, the southern tip of Greenland and the Mediterranean areas. At T159, the positive anomaly spans all the mid-latitudes of the Eurasian Continent.

The only area with negative anomalies that remains in both T106-159 is in the Pacific, east of Japan. Also, a few areas of weak negative anomaly in T106 over the NW American continent and Greenland are present.

The strong positive anomalies over continents at T106-159 could hint that the restriction for cyclone counting of tracks >24h and >1000km doesn't get rid of all the thermal lows and monsoon-related pressure minima, that are overestimated in the ECHAM5 runs with higher resolution.

Before starting with the oceanic track density anomalies at T106-159, a short reminder:

In section 5.1.2, it was addressed in the seasonal cycle of simultaneous cyclone number that resolutions T106-159 had a peak number during summer time over both oceans, whereas this peak, at the ERA-Interim reanalysis (reality), just appeared in the Pacific ocean.

Well, in fig. 5.15 middle-right and lower-left maps (T106 and T159 respectively), it can be seen that there is a positive track density anomaly in the Pacific near the Kamchatka Peninsula, and near the southern tip of Greenland in the Atlantic. The area of negative anomaly near Japan compensates the positive one further north, and makes the cyclone number peak in summer match with the Era-Interim reanalysis. In the Atlantic, though, the only anomaly is the positive one over S Greenland. Since nothing compensates it, the cyclone number peak in summer at T106-159 in the Atlantic doesn't appear in the ERA-Interim reanalysis.

This shows that the match of the cyclone number summer peak over the Pacific at T106-159 and ERA-Interim is just by chance, because two areas of lower and higher cyclone activity compensate the overall cyclone number over the ocean.

The issue of increased cyclone activity over S Greenland has been addressed *by Hanley and Caballero (2012)* when tracking cyclones with SLP fields: their results describe this area as problematic, with a signal of enhanced cyclogenesis and spurious track splitting due to a lee

trough effect of Greenland's topography. This effect doesn't appear when tracking with vorticity maxima, thus one has to take this problematic area with special caution.

In the study described here, multicentre cyclones are not dealt, so a track that splits into two would appear as a generation of a new cyclone and increase the track density in the neighbouring area. One could wonder whether the effect addressed for S Greenland could be extrapolated to other areas of pronounced topography in this study, such as the Himalayas, the Kamchatka Peninsula and the Rockies.

In the monthly cyclone generation maps in Appendix II (figure II.1, no min P limit), if one compares the central column (T159) with the right column (ERA-Interim), for June-July-August there are indeed cyclone generation maxima over the above mentioned regions.

The maximum of cyclone generation over S Greenland is exaggerated at T159, so it would explain the positive anomaly of summer track density in the neighbouring areas in figure 5.15.

There is an area east of Kamchatka where cyclone generation is quite higher at T159 than in ERA-Interim, explaining the increased summer track density near that region in figure 5.15.

The increased track density over Mid-West US and central Asia at T106-159 could be a combination of spurious track splitting and tracked thermal lows, that happen more in those model runs than in ERA-Interim.

All of this being said, one could argue that the track density differences of T106-159 with ERA-Interim in summer (also the different summer cyclone number peaks from section 5.1.2) could be an artefact of merging-splitting events in multicentre cyclones that cannot be dealt with the tracking scheme used to obtain the data packages.

This way, the track density / cyclone number differences could be a result of a different behaviour of multicentre cyclones near areas of problematic topography at the ECHAM5 higher resolutions able to produce similar track densities to reality (i.e. T106 and T159).

Also, the lower track densities / cyclone number at lower resolutions could be the result of the inability of such a low resolution to capture multiple centres of a cyclone within a relatively short distance.

- Figure 5.16 shows the winter track density differences from ERA-Interim:

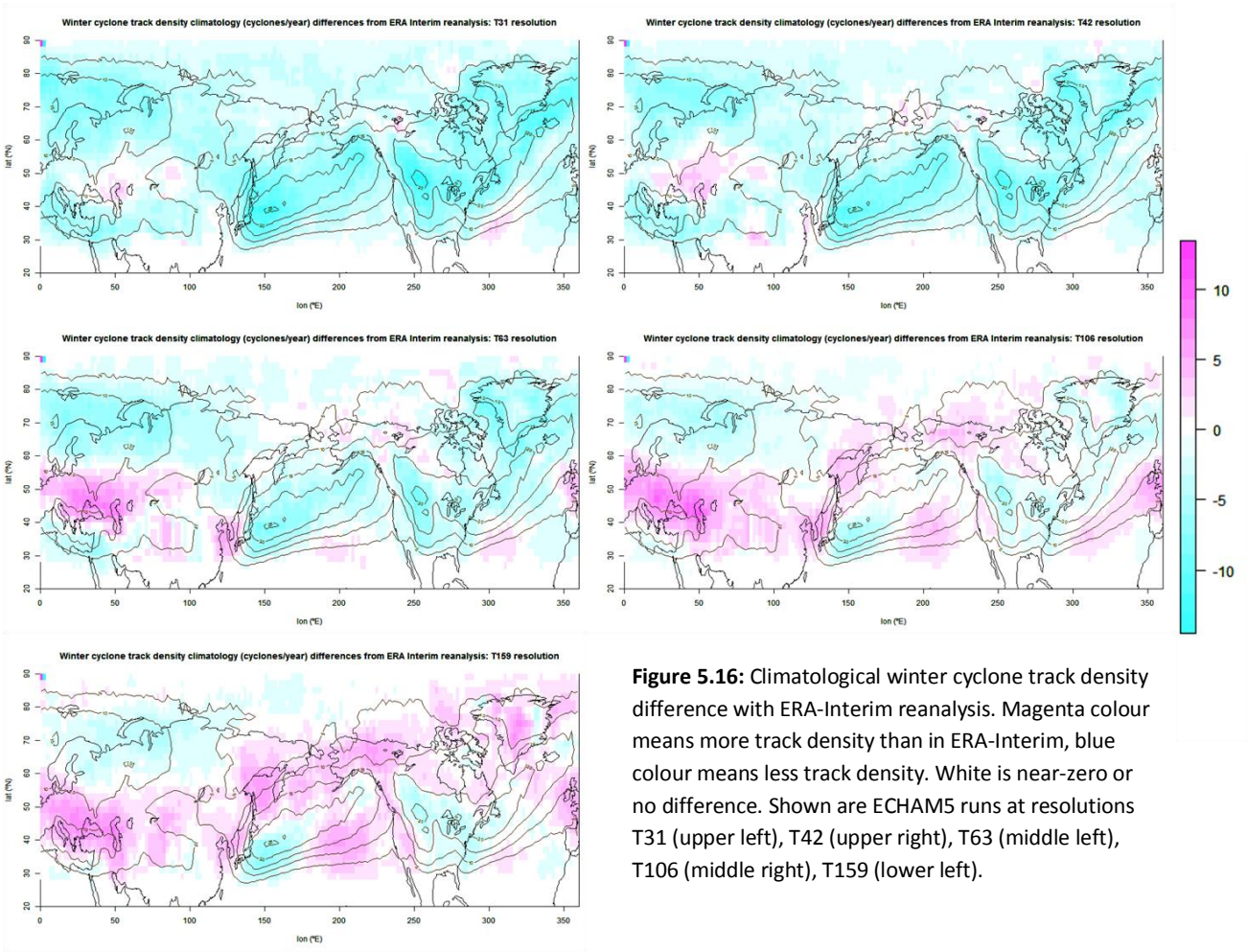

Figure 5.16: Climatological winter cyclone track density difference with ERA-Interim reanalysis. Magenta colour means more track density than in ERA-Interim, blue colour means less track density. White is near-zero or no difference. Shown are ECHAM5 runs at resolutions T31 (upper left), T42 (upper right), T63 (middle left), T106 (middle right), T159 (lower left).

If one looks at resolutions T31 and T42 (upper row) at fig. 5.16, it can be observed that, analogously to summer, they show predominant negative track density anomalies. The most negative anomalies are placed in the areas with highest track density drawn with the contours (as in the track density maps for all cyclones in section 5.1.7 for ERA-Interim, maxima over the Pacific, area near US-Canadian border, and the Atlantic).

One area of positive anomalies over Eastern Europe appears in both T31-42, surrounded by negative anomalies over N Europe and the Mediterranean Sea.

At T63 (middle left map) the area of positive anomaly over E Europe enlarges and spans from France to Central Asia. There is a clear symmetric contrast between N Europe, with negative anomalies, and S Europe with positive anomalies.

The negative anomaly over the Mediterranean Sea is still present as in T31-42. The rest of negative anomalies concentrate in the areas with highest track density as before, but in the surrounding areas some positive anomalies appear.

The anomalies of major interest here are the ones from T106 and T159 since in section 5.1.7 the track density distributions for all cyclones (fig. 5.8) were very realistic, and the overall number of cyclones that they produce was similar to that at ERA-Interim reanalysis.

In section 5.1.7 it was already addressed that the Pacific high track density area was broader than in ERA-Interim, that the maximum over Mid-West US was underestimated and that the track density was increased over Europe.

Here, at T106-159 (middle right map and lower left map respectively in fig. 5.16) the contrast between N Europe (negative anomaly) and S Europe (positive anomaly) is present again as in T63. The negative anomalies over the Pacific and Atlantic track density maxima contours are surrounded by positive anomalies much more prominent than at T63. For the case of the maximum contour near Mid-West Us / Canada, there is also a negative anomaly centred there, followed by positive anomalies immediately to the West.

As explained before for the track density differences in summer, the Rockies are a problematic area, and the distribution of the track density anomalies (negative East of the Rockies and positive to the west) hints that the underestimation of cyclonic activity seen earlier in section 5.1.7 may be caused by a slight shifting of the lee trough effect in the T106-159 resolutions. The displaced cyclogenesis would add extra track density in areas with lower track density leading to a less pronounced maximum in that area.

The anomalies at fig. 5.16 over Europe show a clear N-S pattern (negative anomaly N, positive S). This clear contrast is also shown in the study by Pinto et al. (2009), where relative track density was compared for different phases of the winter North Atlantic Oscillation (NAO).

For NAO++ (meaning a very positive NAO phase: lower sea level pressure over Iceland and higher at the Azores than usual) the highest relative track density of non-extreme cyclones was concentrated in N Europe.

For NAO-- (very negative NAO phase, higher SLP over Iceland and lower over Azores than usual) the relative track density of non-extreme cyclones was more-less the same over N and S Europe, meaning that the NAO phase modulates the cyclone track density in a way that less cyclones occur over N Europe and more over S Europe with negative NAO phase.

The anomalies over Europe seen in fig. 5.16 hint a predominant NAO phase at T106-159 more negative than in ERA-Interim, that would lead to the negative track density anomalies over N Europe and positive anomalies over S Europe. One has to remember that the time period of this study (1982-2009) had a very predominant positive winter NAO phase, which is captured in the ERA-Interim reanalysis.

In the ECHAM5 model runs, though, the atmospheric component is free (just sea surface temperature (SST) and ice coverage are prescribed), and the same predominant positive winter NAO phase does not necessarily have to appear.

This means that the prescribed oceanic SST do not force a certain NAO phase state in the atmospheric component of the model, and different phases develop even when the atmospheric processes do not feed back onto the oceanic SST. This would explain not just the track density anomalies over Europe, but also the ones over the N Atlantic: their distribution matches a (climatological) mean state without a predominant NAO+ phase.

In addition, a similar process happens in the N Pacific: the negative track anomalies found near Japan and Alaska (cyclone tracks tend to concentrate between these areas with stronger Aleutian Low, see section 2.4, figure 2.3) and positive anomalies in the surrounding areas (cyclone tracks tend to disperse throughout the N Pacific with weaker Aleutian Low) suggest that the Aleutian Low is on average weaker in the ECHAM5 model than in the ERA-Interim reanalysis.

Resuming: the winter track density anomalies from ERA-Interim at T106-159 over the oceans and Europe are a result of a different atmospheric mean state: the prescribed SST do not force a similar predominant NAO phase and track density distribution over the N Atlantic and Europe. In the same way, in the N Pacific, a similar mean Aleutian Low strength is not forced, and the corresponding track density distributions change.

This is another source of differences between the ECHAM5 model runs and the ERA-Interim reanalysis to take into account, apart from the proper representation and behaviour of multicentre cyclones addressed earlier.

5.2.4: Track density / deepening ratios between oceans

Procedure:

In this section, the track density and deepening event density want to be compared between the Atlantic and Pacific oceans. The track density and deepening event density maps obtained in sections 5.1.7 and 5.1.8, respectively, are used for this purpose.

Instead of taking the whole areas designated for both oceans in fig. 5.1, only the most representative areas near the density maxima are taken as shown in figure 5.17. These areas are East of Newfoundland and South of Greenland (44-56ºN and 300-320ºE) for the Atlantic, and East of Japan and South of Kamchatka (34-50ºN and 140-170ºE) for the Pacific.

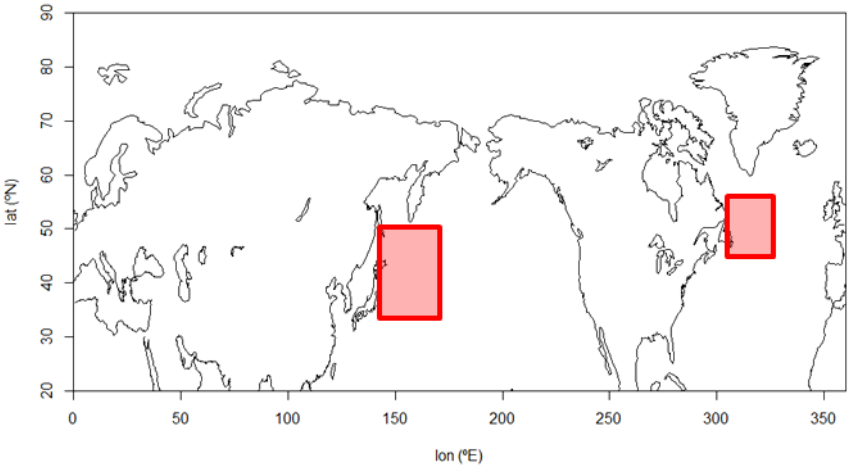

Figure 5.17: Areas taken to calculate the track / deepening event density ratios between the Atlantic and Pacific oceans: red boxes.

For each of the 6 DATA sets, the mean density in each of the red area in fig. 5.17 is computed. Also, the standard deviation (sigma) of the density values within the grid boxes in those areas is calculated.

The ratio between Atlantic and Pacific will be represented as a diagram with the mean density in the Atlantic red area in the X-axis, and the mean density in the Pacific red area in the Y-axis.

A line crossing (0,0) and the point corresponding to the ERA-Interim reanalysis is drawn in the diagram to see if the ECHAM5 resolutions are close to the same ratio.

Error bars at 95% confidence are drawn as well, using this formula: $\frac{1{,}96 \times sigma}{\sqrt{n}}$

being n the sample size: 7x11 grid boxes in the Atlantic, and 9x16 grid boxes in the Pacific (there is one grid box every 2º).

A diagram is obtained for all cyclones, 10% strongest cyclones, 1% strongest cyclones, and deepening events of 20hPa/24h and 32hPa/24h.

Results:

Figure 5.18 shows the track density ratios between the Atlantic and Pacific oceans for all cyclones (left), 10% strongest cyclones (centre) and 1% strongest cyclones (right). The data used is the same as in the track density maps (figures 5.8, 5.9 and 5.10 respectively) from section 5.1.7. The ratios were made averaging track densities over the areas shown in fig. 5.17, near the density maxima.

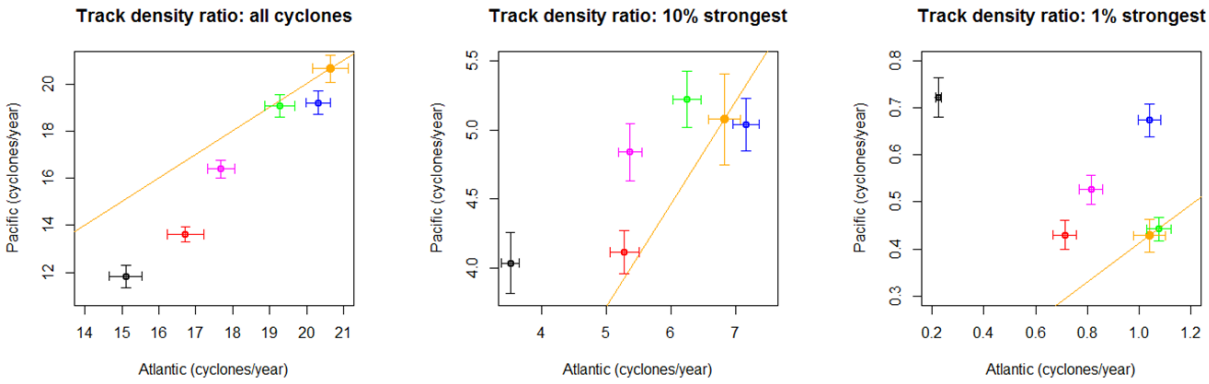

Figure 5.18: Cyclone track density ratios between the Pacific and Atlantic oceans. Shown are ratios for all cyclones (left), 10% strongest cyclones (centre) and 1% strongest cyclones (right). Track density averaged over the areas designated for each ocean in figure 5.17. Error bars at 95% confidence. Orange line represents the same ratio as the ERA-Interim reanalysis. Colours of the points and error bars correspond to coloured text on the lower right part.

- T31
- T42
- T63
- T106
- T159
- ERA- Interim

In the left diagram from fig 5.18 (ratio for all cyclones), it can be seen that the track density difference at the lowest resolution gets fixed almost linearly with increasing resolution: each higher resolution of the ECHAM5 runs is closer to ERA-Interim in the very same direction.

Although being very close, if one looks at the 95% confidence intervals, the higher resolutions (T106-159, green and blue respectively) have not the same cyclone numbers at each ocean as ERA-Interim (orange). This has to be dealt with caution, because the same area is used for the track density averaging in all model runs, and their track density maxima don't necessarily have to be placed exactly there.

In the diagram for the 10% strongest cyclones ratios (centre graphic from fig. 5.18), that linear approach to the ERA-Interim ratio with increasing resolution doesn't happen this time, but still the higher resolutions T106-159 (green and blue) are the closest to the ERA-Interim mean track densities at the Atlantic and the Pacific.

Although T42 (red) has much lower track densities, it has the closest Atlantic-Pacific ratio to reality (ERA-Interim ratio is the orange line). Note that the scale at which track density increases with resolution is not the same at both oceans: Pacific goes from 4 (T31, black) to 5.3 (T106, green) cyclones/year, whereas the Atlantic goes from 3.5 (T31, black) to 7.5 (T159, blue) cyclones/year. The Atlantic is again more sensitive to resolution as in earlier sections.

In the diagram from the right in fig. 5.18 (1% strongest cyclones), the Atlantic-Pacific ratio getting closer to reality with higher resolution is not clear at all:

T31 point (black), as always, lays furthest from ERA-Interim. T106 (green) ratio and track densities at both oceans are almost identical to ERA-Interim. T42 (red), T63 (magenta), and T159 (blue) are spread more-less at the same distance from the ERA-Interim point.

As before, the scale at which the Atlantic track densities vary at different resolutions is bigger than in the Pacific (Atlantic is more sensitive to resolution), but this time the track density at the Pacific is higher at the lowest resolution T31.

Figure 5.19 shows the extreme cyclone deepening event density ratios between the Atlantic and Pacific oceans for 20hPa/24h events (left) and 32hPa/24h events (centre). The data used is the same as in the event density maps (figures 5.11 and 5.12 respectively) from section 5.1.8. The ratios were made averaging event densities over the areas shown in fig. 5.17, near the density maxima.

At both diagrams from fig. 5.19 it can be noted that T159 (blue) event densities are closest to ERA-Interim (orange), but their Atlantic-Pacific ratio is not: the closest Atlantic-Pacific ratio (closest point to orange line) to reality for 20hPa/24h events is at T42 (red), and for 32hPa/24h events is at T106 (green). T31 point (black), as always, lays furthest from ERA-Interim.

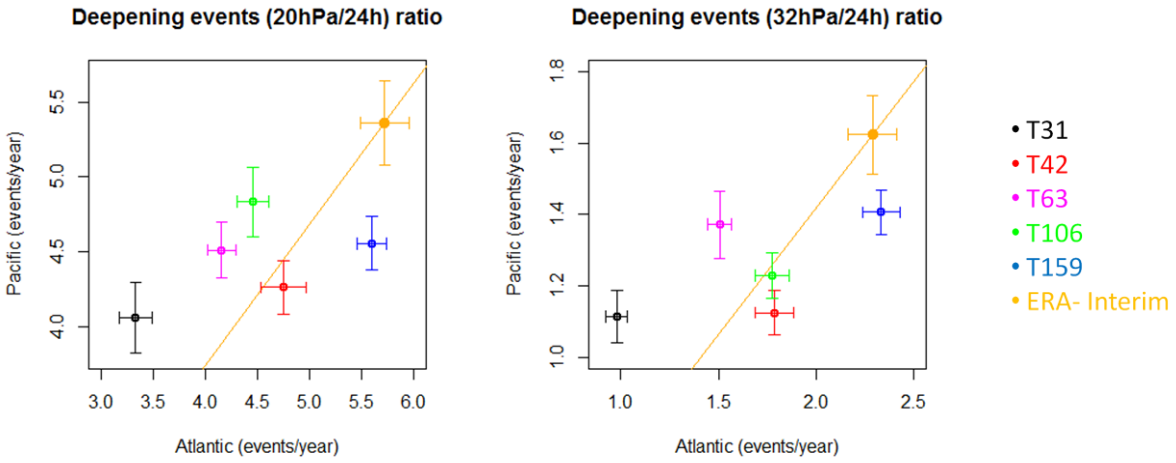

Figure 5.19: Extreme cyclone deepening event density ratios between the Pacific and Atlantic oceans. Shown are ratios for 20hPa/24h deepening events (left) and 32hPa/24h events (centre). Event density averaged over the areas designated for each ocean in figure 4.17. Error bars at 95% confidence. Orange line represents the same ratio as the ERA-Interim reanalysis. Colours of the points and error bars correspond to coloured text on the right part.

In both deepening event types the T42-63-106 points (red, magenta and green respectively) are spread more-less at the same distance from the ERA-Interim point (orange), so again it cannot be said the track densities and Atlantic-Pacific ratios are better represented by ECHAM5 with increasing resolution in a constant way as in the track density diagram for all cyclones (fig. 5.18, left). There is no better performance between T42-63-106.

As before, the Atlantic is more sensitive to resolution: the track density changes with resolution in the Atlantic have a bigger scale compared to the Pacific.

5.2.5: Track zonality comparisons

Procedure:

To calculate track zonality, the algorithm takes track density maps obtained at section 5.1.7. It takes the densities at the areas defined for each ocean in fig. 5.1, and creates the following points:

-Every 2º latitude it calculates the track density maximum, takes the longitude corresponding to the maximum and stores the location.

-Every 2º longitude it calculates the track density maximum, takes the latitude corresponding to the maximum and stores the location.

If several grid boxes have the same maximum density the algorithm creates several points. With the list of points of each ocean, a linear fit is applied. The line obtained will represent the preferred linear path of the cyclone tracks, and its slope the zonality of the cyclone tracks.

This is done with the track densities of all cyclones, 10% strongest cyclones and 1% strongest cyclones, so for each ocean there will be three diagrams comparing the lines of the 6 DATA sets.

Results:

Figure 5.20 shows a comparison of track zonality between the ECHAM5 runs and ERA-Interim at the Atlantic (left column) and the Pacific (right column), taking all cyclones (upper row), the 10% strongest cyclones (middle row), and the 1% strongest cyclones (lower row).

All the linear fits made for the longitude/latitude maxima points are put in the same space so one can distinguish not just the zonality of the track density maxima (more zonality: less slope), but also shifts of the track linear fits (same slope, but moved to the N/W or S/E)

In the upper row (all cyclones) in fig. 5.20, it can be seen that in both oceans the cyclone tracks have more zonality (i.e. less slope) with increasing resolution of the ECHAM5 model runs.

For the Atlantic (upper right) all linear fits from ECHAM5 runs have less slope than the ERA-Interim reanalysis. The T106 (green) and T159 (blue) have most zonality (less slope) of all, and the ERA-Interim line (orange-dotted) is clearly shifted northwards. As commented in section 5.2.3, this is a consequence of the prevalence of NAO+ phase during the time period (1982-2009) of this study: during positive NAO phase, cyclones tend to pass mainly over N Europe, and during negative NAO phase, more cyclones move across S Europe. That is captured in the ERA-Interim reanalysis, but in the ECHAM5 runs (specially the higher resolutions) the symptom is that the NAO+ phase doesn't dominate that much, more cyclones pass through S Europe instead of N Europe and thus the mean track zonality increases (i.e. less meridional slope in the upper-left graph in fig. 5.20.

For the Pacific, zonality also increases with resolution, but this time the higher resolutions T106-159 (green and blue) match very well with the ERA-Interim fit (orange-dotted line)

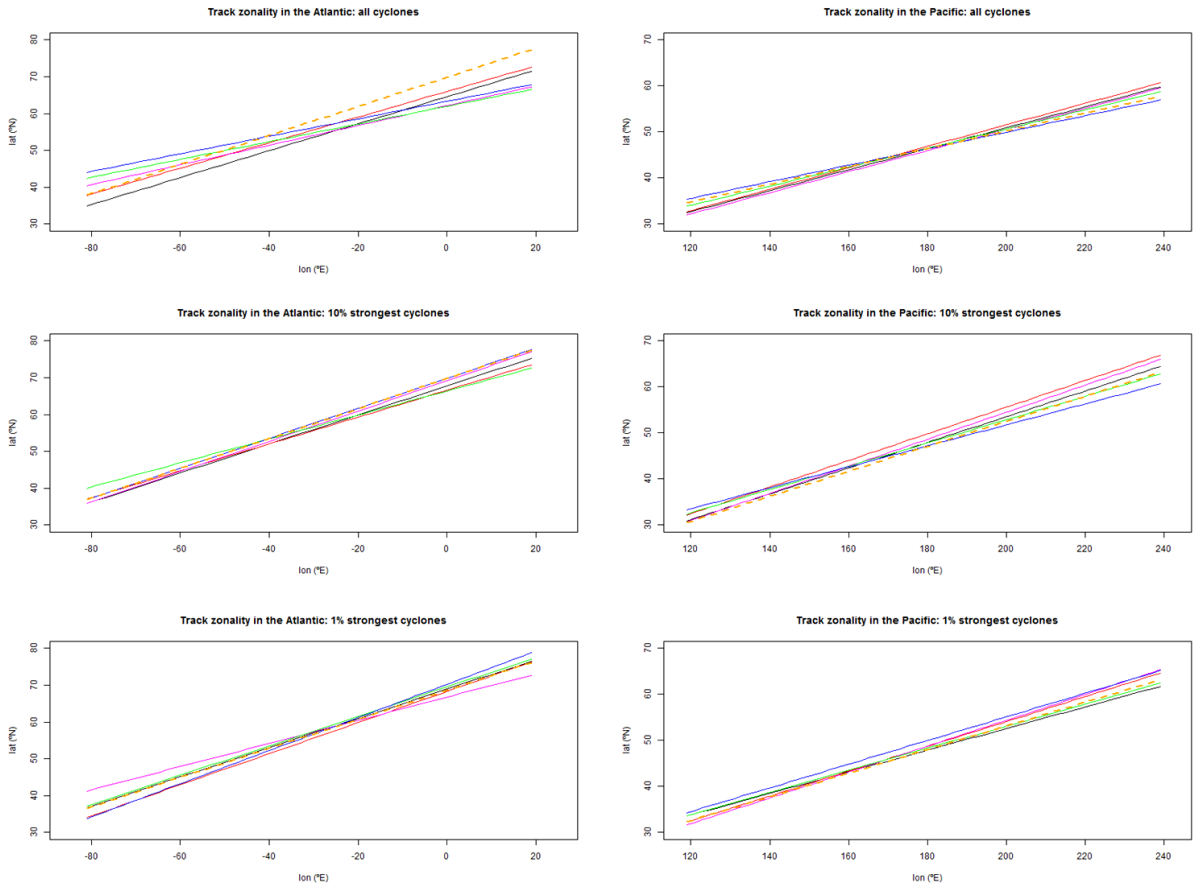

Figure 5.20: Comparison of track zonality for Atlantic (left column) and Pacific (right column). Upper row is for all cyclones, middle row for the 10% strongest cyclones and the lower row is for the 1% strongest cyclones. All lines are linear fits for the track density maxima as detailed in section 3.4.5. Color lines correspond to model runs from the coloured text on the lower right.

When it comes to the 10% strongest cyclones (middle row), the Pacific (right graphic) shows the same tendency as for all cyclones (upper row): less slope at higher resolutions. This time, the T31-42-T63 (black red and magenta) lines have the same slope as ERA-Interim, but they are a bit shifted to the N. T106-159 have again lower slope than the rest, which is a result of the broader areas of high track density seen in this resolutions at section 5.1.7, figs. 5.8 and 5.9.

In the Atlantic, there is no clear tendency: T159 has the highest slope and matches very well with the fit from ERA-Interim, T31-42-63 are very close to T159 and ERA-Interim, and T106 has the lowest slope.

In the case of the 1% strongest cyclones (lower row), in the Atlantic all resolutions have more-less the same slope but T63 (magenta) that has the lowest and T159 (blue) has a bit more slope.

In the Pacific, T31 (black) and T106 (green) have less slope, and T159 has the northernmost linear fit. No clear tendency can be described for any ocean this time.

6: OUTLOOK AND CONCLUSIONS

6.1: Comments for the improvement of the study

Before starting with the conclusions found in this study, first a few comments have to be made about its limitations and ways to improve it.

The ECHAM5 model runs

The data from the ECHAM5 model runs used in this study come from resolutions T31 and T42 (with 19 vertical levels) and T63, T106 and T159 (with 31 vertical levels), all of which have the top level at 10hPa altitude. Meanwhile, the ERA-Interim reanalysis is carried out at T255 and 60 vertical levels ending at 0.1hPa altitude.

Middle atmosphere ECHAM5 configurations with 39 or 90 vertical levels ending at 0.01hPa also exist, at higher horizontal resolutions than T159. Comparing the performance of an ECHAM5 run with horizontal and vertical resolution close to those used at the ERA-Interim reanalysis would give more information about the possible processes that lead to the differences in cyclone properties and spatial distribution between the ECHAM5 runs and ERA-Interim.

Ulbrich et al. (2008) suggest that the ECHAM5 model provides realistic results when studying the storm track activity in the Northern Hemisphere with a resolution of T63 and 19 vertical levels. The results (section 5) from the study done here suggest the opposite.

Pinto et al. (2009) also suggest that the T63 resolution of the ECHAM5 model simulates extratropical cyclones realistically. It has to be taken into account that the NCEP-NCAR reanalysis data that were used for comparison in that study have also a truncation of T63.

Thus, the resolution of the data used as “reality” is important when assessing when a model gives realistic extratropical cyclones.

An improved way to accomplish the comparison made in this study would be interpolating the ERA-Interim SLP fields onto the same truncations of the ECHAM5 model runs before doing the detection and tracking, and then compare the properties of the cyclones appearing at the same resolution of ECHAM5 and ERA-Interim.

The tracking scheme

Although the software used to obtain the data packages did undergo some improvements, it originally dates back to the year 2000 *(Grigoriev et al., 2000).* The closest-neighbour search done for cyclone tracking doesn't take into account the trajectory and velocity of the cyclone and might confuse two cyclones that are close to each other, having more trouble the faster the cyclones move.

Besides, it doesn't distinguish cyclones with one pressure minimum from those that have multiple centres of minimum pressure. In the case of a multicentre cyclone this leads to double-counting for each extra min P centre in the same cyclone. It also leads to double-counting when a cyclone splits or when two cyclones are about to merge and their centre's paths are still very close to each other.

Newer tracking techniques avoid all these problems with schemes that are consistent with the cyclone's movement (*Wernli and Schwierz (2006)* and *Hanley and Caballero (2012)*), and are straightforward while taking into account more processes.

A relatively novel way to deal with multicentre cyclones is by grouping those min P centres within the same closed pressure contour *(Hanley and Caballero, 2012)* and counting them as just one cyclone.

In the study done here, for cyclone track densities, an almost constant size around the cyclone centre was counted in the corresponding grid boxes. A much more objective way to define the area affected by a cyclone would be by counting the grid boxes within a defined closed pressure contour around the cyclone's centre(s), which would count the exact size of the cyclone at every step of its lifetime. Thus, contour mapping of the SLP fields would give the possibility to obtain cyclone track densities and statistics much more realistic than the ones obtained in this study.

In addition, it would tell whether the increased cyclone number in the higher resolutions of the ECHAM5 runs corresponds to missed, too shallow or too small cyclones to be resolved in the lower resolution runs, or to extra min P centres within the same low-pressure system (in which case the cyclone is not missed by the lower resolution, but double-counted in the higher resolutions, actually).

This is to address that using the most up-to-date cyclone detection and tracking schemes (that are much more complete and still work in a simple way) more information could be obtained from the same model runs used in this study.

The couple of problems found in the data also have to be taken into account: track splitting every New Year, and the missing of cyclones in Dec 2003 in the ECHAM5 T63 run due to a defect in the data storage (detailed in Appendix I.2) both of which being as well attributable to the functioning of the tracking scheme.

Restrictions and cyclone selection criteria

In this study, only cyclone tracks of >24h and >1000km are used to obtain the results. This was to get rid of continental thermal lows, monsoon-related cyclones and stationary lows in any statistic or track/event density.

If one looks at figure I.2 from Appendix I, the upper and middle right reconstructed tracks (which fulfil these criteria) seem to be looping around the same point, adding distance in every time step, but remaining in the same area during their lifetime. This is an example to show that probably those limits are not restricting enough.

In both figures II.1 and II.2 from Appendix II, enhanced cyclone generation is observed over land during summer time at T159 resolution (central column) compared to ERA-Interim (right column), which again hints on the not total purge of the undesired thermal lows.

Continental regions of pronounced topography (for example Greenland or the Rockies), were mentioned in section 5.2.3 as problematic for their role in cyclogenesis and track splitting. For the case of the Rockies and the Himalayas, they lay at latitudes where the exaggerated cyclone generation and track density at higher ECHAM5 resolutions (compared to ERA-Interim) could be explained by any of the following: different multicentre cyclone behaviour, exaggerated thermal low formation, or spurious track splitting.

A comparison of the results obtained in this study with the above mentioned restrictions with the same procedure done with much more restrictive criteria, combined with contour mapping (advantages explained above) would give a hint on which is the main cause.

To finish with the criticism in this section, all of the above explained limitations are the same for all the ECHAM5 runs and the ERA-Interim reanalysis data sets, so their interference is very small on the main purpose of this study, which is the comparison of the cyclone characteristics along these data sets, and not their most realistic representation. On the other hand, the application of the different procedures proposed in this section would improve the quality of the results.

The methodology of this study, with its limitations and leaving some open questions, is enough to accomplish the comparison of cyclone characteristics between the ECHAM5 runs and the ERA-Interim in a very simple but efficient way.

6.2: Summary

A comparison of many different extratropical cyclone characteristics has been carried out between ECHAM5 runs at several resolutions (T31-42-63-106-159) and the ERA-Interim reanalysis (taken as reality).

Climatologies

All ECHAM5 runs reproduce the climatological seasonal cycle of minimum pressure (section 5.1.1) and simultaneous cyclone number (section 5.1.2) with a parallel timing. Higher resolutions produce more cyclones and reach lower minimum pressures (expectable from more detailed pressure gradients).

For the climatological distributions of cyclone min P relative frequencies (section 5.1.3), the lower resolutions have their distribution moved towards lower min P in the Pacific, and towards higher min P in the Atlantic. This means that with lower spatial resolution, the strength of the cyclones (in terms of min P) tends to be underestimated in the Atlantic and overestimated in the Pacific.

The climatological distributions of the relative frequencies of cyclone lifetime (5.1.4) and track length (5.1.5) show the same behaviour: cyclone tracks tend to be longer in time and space at lower resolutions, because the cyclone development and strengthening is slower. The Atlantic distributions are more sensitive to resolution change than the ones from the Pacific.

In the climatological intensification rate distributions (5.1.6), it is noted that the relative frequency of the extreme intensification rates (positive or negative) is higher with increasing resolution (i.e. rapid cyclone development happens more often at higher resolutions). Also, the Atlantic distribution reaches more extreme values (it is broader) than the Pacific one.

Comparing winter cyclone track density maps (section 5.1.7), only T106 and T159 resolutions show track densities comparable to ERA-Interim in terms of magnitude and spatial allocation when taking all cyclones and the 10% strongest cyclones. When just counting the 1% strongest cyclones, higher resolutions tend to be closer to ERA-Interim track densities but

none of them represents them properly. In all cases the lower resolutions T31-42-63 show less track density, and the Atlantic has the biggest track density differences with increasing resolution (again, it is more sensitive to resolution).

Comparing winter cyclone deepening event density maps (5.1.8), a similar thing happens: higher resolutions tend to be closer to ERA-Interim event densities but none of them is realistic. The lower resolutions T31-42-63 show less event density and the Atlantic is more sensitive to resolution.

Sections 5.1.7 and 5.1.8 (track and deepening event density maps) show that when the cyclones that are counted in the maps are more extreme, the performance of the ECHAM5 runs looks worse.

Relationships between variables

Minimum pressure vs lifetime (5.2.1) and track length vs lifetime (5.2.2) 100-cyclone averaged relationships confirm what was seen in sections 5.1.3 to 5.1.6: with increasing resolution cyclones tend to develop faster, needing a shorter lifetime to reach the same min P or track length. The Atlantic is more sensitive to resolution change, and (in contrast to the Pacific) shows important differences from ERA-Interim at lower resolutions.

The summer and winter track density differences between the ECHAM5 runs and ERA-Interim (5.2.3) show the following:

-The negative track density anomalies are biggest where the track densities at ERA-Interim are higher at lower resolutions T31-42 especially, hinting that there the counting of multicentre cyclones plays an important role.

-Positive track density anomalies appear near areas of pronounced topography (Greenland, the Rockies or the Himalayas) which indicates exaggerated cyclone generation / track splitting in these problematic areas *(Hanley and Caballero, 2012).* Also, positive anomalies appear in mid-latitude continental areas during summer because of non-removed thermal lows.

-There is a clear North-South winter track density anomaly contrast over Europe at higher resolutions T106-159 that matches perfectly the track density changes with NAO phase addressed by *Pinto et al (2009).* This explains the track density anomalies over Europe, and tells that, in the Atlantic, prescribed oceanic SST and ice coverage do not force the same atmospheric mean state (the predominant positive winter NAO phase that occurred during the

time period studied here, 1982-2009, appears in the ERA-Interim reanalysis but not in the ECHAM5 runs forced with the same observed SST during this period).

Since the track density is very dependent on the NAO phase, this would in turn explain why the Atlantic is more sensitive to resolution change (the SST contrasts get smoothed with lower resolution and won't force towards the real atmospheric mean state that much), and why the performance of the ECHAM5 runs gets apparently worse when counting extreme cyclones (their occurrence is even more dependent on the NAO phase as showed by *Pinto et al. (2009)*).

For extreme cyclones in the Atlantic, comparisons should be made taking situations happening during the same NAO phase to discern whether for that NAO phase the track / deepening event densities are similar to ERA-Interim (in which case the cause of the differences would be the predominance of other NAO phase and not an unrealistic representation of extreme cyclones in the model run).

-A similar process concerning the strength of the Aleutian Low is responsible for the differences in track density anomalies over the Pacific. As explained in section 2.4, this would mainly affect just the spatial distribution of the cyclones and not their intensity or other properties. This is why the Pacific is less sensitive to horizontal resolution change than the Atlantic in many of the result sections.

The track / deepening event density ratio diagrams (5.2.4) show that the improvement of the veracity of cyclone characteristics with increasing resolution is not constant (just in the case of all cyclone track densities the track density and ratio come closer to the values of ERA-Interim with increasing resolution in a linear and constant way).

The track zonality comparison (5.2.5) captures the increased zonality and southward shifting of the cyclone tracks in the Atlantic in the ECHAM5 runs compared to ERA-Interim (at all cyclones) due to a less positive predominant winter NAO phase. It also shows the increased zonality with higher resolution in the Pacific (all cyclones and 10% strongest cyclones) due to a broader distribution of the high track density area.

6.3: Concluding remarks

The main goals of this study were to describe the sensitivity of extratropical cyclone characteristics to horizontal resolution, and to assess at which resolution they start being realistic.

Concerning the first question, cyclone characteristics are indeed very dependent on resolution in the ECHAM5 runs compared to ERA-Interim in this study. As expected from *Blender and Schubert (2000)*, *Jung et al., (2006)*, fewer cyclones are detected at lower resolutions.

A new finding is that the Atlantic Ocean shows much higher sensitivity to resolution change than the Pacific, and the track density anomalies over the Atlantic and Europe suggest that the predominant NAO phase is not forced by the prescribed SST in the ECHAM5 model. This in turn would affect the representation of extreme cyclones whose occurrence depends a lot on the NAO phase *(Pinto et al. 2009).* In the Pacific, the mean atmospheric state also differs from the reanalysis (Aleutian Low strength), but only affects cyclone spatial distribution and not other properties.

The cyclone characteristics get more realistic the higher the resolution of the ECHAM5 is, but not in a constant way (in contrast with *Roeckner et al., 2006*). This relationship gets less clear when taking more extreme cases.

Concerning the second goal of the study, T106 and T159 have a realistic representation of cyclones in most of the cases, in contrast with earlier studies by *Ulbrich et al., 2008* and *Pinto et al., 2009* that suggest T63 having realistic cyclones. This has to be taken with caution since the set describing "reality" in this study has a higher resolution T255. Also, all resolutions match much worse with ERA-Interim when taking extreme cyclones.

Four main processes are found responsible for the differences in the cyclone number and densities between the different resolutions of the ECHAM5 runs:

-The double counting of multicentre cyclones and related merging / splitting events.

-Different lee-trough effect on cyclones that pass over pronounced topography

-Tracked and non-removed thermal lows

-A different mean atmospheric state not totally forced by the prescribed SST and ice coverage.

To discern how big is the role of each one of those, a more advanced cyclone detection and tracking algorithm should be used (with the need of contour mapping to deal with the multicentre cyclones), along with more restrictive cyclone selection criteria.

Also, it would be interesting to compare the different ECHAM5 runs with the ERA-Interim data interpolated onto lower spatial resolutions to remove the effect of smoothed SLP fields at lower resolution when detecting and tracking the cyclones, as well as using an ECHAM5 run with similar resolution to the original ERA-Interim reanalysis data to compare without any significant resolution difference and detect problematic areas.

APPENDIX I

I.1: Data format

The cyclone tracks are grouped into one file every year. The data file has extension ".trk" and is similar in appearance to an ASCII file. Figure I.1 shows an example of the distribution of the cyclone track information in the file.

It has to be pointed out that the file format ".trk" cannot be computed straight away with the software used for this study (mathematical software "R" by ***cran***.*r-project.org*). Thus, a format change is required for computation (described in Appendix I.3).

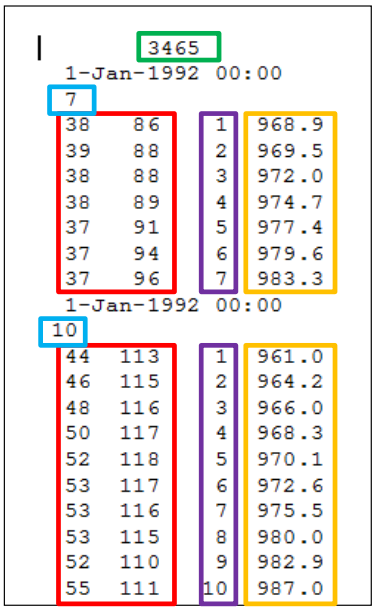

Figure I.1: Screen caption of the beginning of the data file with cyclone tracks of year 1992 from ERA-Interim reanalysis. Highlighted in color boxes:

- **Number of cyclones in that year**
- **Lifetime of the cyclone (time-steps)**
- **Spatial coordinates of the cyclone centre (polar stereographic projection 181x181)**
- **Time coordinates during the cyclone's lifetime**
- **Central (minimum) pressure (hPa) at each time**

The data files consist, for each year, of a list of all the cyclones and the properties of their centre during the cyclone lifetime. These properties are: location, time of the year and central (minimum) pressure. The first green header tells the number of cyclones that are stored in that year. The blue header tells the lifetime of each cyclone on top of its information. These two headers (green and blue) will guide the R algorithm when pre-processing the data into an ".RDat" file (see Appendix I.3) that can be handled and computed with the R programme.

Below the blue header the information of the cyclone track is stored. The first two columns (red boxes) show the spatial location of the cyclone centre at each time, in polar stereographic projection coordinates 181x181, so both columns will range from 1 to 181.

Inside the violet box the time coordinate is placed. The data are of 6h time resolution (4x daily), so the number of time steps in each year will be 1460 (1464 in leap years). Therefore the values in the violet column will lay within the 1:1460/1464 interval.

The last column (orange boxes) shows the pressure in hPa of the cyclone centre for each time.

Also, the corresponding date when each cyclone starts is shown on top of its information, but this is redundant since a time coordinate (violet boxes) is given already, and is not assigned any use when storing the data into another format (Appendix I.3).

I.2: Data problems

There are two features in the data that caused problems while computing the results. The cyclone track information of year 2003 from the ECHAM5 T63 resolution ends on 6th of December, making the cyclones from almost all that month to be missed. For this reason winter 2003/04 of T63 resolution is discarded from any statistic or climatology.

The second and most important problem is that the cyclone tracks are “cut” every year because the cyclone tracking procedure is seemingly reset. The cyclone tracks that start at the end of December and finish at the beginning of January of the next year are in practice divided into two: for December, just the part of the track until the last time coordinate of the year (1460 or 1464) is saved; for January, the part of the track from time coordinate 1 onwards is saved like another different cyclone. All of this with the limitation that any cyclone has to have a lifetime of at least 4 time steps.

This leads to the following scenarios. As an example, if one hypothetic cyclone has a total lifetime of 8 time steps distributed like so: 6 in December and 2 in January; the cyclone is saved in December with a lifetime of 6 time steps, and the 2 steps of January are lost: they won’t be saved in the data, because the algorithm recognizes that as a new, short cyclone of just 2 steps and discards it. In the contrary case, the same would happen if there were 2 steps in December and 6 in January: the track part in December would be discarded.

In the case of a hypothetic cyclone of 6 time steps, that lays 3 in December and 3 in January, the entire track is lost, even though it actually meets the minimum lifetime criterion.

This happens to a small part of the cyclones compared to the total number of them, but affects winter statistics and climatologies in a subtle way, thus diminishing their consistency. If the climatological mean number of simultaneous cyclones is computed at every time step with the raw data to show the climatology of the seasonal cycle of cyclone number (as in section 5.1.2), it drops very significantly at the beginning and the end of the year.

Being this the most obvious example of the problem (and how it was found out), it also may affect other statistics strongly: for example, by hiding very intense cyclone strengthening events (extreme pressure drops within 24h, named “bombing” or “explosive” cyclogenesis by the media). These cases are rare and are almost entirely delimited to winter time, making the loss of one single event that (very inconveniently) happened around New Year, to be very significant for the climatological mean number of these type of events in that area.

This problem can be solved partially, reconstructing the cyclone tracks that jump year by linking the two track parts of December and January so they can be accounted properly in the statistics and climatologies (see full procedure in Appendix I.4). Yet, the track parts shorter than 4 time steps are not within the data files and cannot be reconstructed, so they will remain missing after the track reconstruction is carried on. However, being the track reconstruction the most that can be done with the data available and not solving the problem completely, it is shown in section 5.1.2 that it does a good job and that the cyclone tracks that couldn’t be fixed were a minority.

I.3: Data pre-processing

The “.trk” files are converted into “.RDat” format for computational purposes with an algorithm that works in the following way:

The data are stored by year, and all files of years 1982-2009 from the same ECHAM5 resolution / ERA-Interim reanalysis are packaged in the same folder.

Referring back to fig. I.1 (Appendix I.1), the algorithm guides itself by the green and blue headers, as well as by the spacing in the chart.

It is programmed with a nested loop to open the 28 files (years) of each data package one by one. Once the file is opened it detects all the rows with blank spacing (where the four columns are not all filled). It can be seen in fig. I.1 (Appendix I.1) that the first row not entirely filled contains the green header, and then the rest are pairs of rows with date (not used) and the blue header, that separate the information of every cyclone track.

The algorithm creates a list with the information of the rows with blank spaces. The first one of the list is the green header (number of cyclones in that year). The amount of blue headers (showing each cyclone's lifetime) appearing in the file must be the same as the number in the green header.

In the example of fig. I.1, the list created by the algorithm would be:
(3465, date, 7, date, 10, ...). It will take the first value (3465) and assign it as the number of iterations to do in the next inner loop, and will read the next 3465 impair positions of the list *(7, 10, ...).* In the first iteration of the inner loop the algorithm will detect the row containing the blue header *(7)* and will read the 7 rows after the header, which contain the first cyclone track information. All the columns in these 7 rows are saved into a predefined array. In the second iteration of the inner loop the algorithm will read the 10 rows after the blue header *(10)* and save all the columns in those 10 rows in the same array. And so on until doing the 3465 iterations with the file, saving all cyclones of that year, and then opening the next file/year of the 28 in the package and doing the same with all.

After all outer and inner iterations are done; the array will contain the information of all cyclones and all years of the ECHAM5 resolution (or ERA-Interim reanalysis) data package. The array is of dimensions (28 x 4000 x 180 x 4), meaning: [year, cyclone, step, information]. The information is stored in the same order as in the original files: variables 1 and 2 for spatial coordinates, 3 for the time, and 4 for the pressure.

For example, [13, 1, 1:7, 4] in the array would correspond to the list of pressures (variable 4, steps 1 to 7) of the first cyclone of the 13th year in the data: 1992 (upper orange box in fig. I.1!!!).

Since the number of cyclones varies every year, and every cyclone has different lifetime, the dimensions have to exceed the maximum of those values in order to not miss any information, and the remaining lots in the array are filled with NA's. The number of cyclones in a year, or the lifetime of a certain cyclone can be easily obtained by "R" by calling the amount of non-NA values in the corresponding dimension.

Defining the array this way makes it possible to handle all the information together. In total, 6 arrays of this type are created for each of the 5 resolutions used from ECHAM5 model and the one from ERA-Interim reanalysis.

At a second stage, the algorithm first converts variables 1 and 2 (space coordinates: 181x181 polar stereographic projection) into geographical coordinates (1 for longitude (ºE) and 2 for latitude in ºN) thanks to a function provided by the data source along with the file packages. Then it expands every array by adding two variables to the last dimension, making the arrays look like (28 x 4000 x 180 x 6), again being [year, cyclone, step, information].

Information variable 5 is assigned to the pressure difference between each step and the one before (variable 4: pressure, at each step, minus variable 4 at step-1), i.e. the intensification rate in hPa/6h.

Information variable 6 is assigned to the distance in km travelled by the cyclone at each step. It is calculated taking the position of the cyclone centre at each step and calculating the distance with the position at step-1 with the following formula:

$$\boldsymbol{Distance} = \sqrt{[\boldsymbol{Ec} \times (\Delta º\boldsymbol{lat})]^{\boldsymbol{2}} + \left[\boldsymbol{Ec} \times (\Delta º\boldsymbol{lon}) \times \boldsymbol{cos}(\frac{\sum º\boldsymbol{lat}}{\boldsymbol{2}})\right]^{\boldsymbol{2}}}$$

Being ***Ec*** the Earth's circumference in km (2 x Π x 6371) divided by 360 (i.e. km per degree). Since the movement of a cyclone in 6h spans only a few degrees of longitude and/or latitude, taking the cosine of the mean latitude to weight the zonal distance will bring an insignificant error in the calculated distance in km. The algorithm accounts for cyclones that cross the Greenwich Meridian (from right below 360ºE to right above 0ºE): if $(\Delta º\boldsymbol{lon})$ is more than 180 it adds 360º to the longitude close to, but East of 0ºE so the difference with the other zonal location is realistic. Since it is squared right after, the resulting sign of the zonal distance in degrees is of no importance.

Summing up, the algorithm converts all six data packages (ECHAM5 resolutions T31/42/63/106/159 and the ERA-Interim Reanalysis) into six arrays of dimensions:
(28 x 4000 x 180 x 6), corresponding to [year, cyclone, step, information].
The information in the last dimension consists of 6 variables being: 1(longitude ºE), 2(latitude ºN), 3(time step), 4(pressure hPa), 5(intensification rate hPa/6h) and 6(distance km).

This array set is given the name “DATA” in order to not repeat “array with cyclone track information of model output...”, and to avoid redundancies, since other arrays are created later on for other purposes.

I.4: Cyclone track reconstruction

In this section the strategy to reconstruct those tracks cut by the year change (problem described in Appendix I.2) will be disclosed. This is carried out in four steps:

-First, for every year, all cyclones ending on 31st of December, and all cyclones starting 1st of January are taken from the DATA and are separated into two new arrays.

This is done by an algorithm that looks at the first and last steps of every cyclone: if the last step of the cyclone has a time coordinate 1460 (or 1464 for leap years), that time coordinate is the last of the year and the cyclone is copied into the array of ending-year-cyclones. If the time coordinate of the first step is 1, the cyclone is copied into the array of starting-year-cyclones.

A back-up array is created for both ending/starting-year-cyclones containing the year and cyclone number in the DATA as tags of those cyclones that were copied.

-In the second step, the algorithm takes the last two positions of all ending-year-cyclones to calculate their last trajectory and projects a “first-guess” position onto 1st of January (one step forward in time), applying the following formula:

$$*\boldsymbol{X}_{t+1} = \boldsymbol{X}_t + (\boldsymbol{X}_t - \boldsymbol{X}_{t-1})$$

Being $*\boldsymbol{X}_{t+1}$ the first guess position and $\boldsymbol{X}_t$ and $\boldsymbol{X}_{t-1}$ the last two positions of the track. This is a similar scheme to the one used by Wernli and Schwierz (2006) and Hanley and Caballero (2012) but accounting for the full distance $(\boldsymbol{X}_t - \boldsymbol{X}_{t-1})$ instead of 75%, since acceleration of cyclones is also observed, especially in winter.

Then the algorithm compares $*\boldsymbol{X}_{t+1}$ of all tracks that end 31st of December (blue track in fig. I.2) with the first positions of the tracks starting 1st of January of the next year (red track in fig. I.2), and if any of them lays less than 500km away from $*\boldsymbol{X}_{t+1}$ the algorithm

connects both tracks, and pairs the tags of the corresponding cyclones in the back-up array created in the earlier step. One limitation is used at this point: if both (blue and red) tracks don't add up a total distance travelled by the cyclone of 1000km the algorithm doesn't connect them, since only cyclones of tracks longer than 1000km will be taken into account in this study.

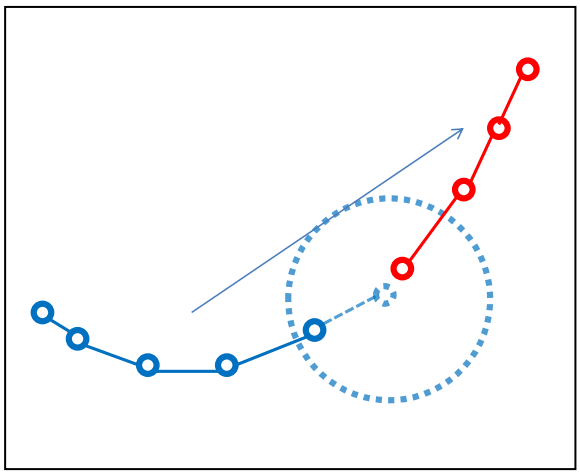

Figure I.2: Representation of the tracking scheme used for reconstruction:
-Blue track ends 31st Dec
-Dotted blue point is the "first-guess" position
-Dotted circle is 500km search distance
-Red track starts 1st Dec
-Arrow indicating space-time direction

-The third step is used when several different tracks are connected to the same one. In this case two scenarios are distinguished:

- Splitting events when one track ending 31st Dec is connected to various starting 1st Jan.
- Merging events when one track starting 1st Jan is connected to various ending 31st Dec.

These events are recognized by the algorithm looking at the tag pairs listed earlier when connecting the tracks. If an ending-year-cyclone tag is repeated, it means that it has been connected to different starting-year-cyclones and the procedure for splitting events is applied. If a starting-year-cyclone tag is repeated, it means that it has been connected to different ending-year-cyclones and the procedure for merging events is applied.

The "dominant" track is defined as the one that is less deviated from its path. Within the distances considered in the scheme for track reconstruction (500km), the large-scale forcing on the cyclones can be considered the same, so the track that suffers less acceleration is the "dominant" for having more inertia, in a simple and useful application of Newton's second law ($F=ma$) to cyclone motion.

For the case of splitting events, represented in fig. I.3, two (red) tracks diverge from the (blue) one ending 31st Dec.

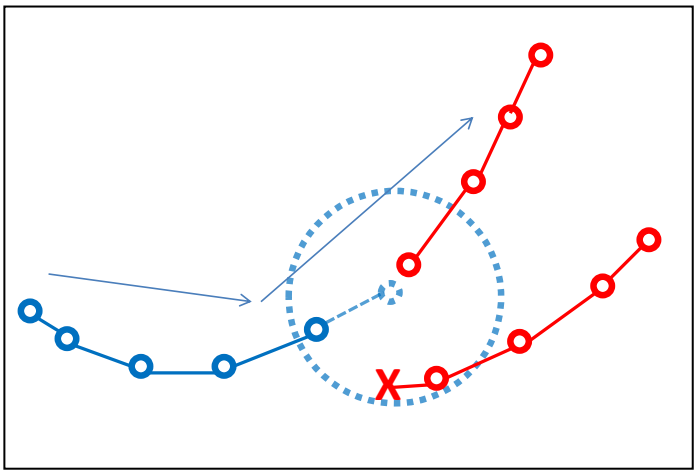

Figure I.3: Representation of a splitting event

-Blue track ends 31st Dec
-Dotted blue point is the "first-guess" position
-Dotted circle is 500km search distance
-Red tracks start 1st Dec
-Red cross indicates discarded track
-Arrow indicating space-time direction

Here the same formula is applicable as when the connecting is done: $*X_{t+1}$ is calculated, and the (red) track starting closer to it is the one that would have suffered less acceleration. Thus the other(s) are discarded and their connection and tag pair is erased from the back-up array.

For the case of merging events, represented in fig. I.4, two (blue) tracks converge onto one (red) starting 1st Jan.

Figure I.4: Representation of a merging event

-Blue tracks end 31st Dec
-Dotted red point is the "first-guess" position
-Dotted circle is 500km search distance
-Red track starts 1st Dec
-Blue cross indicates discarded track
-Arrow indicating space-time direction

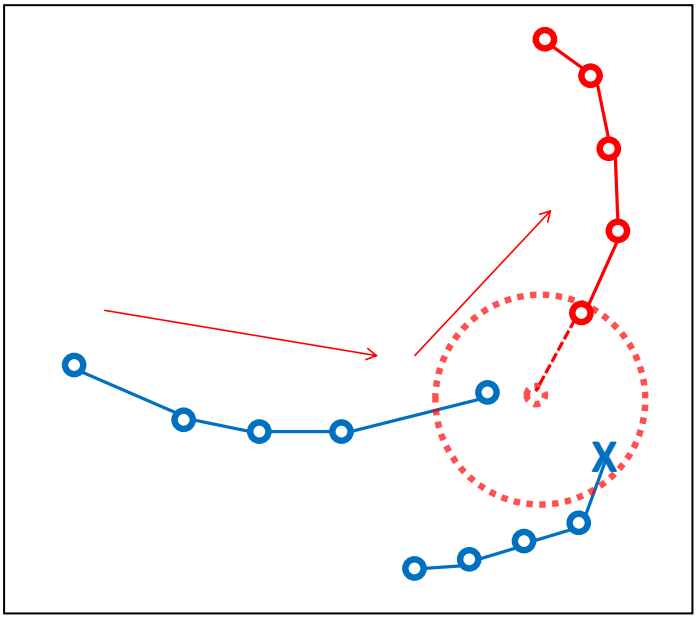

Here the "first-guess" positions following the blue tracks would point to the red track more or less equally, so the procedure goes the other way round: $*X_{t-1}$ is calculated for the red track (projection one step backward in time onto 31st Dec as in fig. I.4) with formula:

$$*X_{t-1} = X_t - (X_{t+1} - X_t)$$

The blue track which has the last position closest to $*X_{t-1}$ is considered the "dominant" since it would undergo less acceleration to follow the red track's path, following the same inertia criterion as for splitting events. The rest of (blue) tracks that lay further are discarded and their connection and tag pair are erased from the back-up array.

-Once the repeated connections from all winters are cleaned-up, the remaining reconstructed tracks have to be put into the DATA. In this last step the back-up array with the tag pairs (with cyclone year and number) of the reconstructed tracks is useful.

For every tag pair the algorithm takes from the DATA the cyclone of year and number specified in the tag.

In the ending-year-cyclones, it puts all the information of its starting-year-cyclone pair after the last step. Since the starting-year-cyclone has time coordinate 1-onwards, 1460 (1464 for leap years) is added in all steps so the time coordinate follows chronological order in the time scale of the ending year.

In the starting-year-cyclones, their information is "cut", all the information of the corresponding ending-year-cyclone pair is put at the beginning (subtracting 1460/64 from its time coordinate so it is in chronological order respect to the scale of the new year), and then the starting information is "pasted" again after the last step of the ending-year-cyclone.

In this way, the cyclone tracks that jump year are represented in both years in the DATA. The time scaling is done to avoid double-counting in some statistics and climatologies: the cyclones which have a negative time coordinate in their first step (because 1460/64 is subtracted from the ending-year cyclone time coordinate in all steps) are not counted.

After all of the above explained procedure in this section is applied to the six DATA arrays, they are ready for the results to be acquired from them.

Further comments and examples of reconstructed tracks

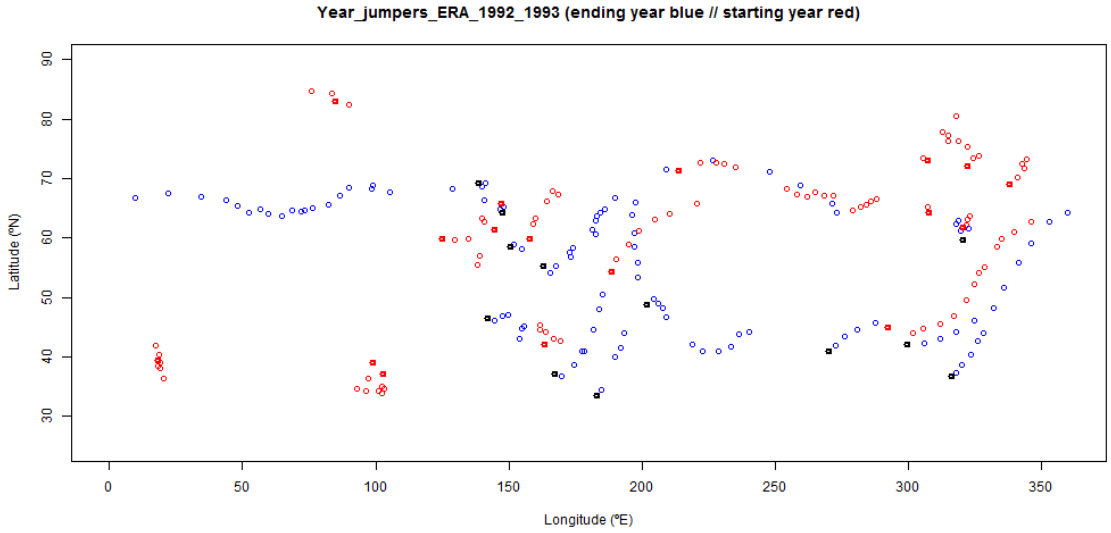

Figure I.5: Map with all cyclone tracks that end the 31st of December 1992 (blue points), and all cyclone tracks that start the 1st of January 1993 (red points), from the ERA-Interim reanalysis data set. Highlighted points (doubled width) are the first position of each track part.

Figure I.5 shows an example of the panorama that the track reconstruction algorithm finds every New Year before starting to search and link the correct parts of the cut tracks.

The track reconstruction scheme used for solving the problem of cut tracks every New Year (explained in Appendix I.2) was chosen because it was the one that offered the best performance: several schemes with different parameters were tried, with a strong increase of cases when multiple tracks were linked to the same ending-year (blue) or starting-year (red) track.

To avoid missing fast-travelling cyclones, the search was not made around the last position of each blue track, but around the projected $^{*}\boldsymbol{X}_{t+1}$ position (with the same formula explained earlier in this section), which takes into account the cyclone's trajectory and velocity:

$$^{*}\boldsymbol{X}_{t+1} = \boldsymbol{X}_{t} + (\boldsymbol{X}_{t} - \boldsymbol{X}_{t-1})$$

The search around the projected $*\boldsymbol{X}_{t+1}$ position using D<600km gave 1008 reconstructed tracks (within all 27 winters and the 6 DATA sets), from which 155 were found to have repeated track parts: multiple track parts linked to the same ending-year or starting-year track part.

With a distance D<500km, 926 tracks were reconstructed, from which 95 had repeated track parts, which tells that the increased number of reconstructed tracks with increased D was mainly due to multiple track linking: a false positive.

When applying the same distance D<500km with the restriction of the total track length being >1000km, 872 tracks are reconstructed and just 52 have repeated track parts. Again, this new restriction eliminates repeated track linking most of the times, and doesn't miss the true tracks that are the goal of the reconstruction algorithm.

In the third step for track reconstruction (detailed in this section), the algorithm deals those 52 tracks as merging or splitting events, applying the cyclone inertia criterion to decide which track is the dominant, ending up with 843 reconstructed tracks (obviously not all of the 52 tracks will be eliminated in the process: when a track part is linked multiple times to others, just one from those multiple links is saved as the dominant, so a bit less than half of those 52 repeated tracks will remain).

Figure I.6 shows the individual tracks reconstructed from all those appearing in figure I.5 that are cut by the year change from 1992 to 1993

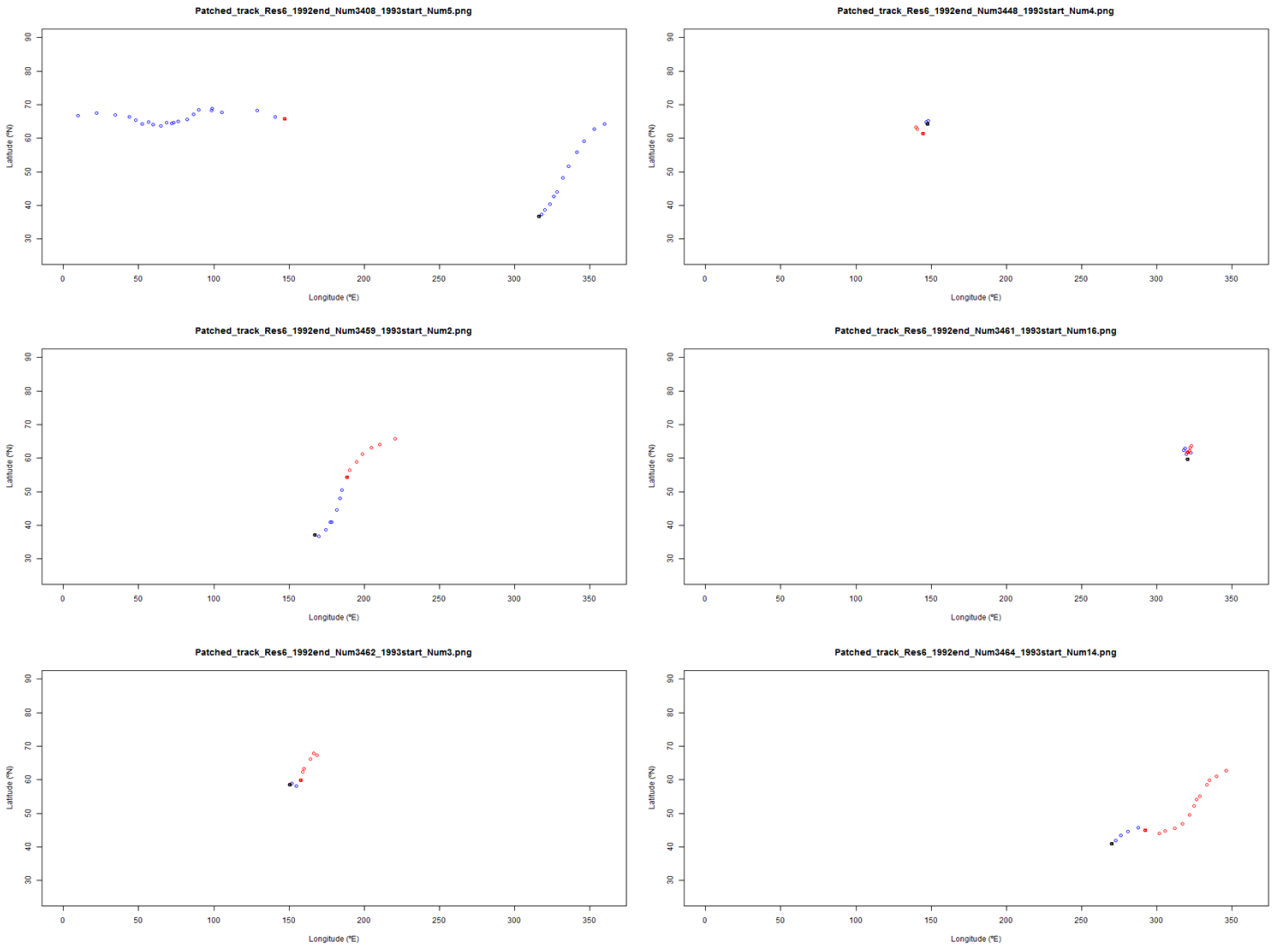

Figure I.6: Maps with all individual reconstructed cyclone tracks sorted by the track reconstruction algorithm from the cyclone tracks that appear at figure I.1. The part of the tracks that end the 31st of December is blue, and the part starting the 1st of January is red. Highlighted points (doubled width) are the first position of each track part.

APPENDIX II: Monthly cyclone generation maps

Here the maps will show where cyclone generation takes place in each month of the year. Only maps for ECHAM5 T31 and T159 resolutions will be made to compare them with the ERA-Interim maps, since the amount of maps will be much higher.

For those three DATA sets, the algorithm will take cyclone tracks of more than 24h and 1000km. No spatial or temporal restrictions are applied as in earlier sections. Once the algorithm checks that the cyclone meets the criteria to be counted, it looks at the information at its first step. The month when the cyclone generated can be computed from the first time coordinate (variable 3 in the DATA array). The +1 count on the map is done for the location of the cyclone at its first step, in the same way as in 5.1.7-5.1.8: in the 5x5 grids area centred at the cyclone's location.

For each of the 3 DATA sets selected, maps of every month are done for each year. January of the first year (1982) is discarded, since it might contain information of cyclones generated earlier in December. As addressed in Appendix I.2, the part of those tracks that happens in January may be stored as a new cyclone, showing more cyclone generation in that month. The track reconstruction (Appendix I.4) solved this problem for the rest of the years, but given that the DATA sets start in 1982 it can't be done for the first month.

For each of the 3 DATA, and for every month, the algorithm makes a mean of all years (28, 27 for January) at each grid box, giving the climatological mean of cyclone generation events in that month.

All of this is done taking all cyclones (for figure II.1), and those with min P <990hPa (for figure II.2).

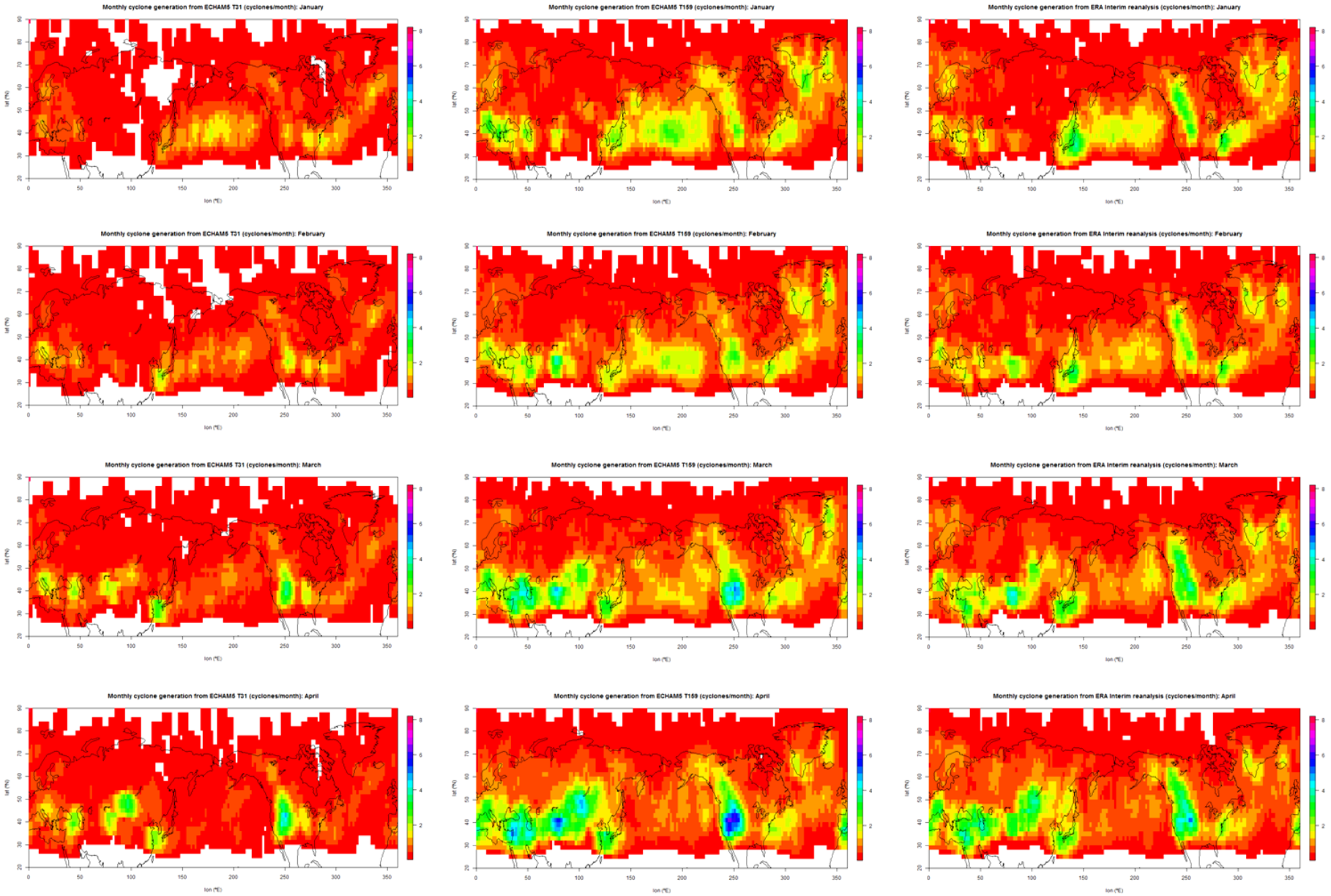

Figure II.1: Monthly cyclone generation maps for ECHAM5 T31 resolution (left column), T159 resolution (central column) and ERA-Interim reanalysis (right column).
1st row is January
2nd row is February
3rd row is March
4th row is April

White spaces correspond to zero generation events per year. Same colour scale used for the rest of generation densities

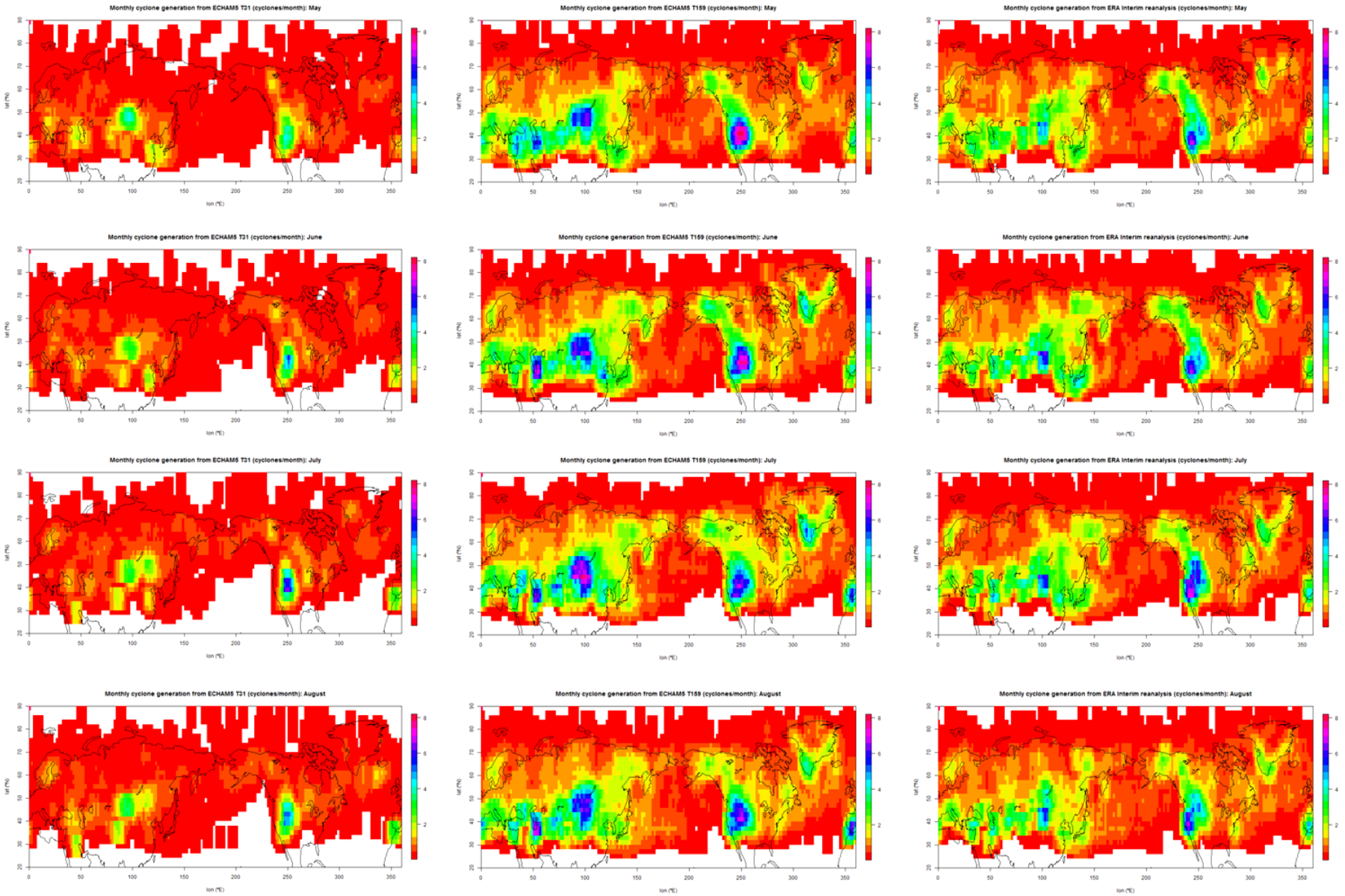

Figure II.1 (continues): Monthly cyclone generation maps for ECHAM5 T31 resolution (left column), T159 resolution (central column) and ERA-Interim reanalysis (right column).
1st row is May
2nd row is June
3rd row is July
4th row is August

White spaces correspond to zero generation events per year. Same colour scale used for the rest of generation densities

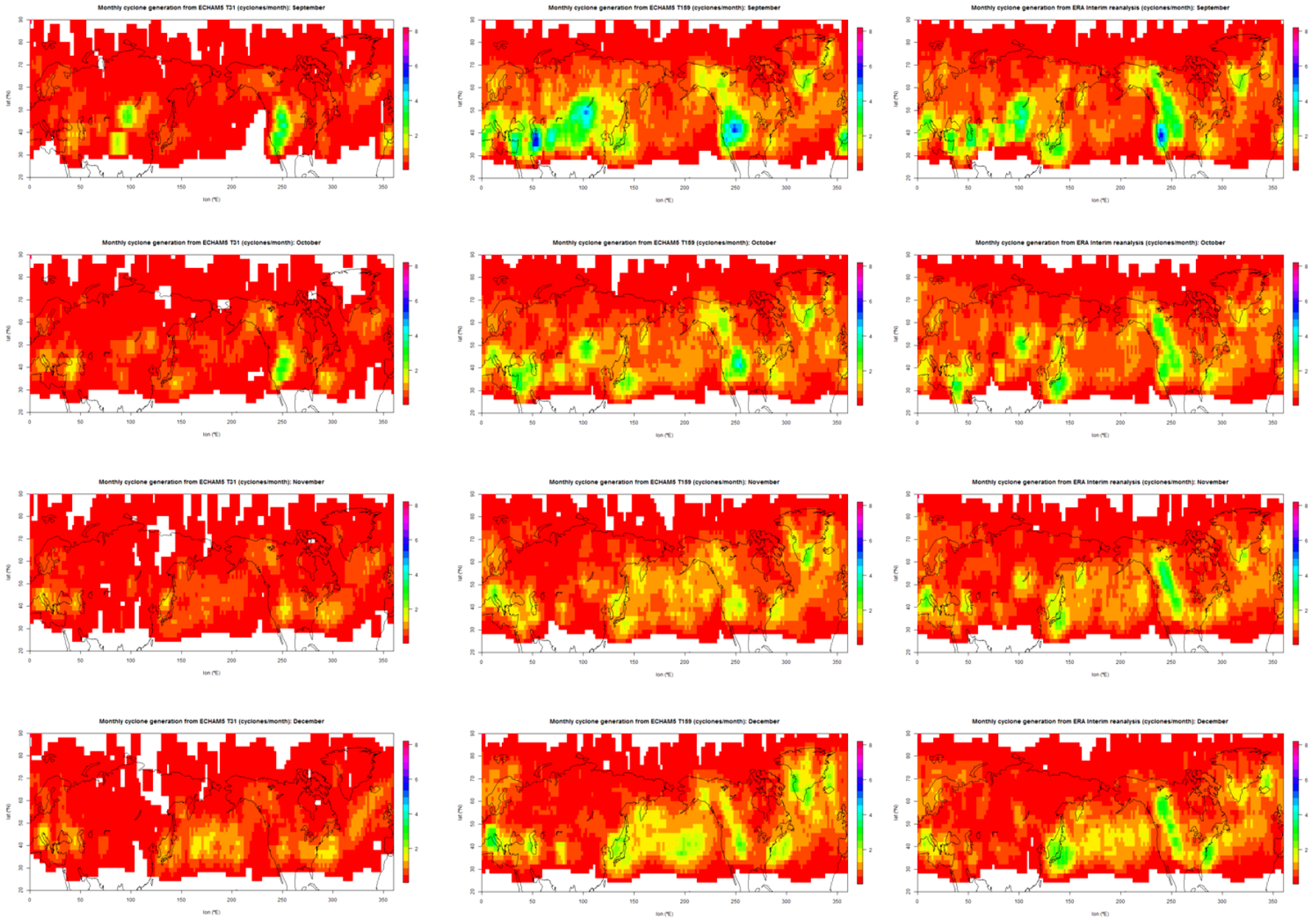

Figure II.1 (continues): Monthly cyclone generation maps for ECHAM5 T31 resolution (left column), T159 resolution (central column) and ERA-Interim reanalysis (right column).
1st row is September
2nd row is October
3rd row is November
4th row is December

White spaces correspond to zero generation events per year. Same colour scale used for the rest of generation densities

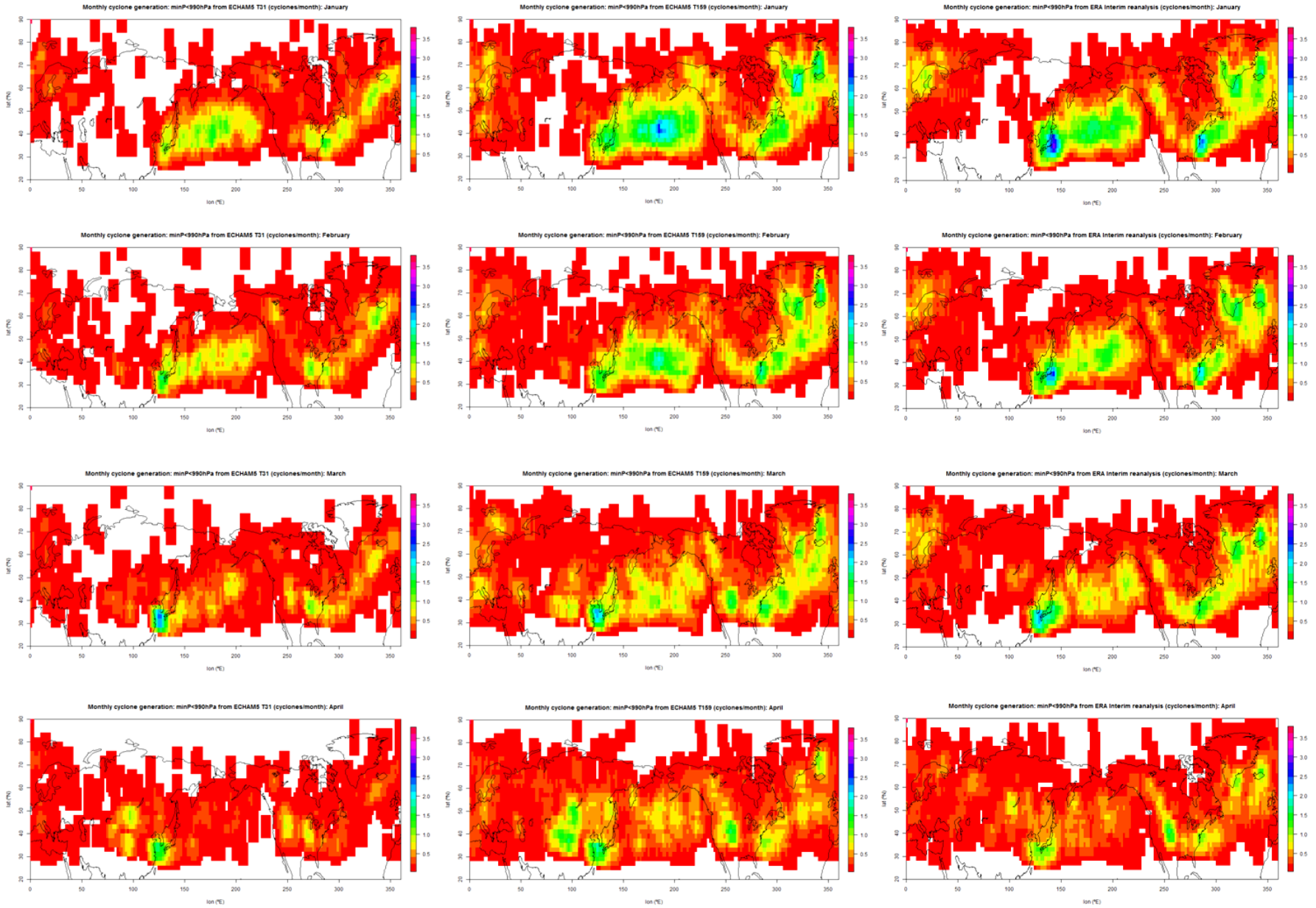

Figure II.2: Monthly cyclone generation maps: only cyclones that reach a min P of 990hPa or lower.

Shown are: ECHAM5 T31 resolution (left column), T159 resolution (central column) and ERA-Interim reanalysis (right column).
1st row is January
2nd row is February
3rd row is March
4th row is April

White spaces correspond to zero generation events per year. Same colour scale used for the rest of generation densities

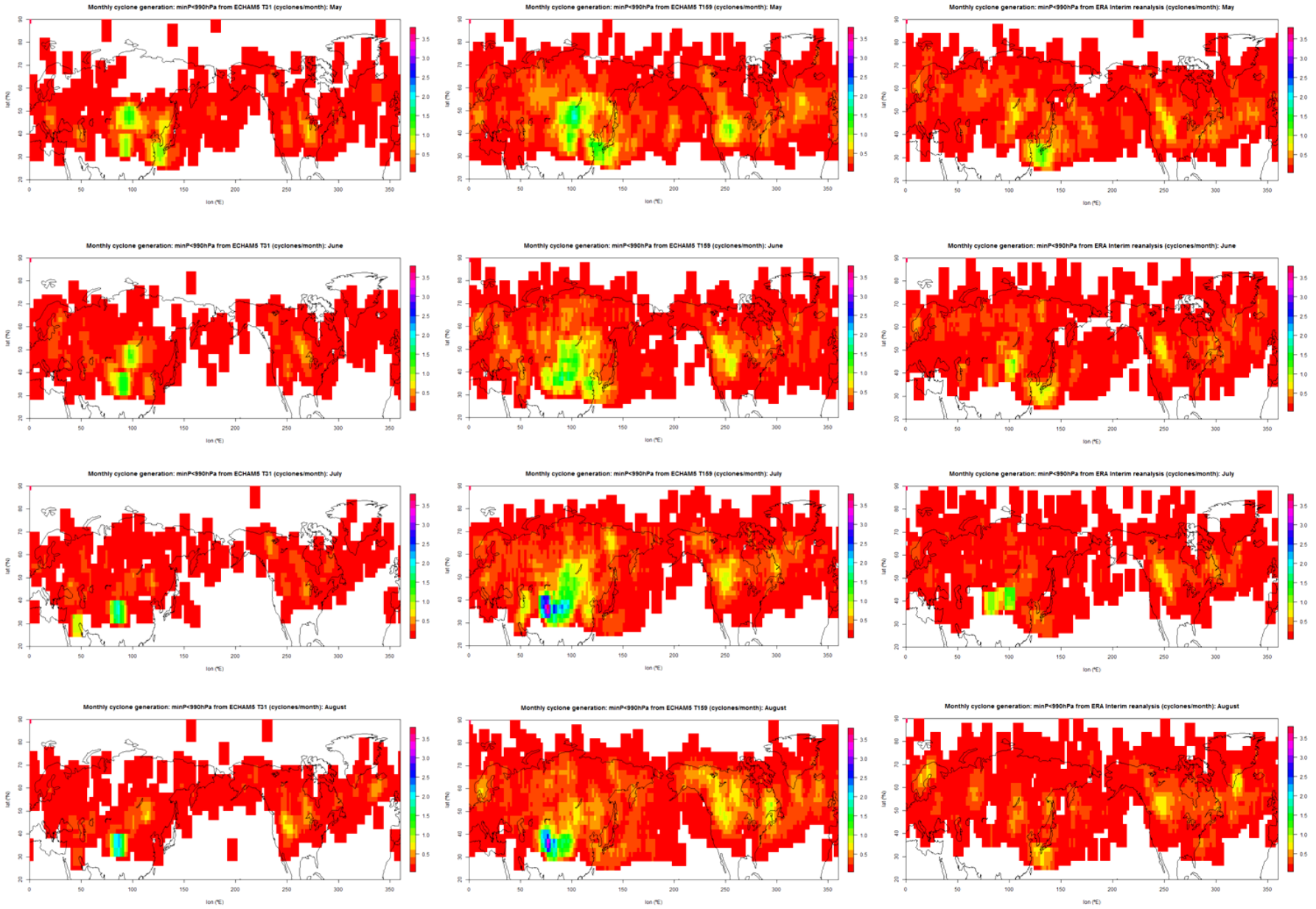

Figure II.2 (continues): Monthly cyclone generation maps: only cyclones that reach a min P of 990hPa or lower.

Shown are: ECHAM5 T31 resolution (left column), T159 resolution (central column) and ERA-Interim reanalysis (right column).
1st row is May
2nd row is June
3rd row is July
4th row is August

White spaces correspond to zero generation events per year. Same colour scale used for the rest of generation densities

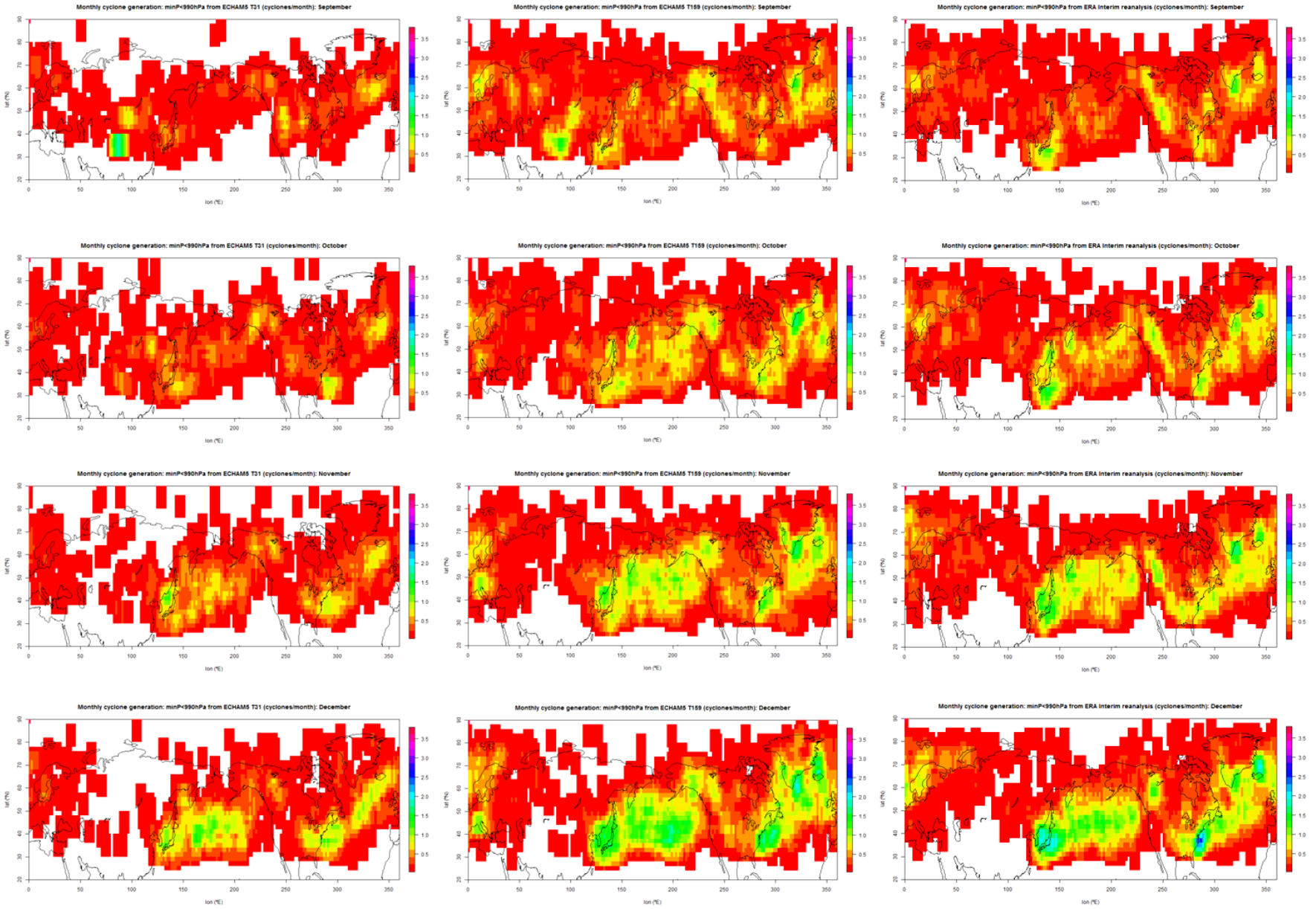

Figure II.2 (continues): Monthly cyclone generation maps: only cyclones that reach a min P of 990hPa or lower.

Shown are: ECHAM5 T31 resolution (left column), T159 resolution (central column) and ERA-Interim reanalysis (right column).
1st row is September
2nd row is October
3rd row is November
4th row is December

White spaces correspond to zero generation events per year. Same colour scale used for the rest of generation densities

ACKNOWLEDGEMENTS

I would like to thank Douglas Maraun and Wonsun Park for their supervising role and guidance during the completion of the thesis. Also, I am grateful to Vladimir Semenov, Claudia Volosciuk and Karl Bumke for their helpful comments and suggestions, and to Natalia Tilinina for providing the data and coordinate conversion algorithm used for the study.

REFERENCES

Bengtsson, L; Hodges, KI; Roeckner, E **(2006):** *Strom tracks and climate change.* Journal of Climate 19, 3518-3543

Blender, R; Shubert, M **(2000):** *Cyclone tracking in different spatial and temporal resolutions.* Monthly Weather Review 128, 377-384

Champion, AJ; Hodges, KI; Bengtsson, LO; Keenlyside, NS; Esch, M **(2011):** *Impact of increasing resolution and a warmer climate on extreme weather from Northern Hemisphere extratropical cyclones*. Tellus Series A- Dynamic meteorology and Oceanography 63, 893-906

Dee, DP; Uppala, SM; Simmons, AJ; Berrisford, P; Poli, P; Kibayashi, S; Andrae, U; Balmaseda, MA; Balsamo, G; Bauer, P; Dechtold, P; Beljaars, ACM; van de Berg, L; Bidlot, J; Bormann, N; Delsol, C; Dragani, R; Fuentes, M; Geer, AJ; Haimberger, L; Healy, SB; Hersbach, H; Holm, EV; Isaksen, L; Kallberg, P; Kohler, M; Matricardi, M; McNally, AP; Monge-Sanz, BM; Morcrette, JJ; Park, BK; Peubey, C; de Rosnay, P; Tavolato, C; Thepaut, JN; Vitart, F **(2011):** *The ERA-Interim reanalysis: configuration and performance of the data assimilation system.* Quarterly Journal of the Royal Meteorological Society 137, 553-597

Evans, JL; Hart, RE **(2003):** *Objective indicators of the Life cycle Evolution of Extratropical Transition for Atlantic Tropical Cyclones.* Monthly Weather Review 131, 909-925

Fortuin, JPF; Kelder, H **(1998):** *An ozone climatology based on ozonesonde and satellite measurements.* Journal of Geophysical Research-Atmospheres 103, 31709-31734

Gibson, JK; Kallberg, P; Uppala, S; Hernandez, A; Nomura, A; Serrano, E **(1997):** *ERA description.* ECMWF Reanalysis Project Report Series, Vol.1, European Centre for Medium-Range Weather Forecasts, Reading, United Kingdom, 72pp.

Grigoriev, S; Gulev, SK; Zolina, O **(2000):** *Innovative software facilitates cyclone tracking and analysis.* Eos Trans 81, 170

Grumbine RW **(1996):** *Automated passive microwave sea ice concentration at NCEP.* NOAA Tech. Note 120, 1-13

Gulev, SK; Zolina, O; Grigoriev, S **(2001):** *Extratropical cyclone variability in the Northern Hemisphere winter from the NCEP/NCAR reanalysis data.* Climate Dynamics 17, 795-809

Hanley, J; Caballero, R **(2012):** *Objective identification and tracking of multicentre cyclones in the ERA-Interim reanalysis dataset.* Quarterly Journal of the Royal Meteorological Society 138, 612-625

Holton, JR **(1972):** *An introduction to Dynamic Meteorology*. INTERNATIONAL GEOPHYSICS SERIES 48. ACADEMIC PRESS, INC.

Hoskins, BJ; Hodges, KI **(2002):** *New perspectives on the northern hemisphere winter storm tracks.* Journal of Atmospheric Science 59, 1041-1061

IPCC **(2007)** *Climate change 2007: the scientific basis. Contribution of working group 1 to the Fourth Assessment report of the intergovernmental Panel on Climate Change.* In: Solomon S, Qin D, Manning M, Chen Z, Marquis M, Averyt KB, Tignor M, Miller HL (eds). Cambridge University Press, Cambridge p996

Jung, T; Gulev, SK; Rudeva, I; Soloviov, V **(2006):** *Sensitivity of extratropical cyclone characteristics to horizontal resolution of the ECMWF model.* Quarterly Journal of the Royal Meteorological Society. 132, 1839-1857

Kalnay, E; Kanamitsu, M; Kistler, R; Collins, W; Deaven, D; Gandin, L; Iredell, M; Saha, S; White, G; Woolen, J; Zhu, Y; Leetmaa, A; Reynolds, B; Chelliah, M; Ebisuzaki, W; Higgins, W; Janowiak, J; Mo, KC; Ropelewski, C; Wang, J; Jenne, R; Joseph, D **(1996):** *The NCEP-NCAR 40-year reanalysis project.* Bulletin of the American Meteorological Society 82, 247-267

Lim, EP; Simmonds, I **(2002):** *Explosive Cyclone Development in the Southern Hemisphere and a Comparison with Northern Hemisphere Events.* Monthly Weather Review 130, 2188-2209

Martinez-Alvarado, O; Gray, SL.; Catto, JL.; Clark, PA **(2012):** *Sting jets in intense winter North-Atlantic windstorms.* Environmental Research letters 7, 2

Nakamura, H; Sampe, T **(2002):** *Trapping of synoptic-scale disturbances into the North-Pacific subtropical jet core in midwinter.* Geophysical Research Letters 29, no16

Neu, U; Akperov, MG; Bellenbaum, N; Benestad, RS; Blender, R; Caballero, R; Cocozza, A; Dacre, HF; Feng, Y; Fraedrich, K; Grieger, J; Gulev, S; Hanley, J; Hewson, T; Inatsu, M; Keay, K; Kew, SF; Kindem, I; Leckebusch, GC; Liberato, MLR; Lionello, P; Mokhov, II; Pinto, JG; Raible, CC; Reale, M; Rudeva, I; Schuster, M; Simmonds, I; Sinclair, M; Sprenger, M; Tilinina, ND; Trigo, IF; Ulbrich, S; Ulbrich, U; Wang, XLL; Wernli, H **(2013):** *IMILAST a Community Effort to Intercompare Extratropical Cyclone Detection and Tracking Algorithms.* Bulletin of the American Meteorological Society 94, 529-547

Pfahl, S; Wernli, H **(2012):** *Quantifying the Relevance of Cyclones for Precipitation Extremes.* Journal of Climate 25, 6770-6780

Pinto, JG; Zacharias, S; Fink, AH; Leckebusch, GC; Ulbrich, U **(2009)** *Factors contributing to the development of extreme North Atlantic cyclones and their relationship with the NAO.* Clim Dyn 32, 711-737

Raible, CC; Della-Marta, PM.; Schwierz, C; Wernli, H; Blender, R **(2008):** *Northern hemisphere extratropical cyclones: A comparison of detection and tracking methods and different reanalyses.* Monthly Weather Review 136, 880-897

Reynolds, RW; Smith, TM; Liu, C; Chelton, DB; Casey, KS; Schlax, MG **(2007):** *Daily high-resolution-blended analyses for sea surface temperature.* Journal of Climate 20, 5473-5496

Roeckner, E; Arpe, K; Bengtsson, L; Christoph, M; claussen, M; Dmenil, L; Esch, M; Giorgetta, M; Schlese, U; Schulzweida, U **(1996):** *"The atmospheric general circulation model ECHAM-4: model description and simulation of present-day climate*". MPI-report No.218

Roeckner, E; Bäuml, G; Bonaventura, L; Brokopf, R; Esch, M; Giorgetta, M; Hagemann, S; Kirchner, I; Kornblueh, L; Manzini, E; Rhodin, A; Schlese, U; Schulzweida, U; Tompkins, A **(2003):** *The atmospheric general circulation model ECHAM 5. PART I: Model description.* MPI-Report No. 349

Roeckner, E; Brokopf, R; Esch, M; Giorgetta, M; Hagemann, S; Kornblueh, L; Manzini, E; Schlese, U; Schulzweida, U **(2006):** *Sensitivity of Simulated Climate to Horizontal and Vertical Resolution in the ECHAM 5 Atmosphere Model.* J. Climate 19, 3771-3791

Rudeva, I; Gulev, SK **(2007):** *Climatology of cyclone size characteristics and their changes during the cyclone life cycle.* Monthly Weather Review 135, 2568-2587

Rudeva, I; Gulev, SK **(2011):** *Composite Analysis of North Atlantic Extratropical cyclones from NCEP/NCAR reanalysis data.* Monthly Weather Review 139, 1419-1446

Sanders, F; Gyakum, JR **(1980):** *Synoptic-dynamic climatology of the "bomb".* Monthly Weather Review 108, 1589-1606

Simmonds, I; Burke, C; Keay, K **(2008):** *Artctic Climate Change as Manifest in Cyclone Behaviour.* Journal of Climate 21, 5777-5796

Simmons, AJ; Burridge, DM; Jarraud, M; Girard, C; Wergen, W **(1989):** *The ECMWF medium-range prediction model: Development of the numerical formulations and the impact of increased resolution.* Meteorol. Atmos. Phys., 40, 28-60.

Sinclair, MR **(1995):** *A climatology of cyclogenesis for the Southern Hemisphere.* Monthly Weather Review 123, 1601-1619

Ulbrich, U; Pinto, JG; Kupfer, H; Leckebusch; GC; Spangehl, T; Reyers, M **(2008):** *Changing northern hemisphere storm track in an ensemble of IPCC climate change simulations.* Journal of Climate 21, 1669-1679

Wernli, H; Schwierz, C **(2006):** *Surface cyclones in the ERA-40 dataset (1958-2001). Part I: Novel identification method and global climatology.* Journal of the Atmospheric Sciences 63, 2486-2507

Yoshida, A; Asuma, Y **(2004):** *Structures and Environment of Explosively Developing Extratropical Cyclones in the Northwestern Pacific Region.* American Meteorological Society, 132, 1121-1142

Yoshiike, S; Kawamura, R **(2009):** *Influence of wintertime large-scale circulation on the explosively developing cyclones over the western North Pacific and their downstream effects.* Journal of Geophysical Research 114

Zhu, X; Sun, J; Liu, Z; Liu, Q; Martin, JE **(2007):** *A Synoptic Analysis of the Interannual Variability of Winter Cyclone Activity in the Aleutian Low Region.* Journal of Climate 20, 1523-1538

Zolina, O; Gulev, SK **(2002):** *Improving the Accuracy of Mapping Cyclone Numbers and Frequencies.* Monthly Weather Review 130, 748-759

ERKLÄRUNG

Ich versichere, dass ich die Arbeit selbstständig verfasst und keine anderen als die angegebenen Hilfsmittel benutzt habe. Weiterhin versichere ich, dass diese Arbeit noch nicht als Abschlussarbeit an anderer Stelle vorgelegen hat.

Die eingereichte schriftliche Fassung entspricht der auf dem elektronischen Speichermedium (Name der Datei: 1000327).

Ich erkläre mich damit einverstanden, dass ein exemplar der Abschlussarbeit der Institutsbibliothek zur Verfügung gestellt wird und stimme einer Veröffentlichung der Arbeit zu.

Kiel, den __ __ ____

_____

Robin Norbert Pilch Kedzierski